POLITECNICO DI TORINO

Master's Degree in Mechatronic Engineering (Ingegneria Meccatronica)

Master's Degree Thesis

Powered exoskeleton hip-joint design for industrial applications

Advisor:
Prof. Luigi Mazza

Candidates:
Ahmed Elbashary
Roberto Maliardo

Co-Advisors:
Prof. Gabriella Eula
Dr. Riccardo Mala
Dr. Marco Pontin

Academic Year 2018/2019

Abstract: Exoskeletons are becoming widespread in the research field nowadays. Those wearable devices can reduce the impact of work fatigue and related injuries.
The aim of this thesis is to provide a complete overview of an assistive exoskeleton that has been developed for industrial applications. Starting from a previous conceptual design, we made some modifications to optimize the exoskeleton structure and efficiency. We pointed out the essential components that form the hip-joint exoskeleton, in terms of actuation system and human-machine interfaces. A detailed design of each mechanical component has been implemented according to the functional requirements and the operating mode, providing a SolidWorks® complete model. Additionally, we make a preliminary bearing calculation to figure out the loads that act on the drive shaft. Lastly, a material selection was performed to understand the different solutions that could be adopted for building different exoskeleton parts. By studying the different specifications of each component, it was concluded that we are working in a safe and efficient zone, trying to provide comfortability and flexibility to the end-user simultaneously.

Table of contents

Chapter 1

Introduction

1.1 Motivation

The main goal of this thesis is to study and design an industrial hip joint exoskeleton that factory workers could wear, since they are constantly exposed to lower back and hip pain. This exoskeleton is aiming to reduce fatigue while performing trunk bending, and to assist defined tasks. There is also the possibility that these exoskeletons could facilitate earlier return-to-work, after an injury. Nowadays, wearable robots such as exoskeletons, which are designed to be used in an industrial field are the fastest growing research topic [1]. Our plan is to define some of the aspects that are dealing with mechanical and electrical details, for a high-level design. In parallel, we try to figure out which are the most effective elements for better functional requirements, that could be used to both fit the high flexibility of the human body, as well as affording the highest efficiency, for a compact and lightweight device.

1.2 Human body movements

The human body is a very flexible structure, composed of synovial joints that allow the body a tremendous number of movements. Each movement is a result of contraction and relaxation of the muscles that are attached to the body bones on either side of the articulations. The primary purpose of a synovial joint is to allow two bones to rotate freely about each other. Some synovial joint like the hip and the shoulder joints are defined as ball-and-socket joints, meant to provide high flexibility around the joint, Ball-and-socket joints allow three degrees of freedom [2]. Other joints are more limited in their range of motion like the ankle joint. For a hip joint exoskeleton, the focus is directed to the hip ball-and-socket joint. The types of synovial joints are shown in (fig. 1).

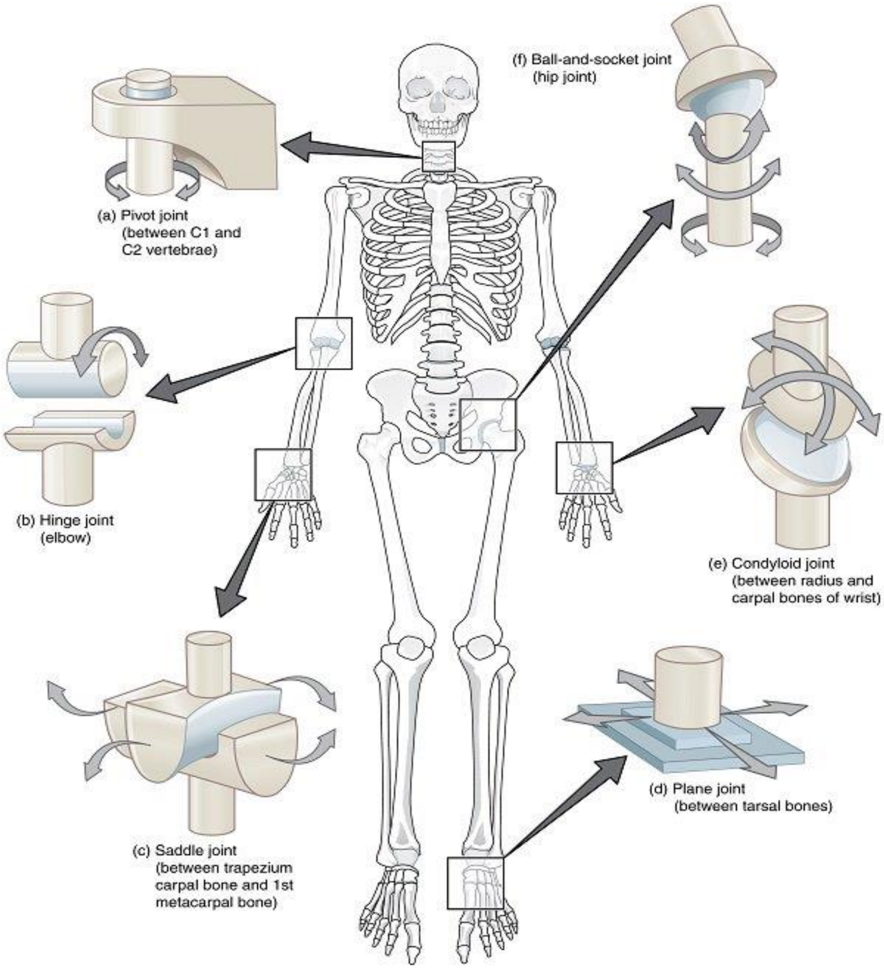

Figure 1: Types of body synovial joints [3]

The human motion are made around three planes of motion, called anatomical planes (fig. 2). A plane is a 2D slice through 3D space. The anatomical planes are three different planes used to divide the human body. We use the three anatomical planes to allow for an accurate description of a location. Those three planes divide the body into three sections [4]:

1- Frontal Plane: Divides the body to the front and back section.
2- Sagittal Plane: Divides the body to the left and right section.
3- Transversal Plane: Divides the body to the top and bottom section.

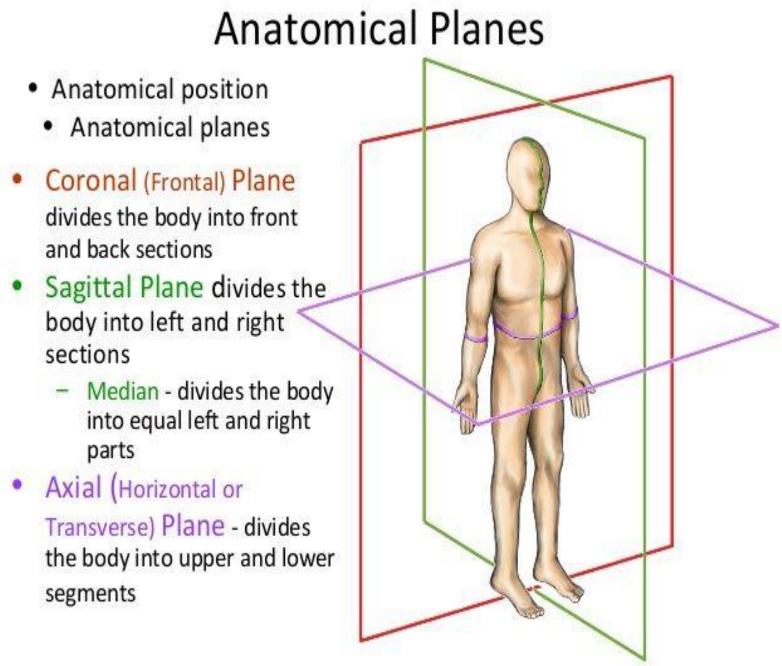

Figure 2: Anatomical Planes [4]

Most human motion involves a combination of two types of motion, the translational motion which is known as the linear motion and rotational motion which is also known as angular motion. Some of these angular motions are mentioned in (fig. 3), which shows both flexion/extensions and abduction /adduction rotation done by the human body as like as other human movements.

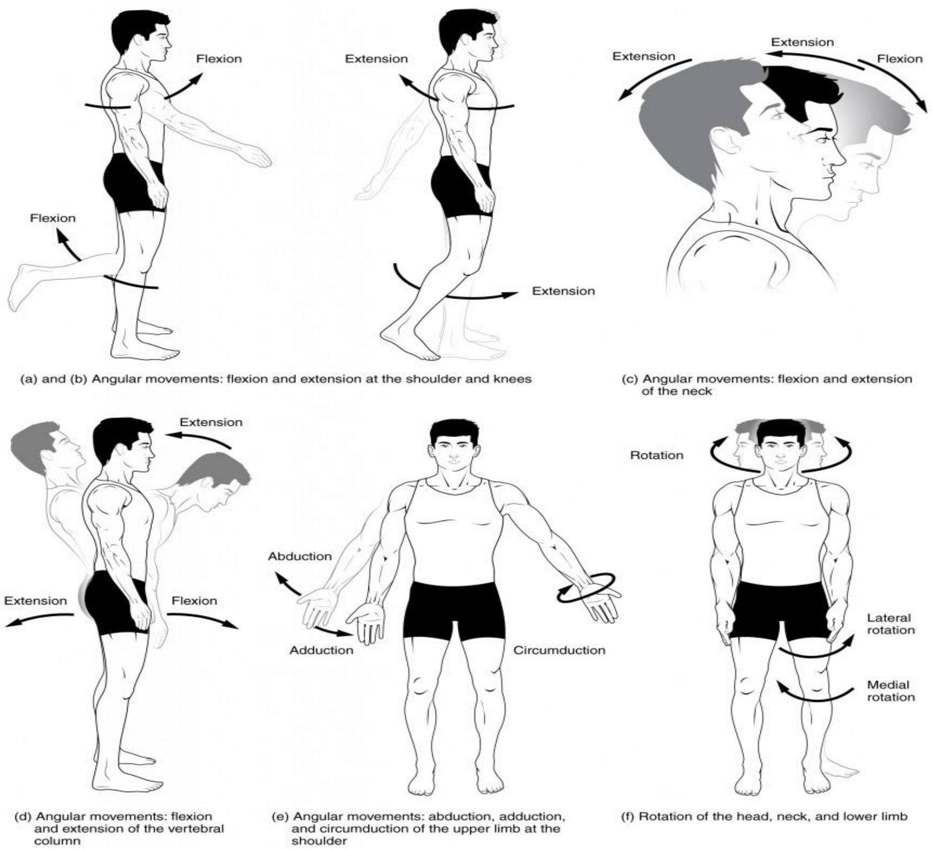

Figure 3: Some body Main Motions [4]

1.2.1 Flexion and Extension

Flexion and extension are the movements that take place within the sagittal plane, include forward or backward movements of the body or limbs. For the spinal column, flexion is a bending of the neck or upper body section forwardly, while the extension is a backward directed motion, like bending backward. Lateral flexion is the bending of the neck or upper body toward the right or left side.

In the limbs, flexion is formed by decreasing the angle between the bones, while the extension is increasing the angle of the joint. For the upper limbs, all forward motions are flexion, and all backward motions are extensions [5].

1.2.2 Abduction and Adduction

Abduction and adduction motions occur within the coronal plane and include median sidelong motions of the limbs, fingers, and toes. Abduction moves the limb laterally away from the midplane of the body, while adduction is the opposing movement that brings the limb toward the body. For example, abduction is holding-up the arm at the shoulder joint, moving it laterally away from the body, while adduction brings the arm down to the side of the body. Abduction and adduction movements are seen at body joints like condyloid, saddle, and ball-and-socket joints [5].

Moreover, as we aim to design a hip joint exoskeleton, we are focusing on flexion and extension, which are the movements that take place within the sagittal plane. Abduction and adduction motions are those which occur within the coronal plane around the hip joint.

1.3 What does Exoskeleton mean?

Originally the word Exoskeleton meant an external skeleton which naturally found in some animals and insects bodies, it adds more protection for their inner soft body and support them to survive in their tough living environments (fig.4), Disparity of the endoskeleton which is internally built in most mammals and in all human beings bodies. The endoskeleton function is to support the body, protect the organs and provide a system of levers on which the muscles can act to produce different kinds of movements [6]. As shown in (fig. 5).

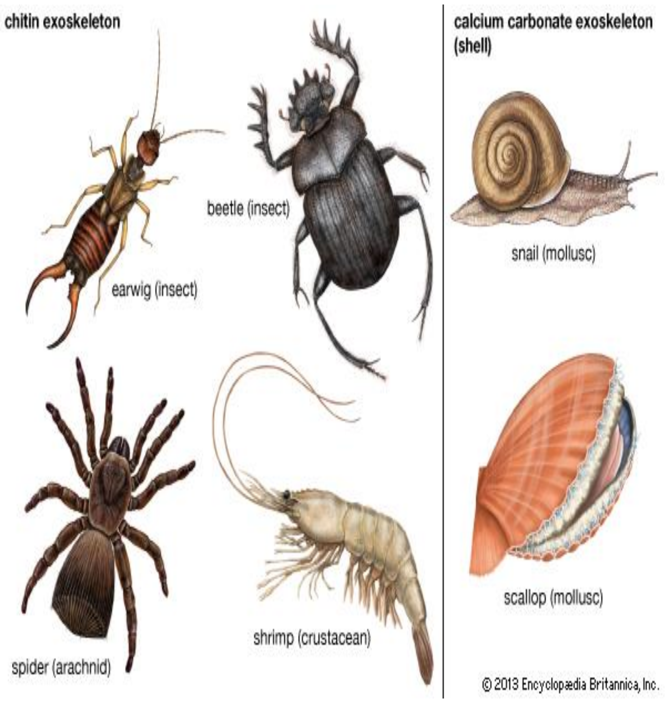

Figure 4: Animals' exoskeletons [6]

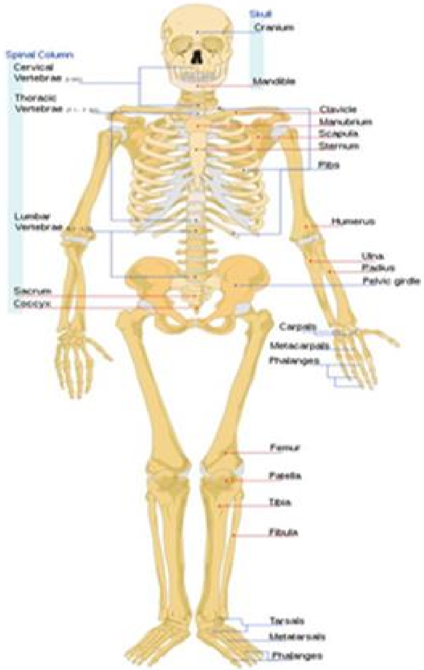

Figure 5: Human endoskeleton [6]

By considering the features provided by animal`s exoskeletons, humans started to develop a wearable robot which could add these features to the human body, that could be used to a variety of applications helping ordinary and disabled people to perform their daily operations in a more comfortable way, taking in count the advantages that an external skeleton adds to them in specific activities.

1.3.1 History of wearable Exoskeletons

Most of the early work related to exoskeletons were conceptual studies that never actually built or tested in real life. A Russian called Nicholas Yagn made the earliest mention of an exoskeleton, Yagn`s running aid patented in 1890 shown in (fig. 6). It was a simple structure containing bow/leaf spring operating parallel to the legs and was intended to boost running and jumping.

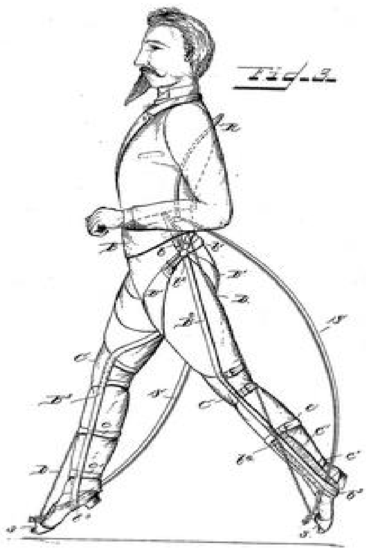

Figure 6: Yagn`s exoskeleton [7]

Many years later in the late 1960s Cornell University and the General Electric Company, financed by the US office of naval research, built a full-body powered exoskeleton, it was an enormous hydraulically powered exoskeleton (680 kg, 30 DOMs) and it contained components for increasing the strength of the arms and legs, it proposed to increase the human strength drastically, it was called Hardiman, as shown in (fig. 7) [7].

Figure 7: Hardiman exoskeleton [7]

In 1986 a new exoskeleton prototype was created by Monty Reed(fig. 8), a united states army ranger who had broken his back in an accident. It was called the LIFESUIT[8], he designed the LIFESUIT, and wrote letters to the military about his plans for the LIFESUIT. In 2001 LIFESUIT One (LSI) was built.

Figure 8: LIFESUIT (LSI) [8]

From this point, the researches related to exoskeletons stared to increase, and they spread in many applications like medical, defense, sports and industrial applications as shown in (fig.9). In our thesis research field, we consider studying and design of the industrial exoskeleton which is helping the worker in his daily working life by reducing the fatigue of lower back group of muscles when they are applied to loads that can affect the worker performance and expose him to have back injuries. Powered hip joint exoskeleton should provide a helping torque, and this helping torque should decrease the loads acting on the lower back muscles, to avoid injuries through multiple daily movements.

1.3.2 Review of some other models

1- Sarcos/Raytheon XOS Exoskeleton: for military use, it weighs 68kg, and it allows the user to lift 90kg with minimal effort, In 2010 XOS 2 was reviled, which gives to the user more flexibility and increases the output power and decreases the power consumption.
2- Ekso Bionics HULC legs: It gives an excellent lifting power compared to his weight which is 24 kg, and it allows the user to carry up to 91kg on a backpack attached to the exoskeleton.
3- Honda legs Exoskeleton: it provides a seat for the wearer, and it weighs 6.5kg.
4- Cyberdyne's HAL5 Exoskeleton: The first cyborg-type wearable robot allows the wearer to lift 10 times as much as they usually could, HAL 5 is currently in use in Japanese hospitals, and was given global safety certification in 2013.
5- ReWalk Exoskeleton: it is a powered hip and knee Exoskeleton enable those with lower limb disabilities, including paraplegia as a result of spinal cord injury, to perform self-initiated standing, walking, and stair ascending and descending.

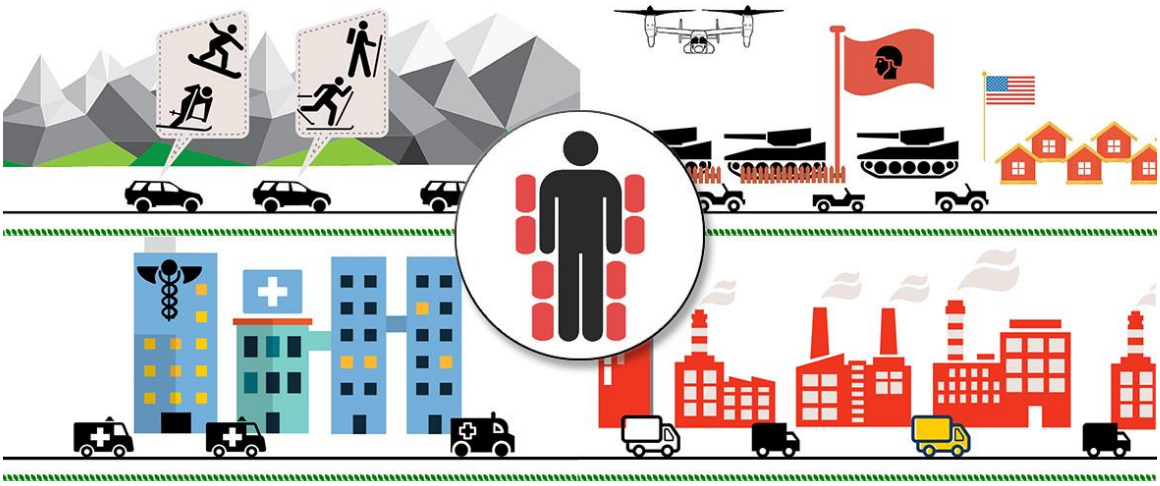

Figure: 9 Exoskeleton applications [9]

Moreover, here are some of exoskeleton researches and manufacturing companies shown in (fig.10)

Figure 10: Exoskeleton producers [10]

1.3.3 Exoskeleton classifications

1- Passive exoskeletons

This class of exoskeletons (fig.11) does not have any power sources, they are composed only by links, joints, and energy storing systems like springs and dampers, and it could be used for:

1- Weight re-distribution: springs and locking mechanisms that transfer the weight of an object around the user into the ground.
2- Energy capture: ankle spring-clutch exoskeletons improve walking efficiency, while spring-dynamo knee exoskeletons are used, as well, to charge a battery.
3- Damping: Its spring or spring-damper passive exoskeletons are used as shock absorbers or vibration reducers.
4- Locking: They are passive exoskeletons designed to be unobtrusive until they are locked into place, allowing the user to crouch or sit in the same position for an extended period.

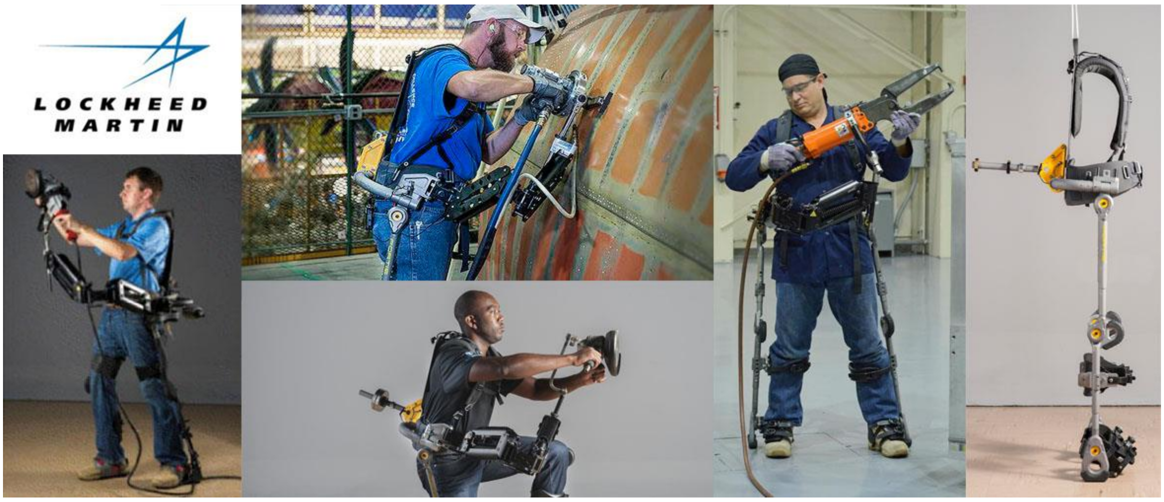

Figure 11: Passive Exoskeletons [12]

2- Pseudo-passive exoskeletons:

This class of exoskeletons has batteries, sensors, and other electronics, but they are not used to provide actuation but uses its electronics to control a variable damper in the knee (fig.12). For example, The C-Brace model which alternatively unlocks slows down the swing of the leg and locks depending on the position of the leg in the gait cycle as determined by the integrated sensors.

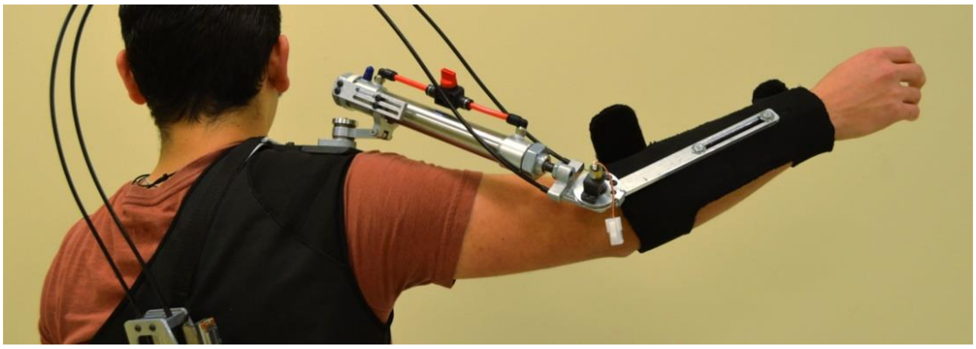

Figure 12: Pseudo-passive exoskeletons [13]

3- Powered exoskeleton

Powered Exoskeletons are an external structural mechanism with joints and links, powered with technologies to mimic the movement of the corresponding to those of the human body.

This class of exoskeletons powered with different kinds of power sources to actuate the links and different elements of the exoskeleton, usually electrical motors or fluid power are used , electronic elements like sensors and transducers built in the system provides a closed loop controlling system, offering feedback on different parameters like speed, position, motion and applied forces. Powered exoskeletons are often used to help in lifting heavy loads and reducing body fatigue for industrial (fig. 13) and militarily uses (fig. 14), they are also widely used for medical reasons as rehabilitation and disable people assessment (fig. 15).

Figure 13: Militarily exoskeleton [14]

Figure 14: industrial exoskeleton [15]

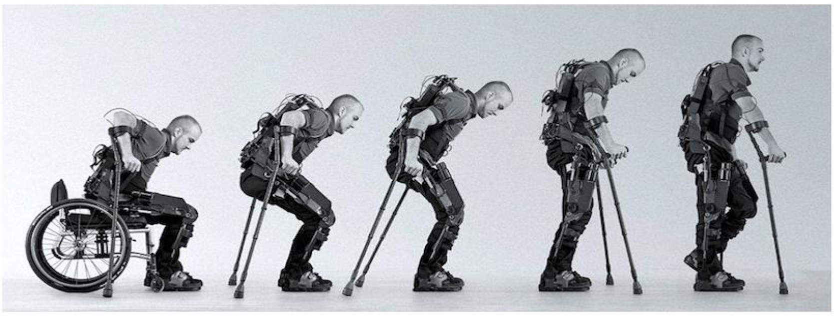

Figure 15: Rehabilitation exoskeleton [16]

1.4 Industrial Exoskeletons

Why industrial exoskeletons are required?

Ergonomics (fig.16) and human safety have always been a critical topic for manufacturing, every day a considerable number of workers are interacting with machines in mass production factories, and even if many research topics are dealing with inverting this relation between workers and machines to a fully automated processes, people are still essential for various roles in the industrial equation, therefore, the importance of ergonomics is clearly affirmed as a result of that more detailed analysis and researches were done to understand better the main ergonomics criticalities that must be faced.[17]

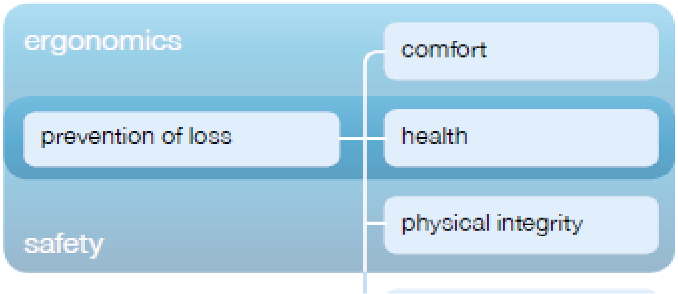

Figure 16: Ergonomics chart [17]

In industry, workers are often subjected to frequent trunk bending in static and dynamic postures, while holding awkward postures in repeated lifting and assembly activities, where the potential for long terms back pain and injuries is significant, lumbar spine disorders such as lower back pain is one of the common joint injuries , approximately 44 million EU workers are affected by musculoskeletal conditions which result in an annual cost of 240 billion euros to the European economy, and the majority of these musculoskeletal problems are related to the lower back pain, and the primary source of back pain is tendon or muscle strain [18].

At this moment the concept of ergonomics and work safe environment became a must, if the activity cannot be eliminated, alternative measures must be applied to safeguard the worker, it also affects optimizing productivity and system performance.

For those reasons, wearable robotics started gaining support from the industrial fields. Industrial Exoskeletons exploded the research field nowadays. Exoskeletons for industry and workplace offers three main advantages:

1- Preserve workers health.
2- Lowering work fatigue which leads to increasing of worker alertness, productivity, and working efficiency.
3- Saving money spent on medical fees.

Industrial exoskeletons is the name given to mostly biomechanical devices that worn by workers. It replicates the structure of the worker`s limbs, muscles, and joints working in tandem with them. It is useful to think in the industrial exoskeletons as wearable robots that take advantage of the worker intelligence and the strength of industrial robots. Exoskeletons are like the traditional robots but the difference is that they work on the idea of physically demanding sensing given by the worker body with some semi-automated operations. At that point we are trying to take the advantages of both traditional industrial robots with entering action done by the human intelligence.

Over time the term (industrial) expanded to include both industrial and commercial sectors, for example the "backX" exoskeleton by SUITX INC (fig.15) is the one which supports back while pending [19]. Companies in the industrial sector derive their profits by providing tangible good, products, and materials. The commercial services sector is made up of companies that primarily derive their profits by providing intangible products and services like transportation, retail, healthcare and energy.

Figure 17: BackX exoskeleton [19]

1.4.1 Classification of industrial exoskeletons

1- **Arms, upper and lower body:** Exoskeleton systems come out in many shapes and forms, including systems that are attached at the hip and others have weight carried by the exoskeleton through to the floor which locks in place, acts as a seat when needed. Others are upper body systems, while still others assist hands in gripping tools to lower fatigue in long time assembly procedures.

2- **Active and Passive:** In contrast to passive exoskeletons which don`t depend on power sources, active exoskeletons increase strength, provide stability and flexibility through a combination of human-guided flexion/extension and locking mechanisms.

3- **Rigid and soft:** Rigid exoskeletons can produce musculoskeletal stress and fatigue due to their weight and structure, as well as the abnormal or constrained movements of the suit. As a result of that problems, some companies are developing new types of soft exoskeletons made of soft, lightweight, compliant materials [20].

Nowadays researchers are working to develop what is called soft exoskeletons(fig.19) which could solve the problem of solid rigid structures and be lighter. Those soft exoskeletons are made entirely out of soft materials excepting some components like batteries and controllers. Power is transmitted by flexible materials only, for example, Bowden cables and air muscles [21].

Advantages of soft exoskeletons

1- More straightforward fitting with different shapes of bodies.
2- More flexibility.
3- Lightweight.
4- Less expensive.

Disadvantages of soft exoskeletons

1- Less strength.
2- Motors and sensors are more difficult to mount.
3- Cannot be used for disables.

Figure 19: Soft exoskeleton [21]

1.5 Our Mission

Our thesis aim is to design a whole exoskeleton containing an hip joint exoskeleton to be used in industrial applications helping the worker to reduce fatigue, to assist in defined tasks as assembly operations.

For designing any engineering system, the engineering design process (fig.20) should be followed to get as output the result we aim to achieve. Those 5 steps are simplifying any engineering design processes [22].

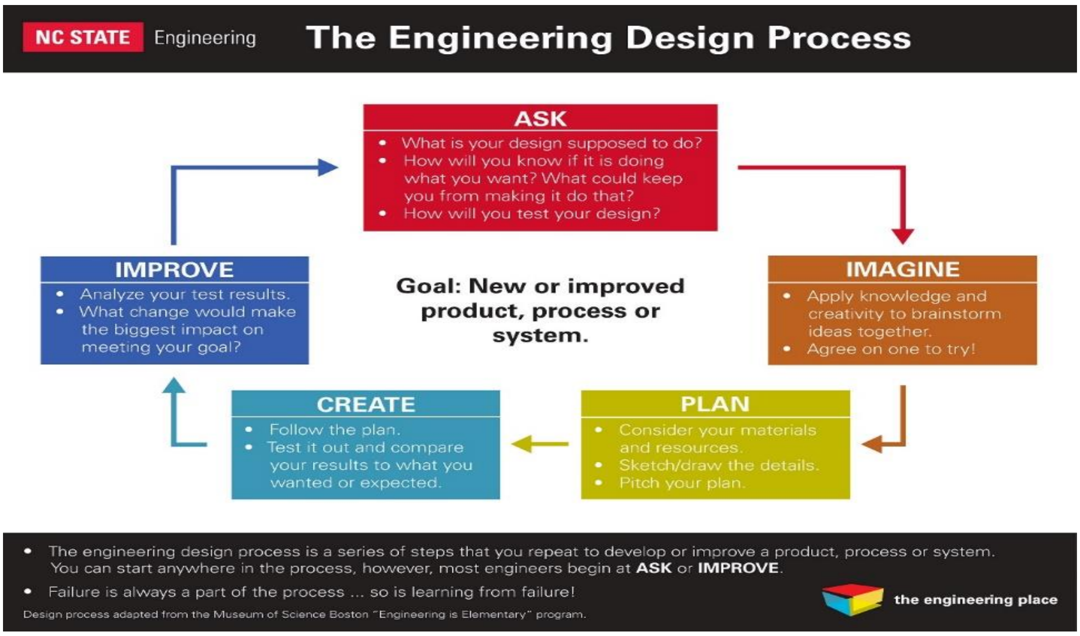

Figure 20: Engineering design process [22]

In the following chapters, we show the steps that have been made following that diagram, starting with the asking step to understand the main function of our system and how does it should work and ending with improvement section — trying to apply our engineering knowledge to build a complete optimized system.

Chapter 2

Hip torque calculations

2.1 Variable definition

The first step we take, before going on with our own work, it's a brief review of the main variable definitions of the previous study.

First, it's the definition of a reference plane to use as a guideline in our design that is the sagittal one and, we assume all the forces and motions lie around the reference axis that is the vertical "z-axis".

Our main variables for the estimation of the torque will be the following angles (*fig.21*):

- ϑ that is the measure of the angle between the vertical axis z and the user trunk.
  We decide to consider the hip flexion as positive direction.
- α, that identifies the angle between the trunk and the thighs.
- β, that identifies the angle between the thighs and the vertical axis.

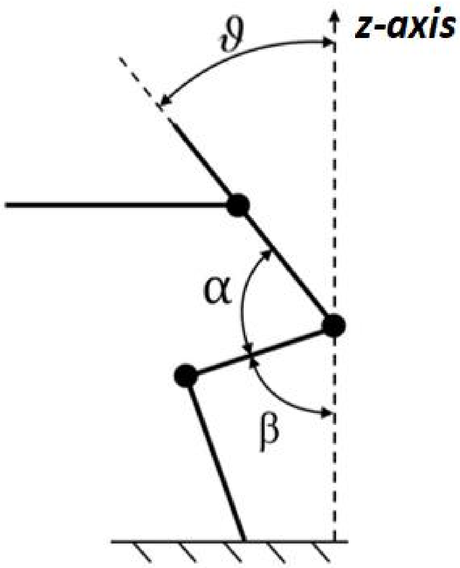

Figure 21: Human body angles and reference axis

Since, as an initial approximation, we consider the exoskeleton to be fixed to the end user, each human body and exoskeleton link angle coincides with each other. Thinking to a future work, it is necessary to distinguish them as it is a human-robot interaction. The consequence is a relative motion between human and exoskeleton, that generates angle shifts.

2.2 Anthropometric data

To ensure an ergonomic and accurate technological design, we refer to the ISO/TR 7250-2:2010 technical report [23], that identifies different statistical summaries of country-specific human body measurements. From this report, we extrapolate data corresponding to the human body mass and weight, selecting as reference subject the 99 percentile Italian man, so that the final required torque is as big as possible, for a worst-case evaluation.
We obtain a height H = 1.883m and a mass M = 103 kg.
These two values are used to evaluate the partial body masses and lengths of the different anatomical portions, according to linear correlation coefficients, found in literature[24], as shown in the following pictures *(fig.22, fig.23)*:

segment	segment length[a]/ body height H
head height	0.130
neck height	0.052
shoulder width	0.259
upper arm	0.186
lower arm	0.146
hand	0.108
shoulder width	0.259
chest width	0.174
hip width/leg separation	0.191
upper leg (thigh)	0.245
lower leg (calf)	0.246
ankle to bottom of foot	0.039
foot breadth	0.055
foot length	0.152

Figure 22: Body segment masses [24]

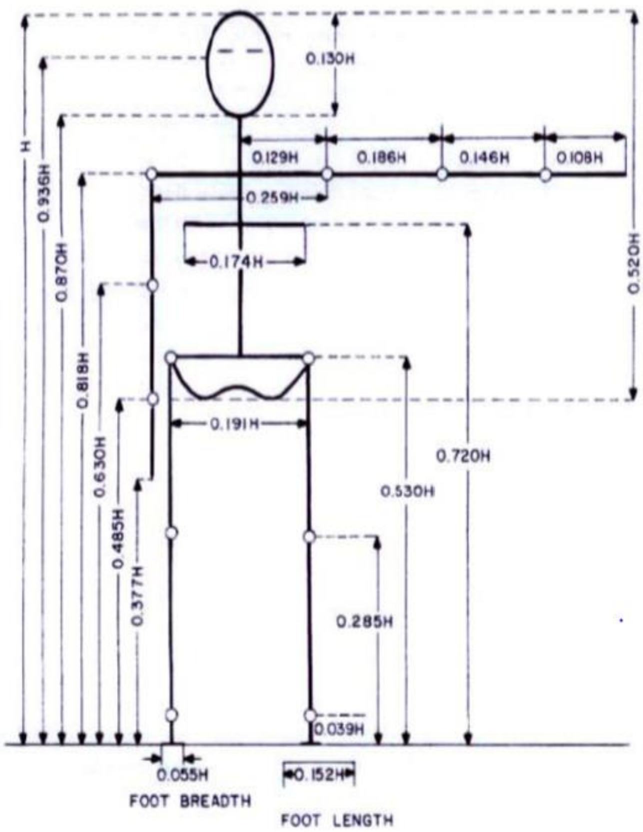

Figure 23: Body segment lengths [24]

Here we report only the values that have been used for the center of gravity (CoG) evaluation:

$m_u = 0.028 \cdot M = 2.884\ kg$	(upper arm mass)
$m_f = 0.016 \cdot M = 1.648\ kg$	(forearm mass)
$m_{hn} = 0.081 \cdot M = 8.343\ kg$	(head and neck mass)
$m_h = 0.006 \cdot M = 0.618\ kg$	(hand mass)
$m_t = 0.497 \cdot M = 51.191\ kg$	(trunk mass)
$L_u = 0.186 \cdot H = 0.3502\ m$	(upper arm length)
$L_f = 0.146 \cdot H = 0.2749\ m$	(forearm length)
$L_{hn} = H - 0.81H = 0.3427\ m$	(head and neck mass)
$L_h = 0.108 \cdot H = 0.2034\ m$	(hand length)
$L_t = 0.5423\ m$	(trunk length)

Table 1: Partial body masses and lenghts

2.3 Weight forces and center of gravity

We can divide the upper body masses in two main contributes, one that is given by the trunk/neck/head region and the other one by the two arms. Those weight forces are:

$$P_t = (m_t + m_{hn}) \cdot g = 584.029\ N \tag{1}$$

$$P_a = 2 \cdot m_a \cdot g = 101.043\ N \tag{2}$$

Where:

P_t is the sum of trunk, neck and head weight forces.

P_a is the two arm weight forces

g is the standard acceleration due to gravity

It's now required to define which are the application points, in terms of levers, on which the weight forces act. For this purpose, we apply the formula of the center of mass of homogeneous bodies. It is important to note that since we are in a uniform gravity field, the centers of masses coincide with the center of gravity [25].

Moreover, we assume parallel legs and arms, meanwhile the axis of the two weight forces are collinear.

We obtain:

$$L_1 = \frac{m_t \cdot \frac{L_t}{2} + m_{hn} \cdot \left(L_t + \frac{L_{hn}}{2}\right)}{m_t + m_{hn}} = 0.3332\ m \tag{3}$$

$$L_2 = \frac{m_u \cdot \frac{L_u}{2} + m_f \cdot \left(L_u + \frac{L_f}{2}\right) + m_h \cdot \left(L_u + L_f + \frac{L_h}{2}\right)}{m_u + m_f + m_h} = 0.3414\ m \tag{4}$$

Where:

L_1 is the distance between hip and center of gravity of trunk, neck and head (fig.24)

L_2 is the distance between shoulder and center of gravity of the arm (fig.25)

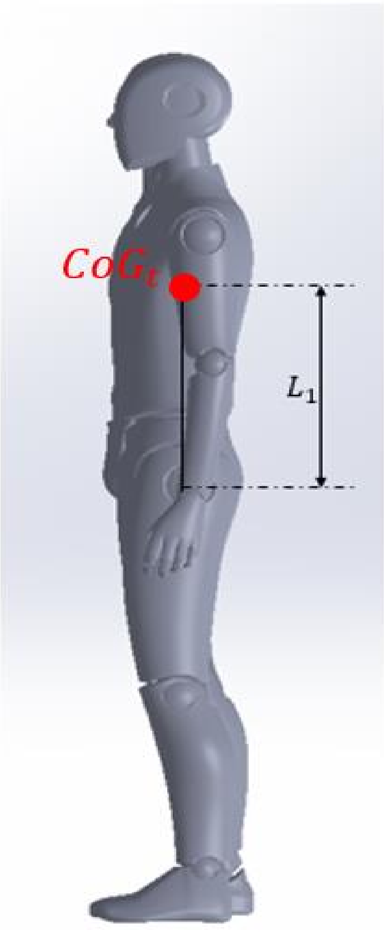

Figure 24: Distance hip – trunk/head/neck center of gravity

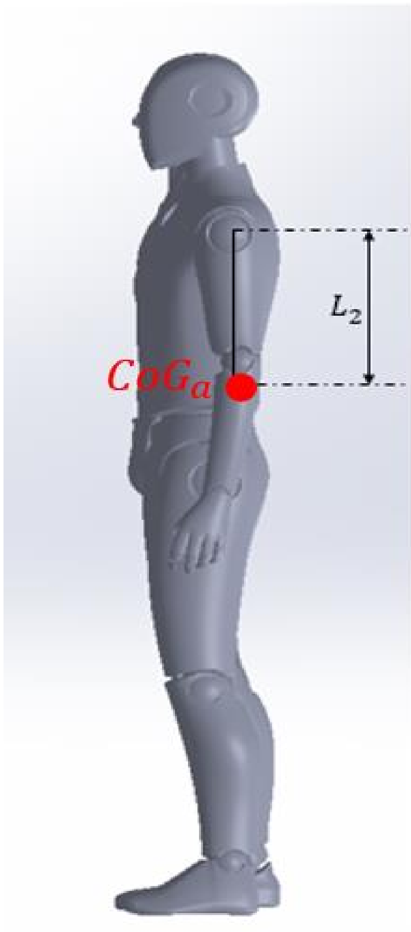

Figure 25: Distance shoulder – arms center of gravity

2.4 Ultimate hip torque

In the final torque evaluation, in the case of static equilibrium, we consider the upper body configuration, in which the trunk and the arms are tilted forward (fig.26).

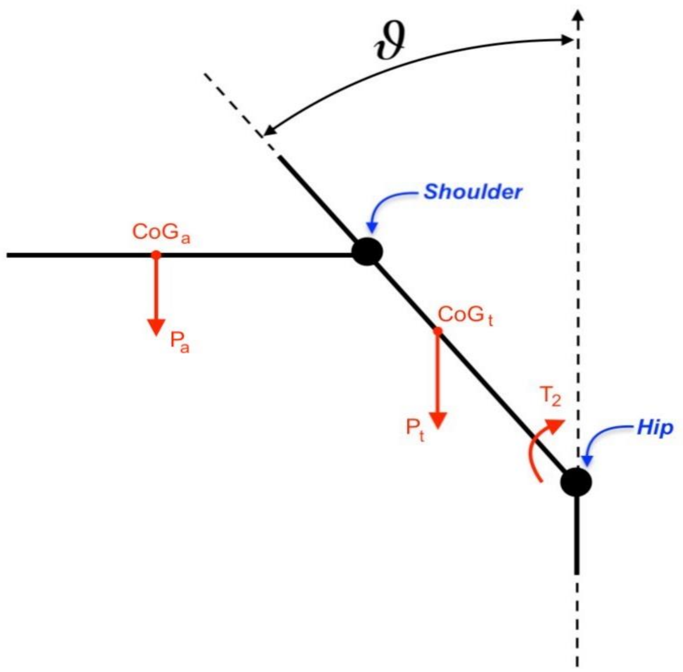

Figure 26: Free body diagram

From this free body diagram, it is possible to calculate the requested torque around the hip, for this examined configuration, obtaining:

$$T_2(\theta) = P_t \cdot L_1 \cdot \sin\theta + P_a \cdot (L_2 + L_t \cdot \sin\theta) \qquad (5)$$

To determine the maximum required torque, that we decided to define as "working torque" $T_2(\theta_w)$, we must choose a reference for the "working angle" θ_w, described as the limit user trunk flexion.
After a long examination we decided to set it to 90°, as the extreme condition in which the user trunk is parallel to the ground. It follows: $\theta_w = 90°$.

This assumption makes the resulting working torque to be:

$$T_2(\theta_w) = 283.89\ Nm \tag{6}$$

This torque is equally split between the two hips, so that we can divide it by two. Furthermore, since we are dealing with an "assistive device", some considerations were made about the rate of assistive torque generated by the actuation system.

It was decided to decrease the assistive holding torque from 70% of the user`s resulting total working torque to be only 30% , this modification had been done after understanding that offering a 70% of the user`s resulting total torque is an exaggerating value, and it's not a reasonable amount of a helping power afforded for a healthy person .

We selected a 30% percentage as it is a safe and reliable value for assisting a healthy person. Now it's possible to determine the final torque provided by each side, with a scaling factor of 0.3 (30%):

$$T_{\text{out}} = \frac{T_2(\theta_w)}{2} \times 0.3 \cong 42\ Nm \tag{7}$$

Starting from this required hip joint torque, that will be given to the harmonic drive (HD) output shaft, and assuming that the clutch will ideally transfer the total torque given by the stepper motor, we can derive the latter driving torque.

The transmission ratio (R) of a harmonic drive is obtained from the virtual work principle, shown in the formula below:

$$R = \frac{T_2}{T_1} = \frac{T_{out}}{T_{in}} \quad , \quad R = \frac{\omega_1}{\omega_2} = \frac{\omega_{in}}{\omega_{out}} \tag{8}$$

Where:

T_1, ω_1 ($= T_{in}$, ω_{in}) are the input shaft torque and angular speed respectively

T_2, ω_2 ($= T_{out}$, ω_{out}) are the corresponding output shaft torque and angular speed

To find a correct R value, it's necessary to define a hip joint angular velocity profile that works during both forward/backward bending.

We assume as valid a trapezoidal 2-1-2 speed profile that best fits our need of a safe motion and a simple control algorithm.
Moreover, adopting this profile we ensure our system to smoothly increase the speed over time, thus preventing body shocks and bumps problems.

It results in the profile depicted below, with a maximum output speed of $\omega_{out} = 5$ RPM (30 deg/s), as shown in the following figure (fig.27).

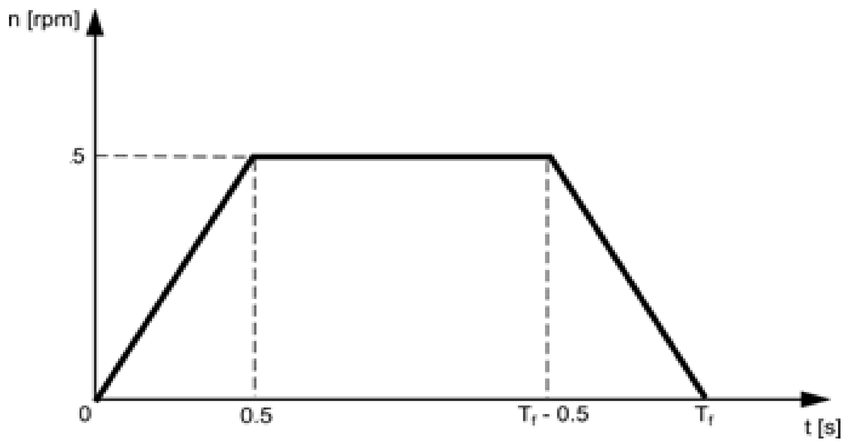

Figure 27: Ideal hip joint angular velocity profile

Note that the maximum output speed value that is the peak bending rotational velocity, it has been selected so that we can find a compromise between the motor size and the speed.

Chapter 3

Optimization of the conceptual design

The target of this chapter is to present the conceptual design that has been previously developed to identify which is the starting point of our project and the relevant main aspects on which we focus our proposed solution.
Moreover, some system requirements are pointed out, in terms of intended functionalities and safety constraints, since those wearable devices present several limitations that could negatively affect the end user.
As those key points are identified, we take care of making the appropriate system modifications to guarantee that the mechanical components can work properly as a whole, in terms of inherent stability and performance.
At the end, it is presented the implementation of a second independent solution, based on an entirely different design.

3.1 System requirements

The implementation of a wearable robot as complex as an exoskeleton should meet some system requirements, aside from assuring the right amount of support at the appropriate time. For this purpose we collect some information that describe the functional and behavioural requirements, to ensure the system to be operationally effective.
Among them we can underline:

1- Range of motion (ROM): Define which are the mechanical angle limits, in terms of maximum back flexion/extension to ensure correspondence with the user limits. It could be useful to adopt some mechanical end-stops that limit the range of motion, even when electric motors do not work correctly, to avoid possible injuries.

2- Alignment between the exoskeleton's hip joint and the anatomical one, as the interaction between the user and the exoskeleton is bidirectional and some kinematic misalignments and mismatch could appear.

3- Human Machine Interface (HMI): The challenge for achieving an optimal exoskeleton-based system is to find the right trade-off between a rigid and a soft structure, as they both have some benefits and constraints.
More in deep, a rigid structure is needed to guarantee the power transmission, to prevent the device slippage with respect to the worker's hip and to provide stabilization and protection against external impacts.
Instead, a soft structure is more suitable to contain the tissues and muscles compression, so to reduce skin irritations and overheating problems. Concurrently, it could counterbalance the inertia, the backlash and the friction contributions due to the stiffness of the actuation unit components.
Moreover, adopting such a flexible kind of material, it could increase human mobility and partially account for the other two degrees-of-freedom of the hip joint (abduction/adduction, internal/external rotations).

4- Dimensional analysis: The examination of the length and width extensions of the entire exoskeleton is necessary, as well as the added mass load, being the user to carry the entire exoskeleton structure.
That's because a relatively higher volume could cause collisions with the environment, but even the impossibility for the user to extend his arms along the two body sides. Additionally, the user is required to accelerate and move the exoskeleton mass when he is moving around, resulting in an increased effort.
Therefore, the user could feel reduced strength and fatigue faster.

5- Operating modes: The exoskeleton is meant to offer three different operational modes. The first one is the "free mode", that should be operated when the user wears the exoskeleton, but it is not required to give support to him (e.g. gait cycle or tasks that do not involve bent-over posture). This mode is associated with the electromagnetic clutch disengagement.

The second operating mode is the “stooping mode”, in which once the exoskeleton reaches the desired inclined position it should lock it in a stationary condition (e.g. when the employer standing farther away from the workstation and he tends to lean-forward). This condition should be satisfied by the stepper motor’s holding torque functionality. The third operating mode is the "bending mode", in which the exoskeleton should provide the right amount of torque when the user is rising from an inclined position to full-erect stance (e.g. when a task has been accomplished). However, it is necessary to emphasise that all these modes should be managed to employ suitable feedback control algorithms, that is not covered in this work.

In conclusion, for the design of an exoskeleton, the primary challenge is to find a trade-off between several aspects, so that the benefits should outbalance the structural limitations.

3.2 First conceptual design

In this paragraph, we provide some general information about the previous solution, from which we have planned our design, in terms of actuation system, back/leg frames, and working principle as relative interaction between all the components.
This solution takes inspiration from the electric SEA (Series Elastic Actuator) system, that is adopted by the existing APO (Active Pelvis Orthosis)[26] exoskeleton, that was realized for assisting older people while walking . This system is the core of the complete structure, and it is composed of four different elements that are: an electric brushless DC electric motor, a single disc electromagnetic clutch, a harmonic drive, and a torsional spring.
Then, to avoid a high lateral encumbrance, a four-bar-linkage mechanism has been designed to be interconnected between the harmonic drive and the torsional spring, so that this mechanism is split in two, as in the APO case.
Moreover, the motor is clamped to one end to the back frame, while the torsional spring is connected to the leg frame, which is free to move inside a bearing that is mounted on the same back frame. The latter is then attached to the human torso through the shoulder straps.

Below are reported two CAD models, to clarify which are the components and the whole conceptual design model (fig.28).

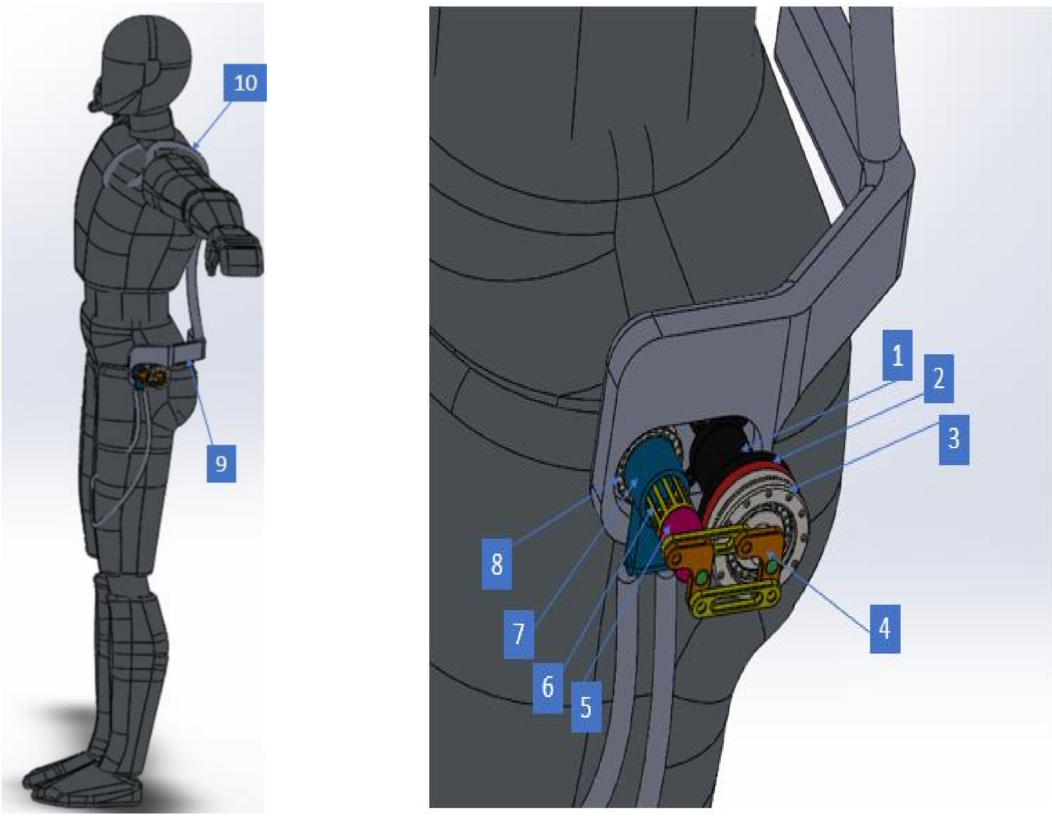

Figure 28: Numbered list of the CAD model components

Component Number	*Component Name*
1	Brushless DC electric motor
2	Single disc electromagnetic clutch
3	Harmonic drive
4	Four-bar-linkage
5	Spacer
6	Torsional spring
7	Leg frame
8	Bearing
9	Back frame
10	Shoulder strap

Table 2: Itemized list of CAD model components

3.2.1 Working Principle

The brushless DC electric motor should be supplied by an external battery that has not been faced in this solution. However, the motor is responsible for delivering the high rotational speed and the low torque to the input of the harmonic drive, passing through the electromagnetic single disc clutch. The presence of the clutch is needed to decouple the load from the motor during the “free-mode”, and it should be electrically activated when needed. Then, thanks to the gear ratio that is provided by the harmonic drive, the system can amplify the torque of the motor, reducing the speed and inverting the rotational direction, thanks to a negative ratio.

Notice that, the selected harmonic drive (fig.29) is composed of three elements that are the wave generator (input), the circular spline and the flexspline (output).

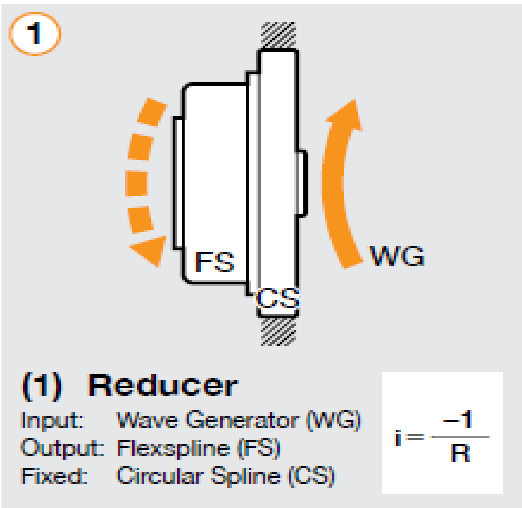

Figure 29: Harmonic Drive elements, gear ratio and rotational directions [27]

Besides, the output torque of the harmonic drive is delivered to the torsional spring, that can store potential energy, and consequently to the leg frame, through the four-bar-linkage mechanism, assuming that between all those components there are no dissipations and power losses. Once the torque is transferred to the leg, a reaction force is sent back through all the transmission system, to the motor and the back frame accordingly.

3.2.2 Advantages and disadvantages

The conceptual design presented above has been taken as a reference to realize an optimized model of the hip joint exoskeleton.
We decided to maintain the advantageous electric powered actuation, as the SEA system is, but we opted to remove the torsional spring since we want to deliver the torque to the leg without any energy absorption by the spring itself.
In addition, we also kept the four-bar linkage, since it is an excellent mechanism to separate the transmission system in two branches, so that we can minimize the occupied space sideways. Furthermore, as second advantage, we can retain the powered joint in correspondence of the anatomical one.
Anyhow, some issues were pointed out and listed below:

1- The electric DC brushless motor is not able to keep and hold the load in a static positioning.

2- The adopted harmonic drive presents some problems for the correct operation of the power transmission. As it is shown in the paragraph 3.2 CAD model, the circular spline that should be fixed is left free to rotate around itself. By consequence, when the flexspline tries to transfer the output torque to the leg frame, through the four-bar linkage, it finds a resistive torque that is much higher than the one required to rotate the circular spline. This leads to the dissipation of the energy provided by the wave generator.

3- The modelled components are designed without any interconnection (in terms of shafts, flange etc.) and they do not respect the dimensional drawings that are provided in the technical manuals of the chosen component manufacturers.

4- The CAD design takes care of only one side of the human body and the contact surfaces are not well specified.

3.3 Proposed solution

Here we introduce our new design, based on the previous considerations. The aim is to show every single element composing the assistive exoskeleton (fig.30, fig.31)
The first modification was applied to the adopted motor. We opted to replace the DC electric brushless motor with a stepper one since this typology can supply an incremental torque, as it divides the complete rotation into several steps that are all equal.
In this way, the motor can hold the load in place when a constant torque is required for the stooping mode.
The selected stepper motor company also provides an integrated optical incremental encoder that allows continuous monitoring of the motor angle.
The second modification was made to reduce the electromagnetic clutch size since we must always keep as a requirement the minimization of the lateral encumbrance of the system. Furthermore, since the motor and the clutch have different shaft diameters, a suitable shaft adapter (including key) has been designed to assure the correct coupling and the torque transmission.
Then, the harmonic drive has been changed for a more compact robotic hip joint, since it is a "Pancake type". This typology also gives the advantage of a repartition of the input torque in two, having two alternate outputs that are sent to the leg and the back, as it is well explained into the Harmonic Drive paragraph.
The four-bar linkage has been kept as it was in the previous solution, with a Z crank form. The output of this mechanism is delivered to a shaft that has an axial extension equal to the one of the first branch (motor, clutch, HD, leg support).
Moreover, a back support meant to transfer the right amount of torque to the human torso has been designed to be connected to the backpack worn by the end-user.
As a final step, we took care of designing all the human-exoskeleton interfaces in terms of waist belt, backpack and leg adjustable straps, needed for a working motion transmission system.
Notice that, since most of the hip joint components need a fixed reference, a preliminary supporting flange has been designed. Thinking to a possible future improvement, a housing should be added to protect all these components against potential corrosions and shocks to which this device could be exposed, due to the nature of the working environment.

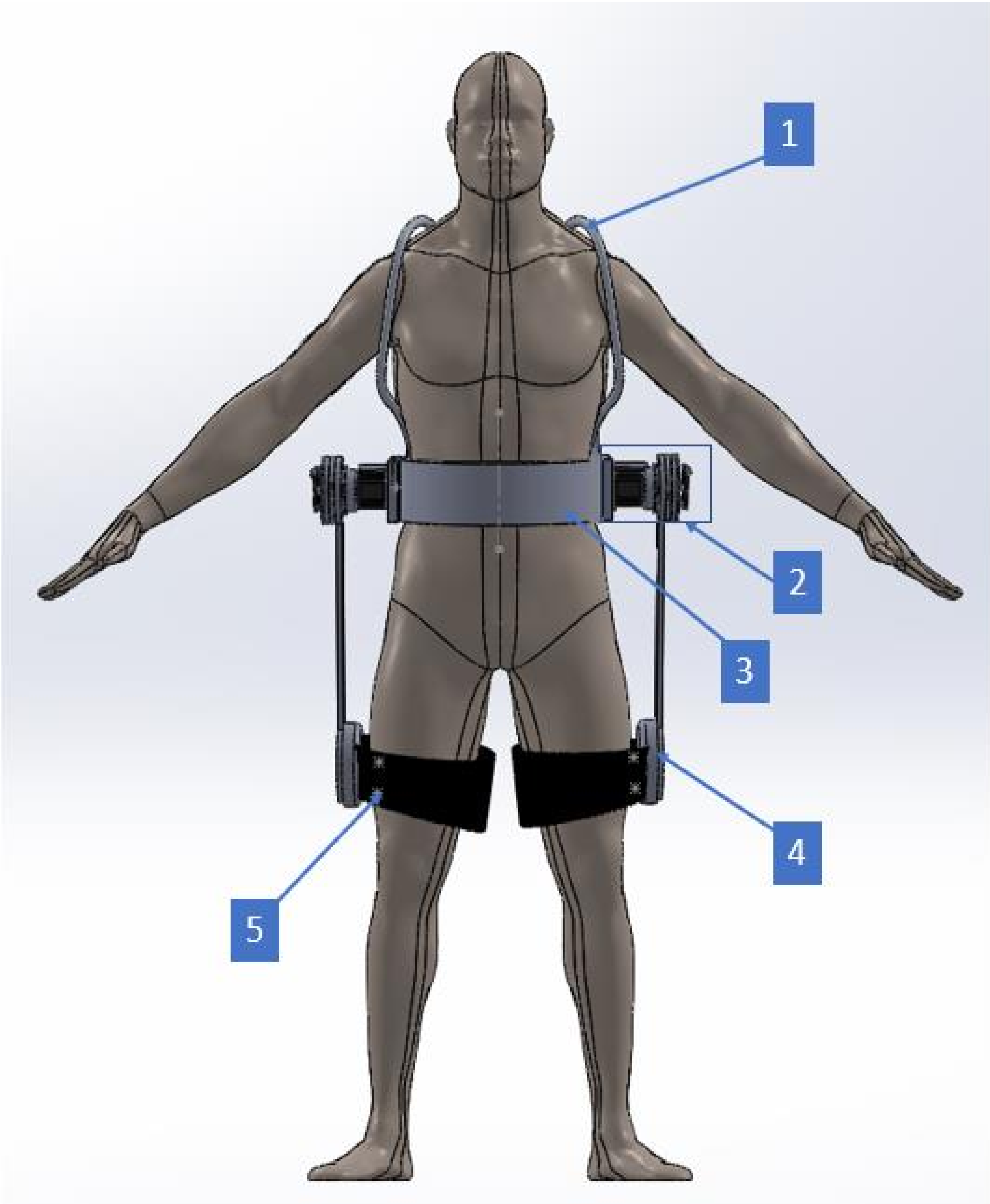

Figure 30: Frontal view of the proposed solution

Component Number	Component Name
1	Adjustable backpack straps
2	Hip joint structure
3	Waist belt
4	Leg frame
5	Adjustable leg straps

Table 3: Main exoskeleton components

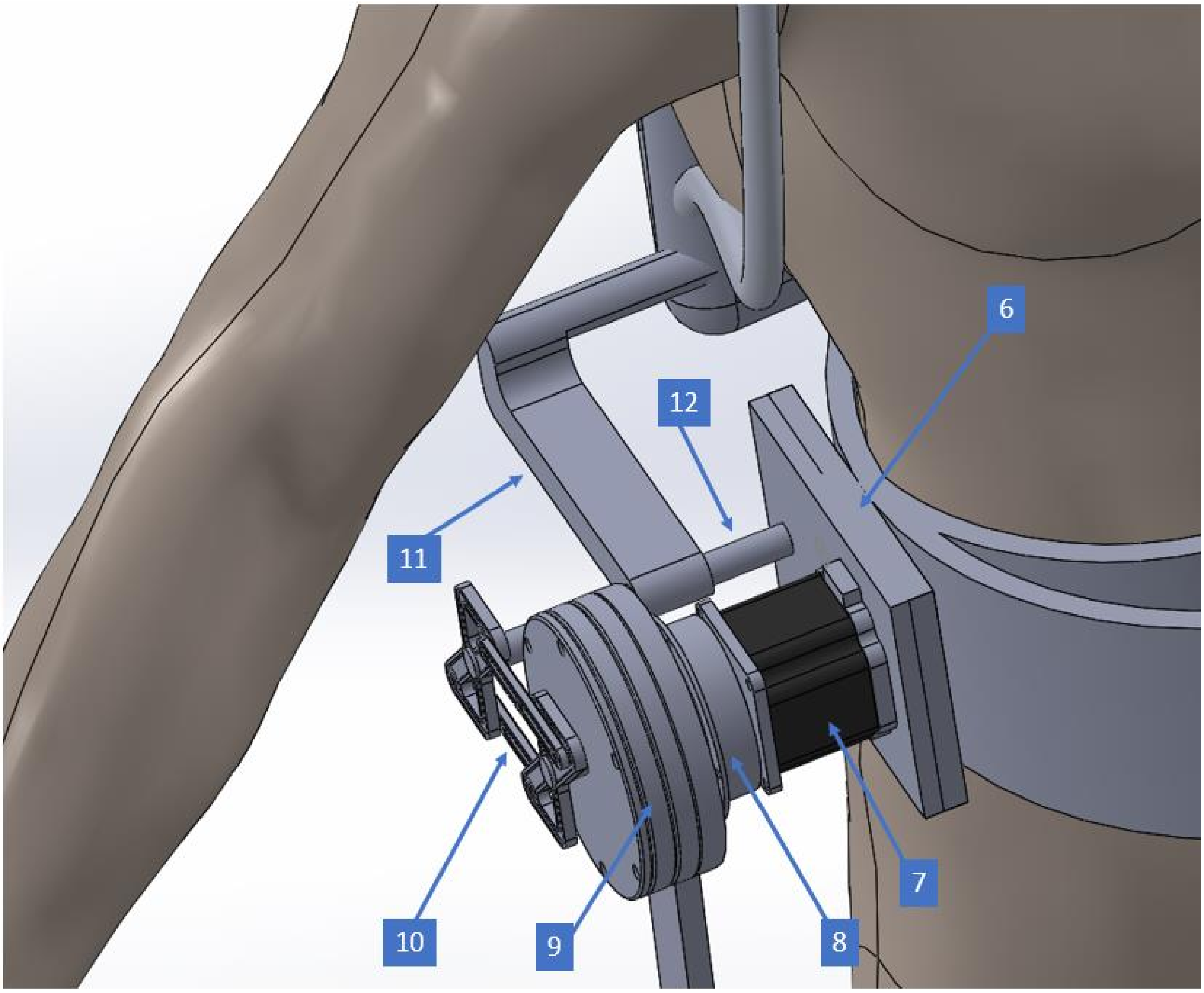

Figure 31: Upper view of the hip-joint components

Component Number	***Component Name***
6	Flange
7	Stepper motor + encoder
8	Electromagnetic single disc clutch
9	Harmonic drive
10	Four-bar linkage
11	Back frame
12	Power transmission back shaft

Table 4: Hip-joint components

3.3.1 Working principle

The working principle is quite close to the first conceptual design solution. Batteries and the electronic controller should be integrated into the backpack, to energize the entire system and to deliver the power to both the motor and the incremental optical encoder, that keeps information of the motor angle. An alternative power supply could be derived from the industrial workstations. Once the motor is energized, it transfers the requested torque to the electromagnetic clutch and consequently to the harmonic drive. In this way the leg support and the four-bar linkage, that are coupled with two different harmonic drive outputs, they can start alternatively rotating through a proper reduction ratio, in the opposite direction. More precisely, the leg support is assumed to be the fixed reference for most of the time, meanwhile, the back receives the assistive torque. Then, it is up to the backpack straps to help the bending movement of the human torso and, concurrently, to the adjustable leg straps to account for the leg rotation.

However, the encoder and the feedback elements are intended to provide "real-time" measurements to the control board, to send as output a control signal to the stepper motor, providing a real-time assistive torque.

The electromagnetic clutch could operate via an additional pushbutton, meant for a "stand-by" phase, which should be manually controlled by the user when the assistive torque is not required (free mode).

Thus, when the pushbutton is pressed the clutch disengages, meanwhile the electronic unit is still energized so that it continuously monitors the feedback information.

In this way when the pushbutton is pressed again, the clutch engages, and the right amount of energy is transferred to the device.

In the next chapter, this solution is studied into details, in order to define a detailed mechanical design of each chosen component.

3.4 Alternative solution

The second alternative solution is totally based on a new design, using different components and a different exoskeleton structure. It is based on the same hip torque calculations of our proposed solution. Following, it is shown the exoskeleton 3D model (fig.32), whose main elements are listed below (Table 5).
Then, we introduce a new concept of the hip joint housing and the details of the power transmission components.

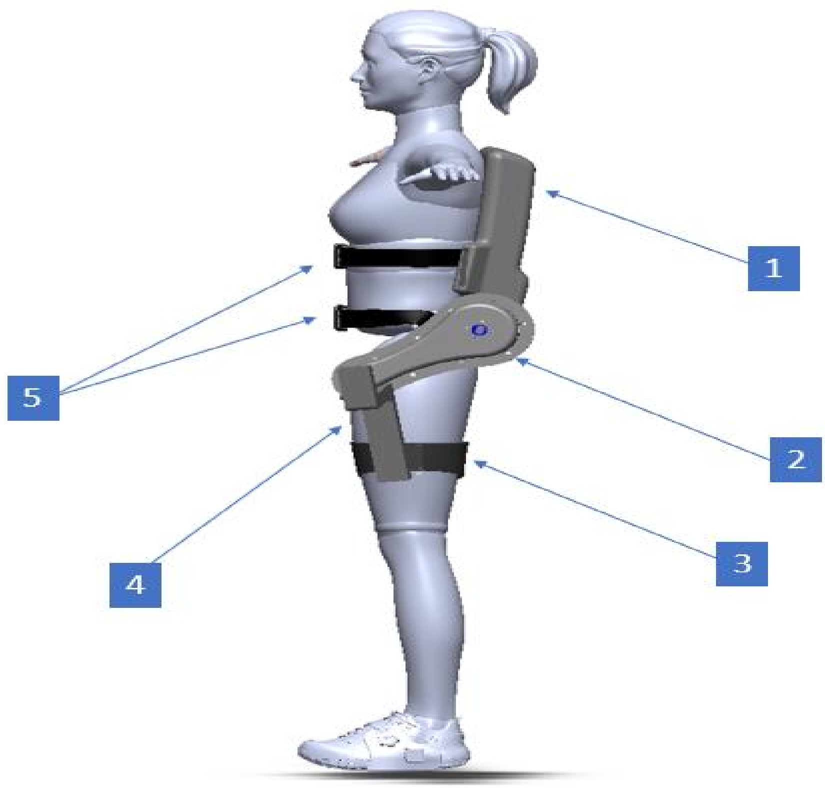

Figure 32: Alternative solution 3D model

Component Number	***Component Name***
1	Backpack containing ECU + electric circuit
2	Power transmission
3	Leg straps
4	Leg frame
5	Adjustable torso straps

Table 5: Alternative solution main components

3.4.1 The new concept of hip joint housing

This new concept is based on the connection between the hip joint lateral axis and the lumbar spine tailbone (L5), as shown in (fig.33), by forming a straight line between them defined as the hypotenuse of a right-angle triangle (red triangle) (fig.34).

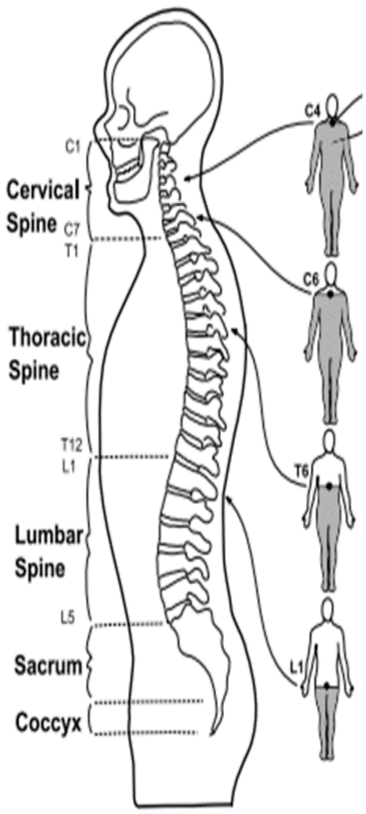

Figure 33: Spinal cord sections[13]

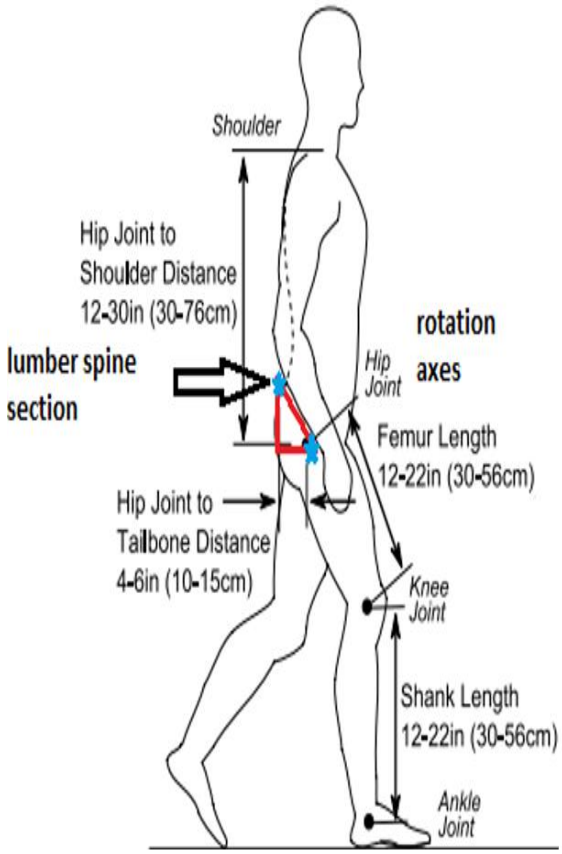

Figure 34: Concept explanitions [13]

By working on those two body points (blue stars), the structure is more fitting the human body topology, providing to it more mobility and flexibility.

Moreover, the motor is placed just above the lumbar spine tailbone (L5), supplying the right amount of requested power to hold the body trunk, which is one of the primary functions of the hip joint exoskeleton.

In this alternative solution, there is no correlation between the motion of the back and the motion of the two legs. All the motor power is supposed to hold the trunk, meanwhile, the legs are freely moving around the hip joint lateral axis.

An additional small size torsional spring could be employed to make smoother motions.

The housing of the hip joint components would be as shown in (fig.35).

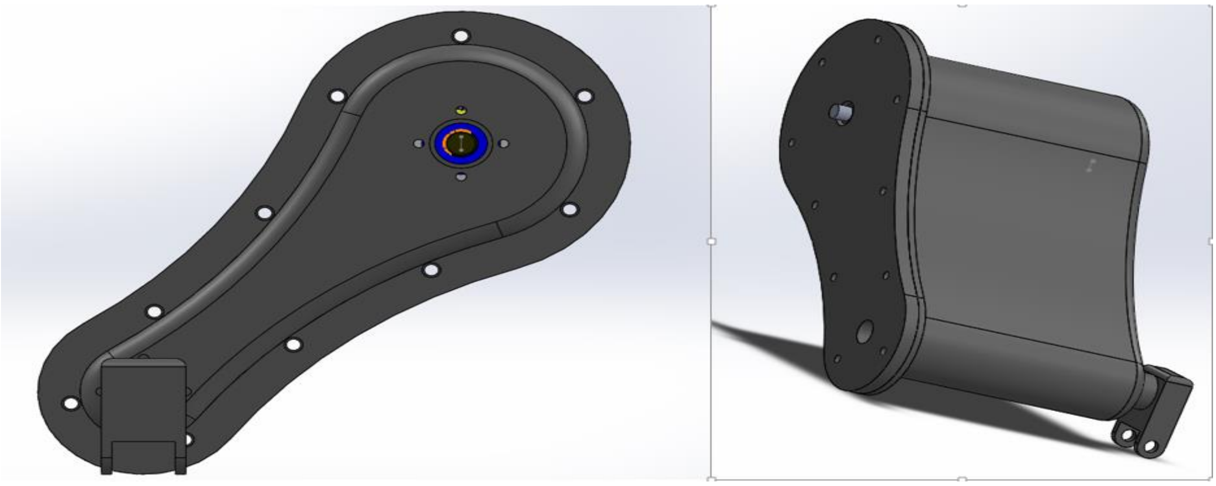

Figure 35: Hip joint housing Solidworks® configuration

3.4.2 Power transmission components

Looking inside the housing, we can identify the following power transmission components (fig.36), and whose main elements are listed below (Table 6).

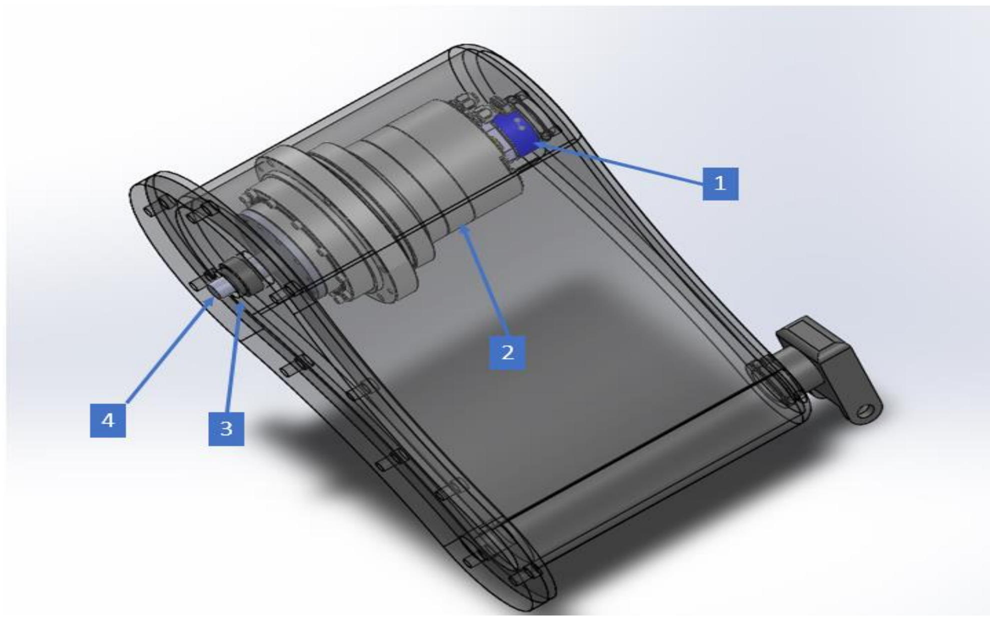

Figure 36: Power transmission Solidworks® configuration

Component Number	Component Name
1	Absolute encoder
2	Servo actuator
3	Radial spherical plain bearing
4	Power transmission shaft

Table 6:Power transmission components

3.4.2.1 Servo actuator

The “SHA-SG” rotary servo actuator is an actuator manufactured by the Harmonic Drive®. It provides high torques and highly accurate rotation operations.
Besides, it is a hollow shaft component containing a brushless servo motor, a harmonic drive, a wide variety of rotation sensors and it could come with or without motor brake (fig.37).
This servo motor could work with both AC and DC voltage currents [28-30].

The main key features are:

1- High torque.
2- Compact and slim design.
3- Light weight.
4- Large center through hole.
5- All-in-one component.

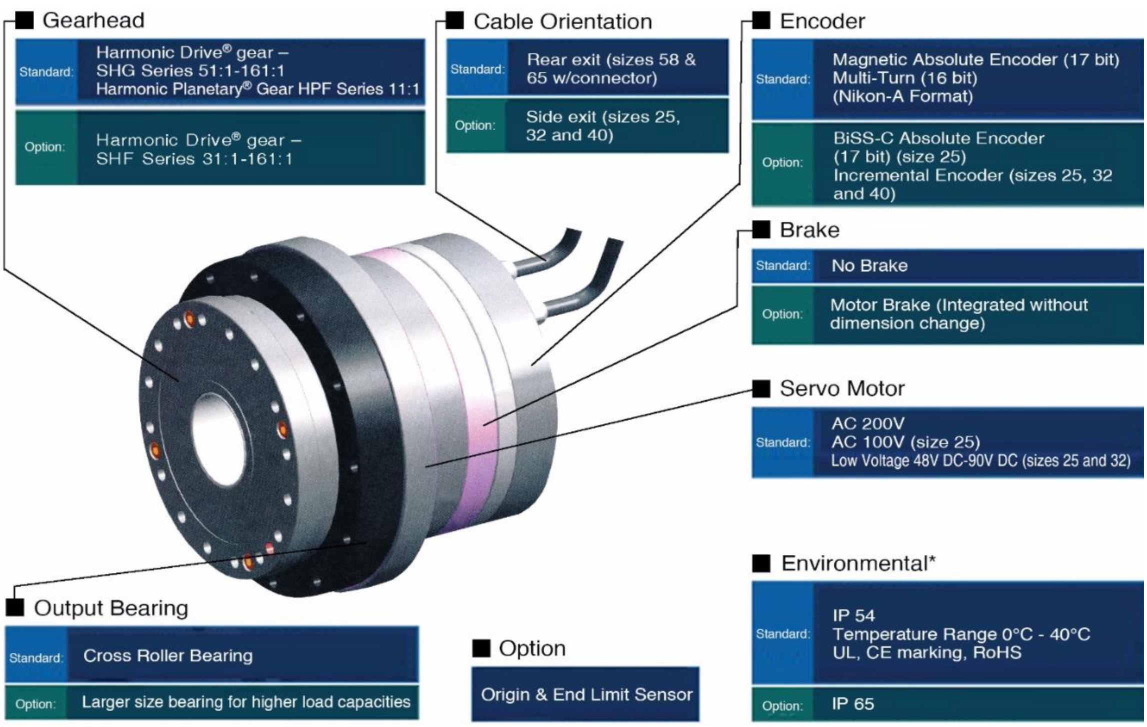

Figure 37: “SHA-SG” rotary servo actuator[28]

 In our study case, the selection of a “all-in-one” solution could save much time in defining, choosing and fitting all components with different dimensions together. The actuator is chosen with the incremental encoder and brake options, keeping in consideration that an absolute encoder is attached to the backside of the actuator.
Moreover, each component has a specific use and function that will be mentioned in the next paragraphs.

1-The servo motor

Servo motor is a self-contained device that rotate part of the machine with high efficiency and precision. The output shaft can be moved to a precise angle, position and velocity that conventional motors do not have.
 Furthermore, servo motors are commonly used in precise position control applications like:

1- Robotics.
2- Metal cutting and forming machines.
3- Antenna positioning systems.

Servo motors are a part of a closed-loop system which contain several parts, as shown in (fig.38):

1- Servo motor.
2- Position pot (encoder or resolver).
3- Microcontroller.
4- Servo control circuit.
5- Shaft.

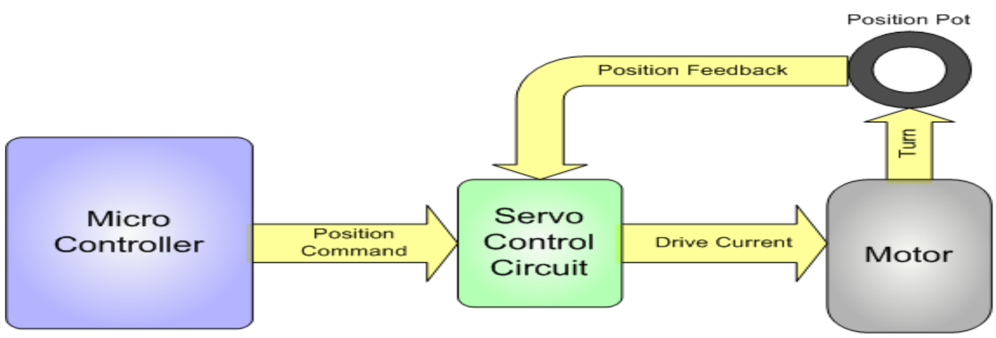

Figure 38: Servo motor closed-loop system [29]

“SHA-SG” Rotary Actuator servo motor is a brushless motor, provided in both AC and DC power supply. For our application, it is more practical to use the DC one, as it could be powered with batteries embedded into the backpack.

2-Gear Head

The gear head is merely a harmonic drive that is directly connected to the servo motor. Besides, meanwhile the input side of the power transmission shaft is coupled to the absolute encoder through a screw system, the output side of this shaft is flanged to the output of the gear head. In this way we can use the mechanical advantage given by the gear ratio, amplifying the torque of the motor.

3-Brake

The brake is used to hold the transmission shaft in place when the power is turned off. Hence, it could be useful to save power consumption when the worker is assuming a leaning forward position for an extended period. Likewise, the brake could be activated by the worker to set the exoskeleton to a fixed position, by deactivating the motor, to prevent overheating.

4-Incremental encoder

The incremental encoder is connected to the motor to provide precise position/speed information of the rotating shaft. However, the best solution is to adopt an additional absolute encoder to keep track of the position even if the shaft is turned while the encoder is off.

Finally, according to the required torque that has been evaluated in the previous chapter, which is equal to 42Nm, we have chosen the “SG” type, “SHA20A-51” model.
This model provides a gear ratio equal to 51 and a maximum working torque of 73Nm, as shown in the technical documentation.
Choosing an actuator that provides a higher torque than our application requires, it is

recommended to not run the device at 100% of its capacity.

Below are shown the specifications and the dimensions of the selected model (fig.39, fig.40).

SG type

Item		Model	SHA20A				
			51	81	101	121	161
Servo Drive				REL-230-18 HA-800□-3D/E-200			
Max. torque*1		Nm	73	96	107	113	120
		kgf•m	7.4	9.8	10.9	11.5	12.2
Allowable continuous torque*1*2		Nm	21	35	43	48	48
		kgf•m	2.1	3.6	4.4	4.9	4.9
Max. rotational speed*1		rpm	117.6	74.1	59.4	49.6	37.3
Torque constant*1		Nm/A	16.5	27	33	40	53
		kgf•m/A	1.7	2.7	3.4	4.1	5.4
Max. current*1		Arms	6.0	4.9	4.5	4.0	3.4
Allowable continuous current*1*2		Arms	2.1	2.0	2.0	1.9	1.6
EMF constant*3		V/(rpm)	1.9	3.0	3.7	4.5	5.9
Phase resistance (20℃)		Ω		1.4			
Phase inductance		mH		2.5			
Inertia moment (without brake)	GD²/4	kg•m²	0.23	0.58	0.91	1.3	2.3
	J	kgf•cm•s²	2.4	6.0	9.3	13	24
Inertia moment (with brake)	GD²/4	kg•m²	0.26	0.65	1.0	1.4	2.6
	J	kgf•cm•s²	2.6	6.6	10	15	26
Reduction ratio			51:1	81:1	101:1	121:1	161:1
Permissible moment load		Nm		187			
		kgf•m		19.1			
Moment stiffness		Nm/rad		25.2×10^4			
		kgf•m/arc min		7.5			
One-way positional accuracy		arc-sec	60	50	50	50	50
Encoder type				Absolute encoder			
Single motor revolution Encoder resolution				2^{17} (131,072)			
Motor multi revolution counter				2^{16} (65,536)			
Output resolution		Pulse/rev	6,684,672	10,616,832	13,238,272	15,859,712	21,102,592
Mass (without brake)		kg		2.0			
Mass (with brake)		kg		2.1			
Environmental conditions			Operating temperature: 0 to 40℃/Storage temperature: -20 to 60℃ Operating humidity/storage humidity: 20 to 80%RH (no condensation) Resistance to vibration: 25 m/s² (frequency: 10 to 400Hz)/Shock resistance: 300 m/s² *4 No dust, no metal powder, no corrosive gas, no inflammable gas, no oil mist To be used indoors, no direct sunlight Altitude: less than 1,000 m above sea level				
Motor insulation			Insulation resistance: 100MΩ or more (by DC500V insulation tester) Dielectric strength: AC1,500V/1 min Insulation class: A				
Mounting direction			Can be installed in any direction.				
Protection structure			Totally enclosed self-cooled type (IP54)				

The table shows typical output values of actuators.
*1: Typical characteristics when combined (driven by ideal sine wave) with our drivers.
*2: Value after temperature rise and saturation when the 320 x 320 x 16 [mm] aluminum radiation plate is installed.
*3: Value of phase induced voltage constant multiplied by 3.
*4: For testing conditions, refer to [1-12 Shock resistance] (P51) and [1-13 Vibration resistance] (P52).

Figure 39: "SHA-SG" rotary servo actuator specefication[30]

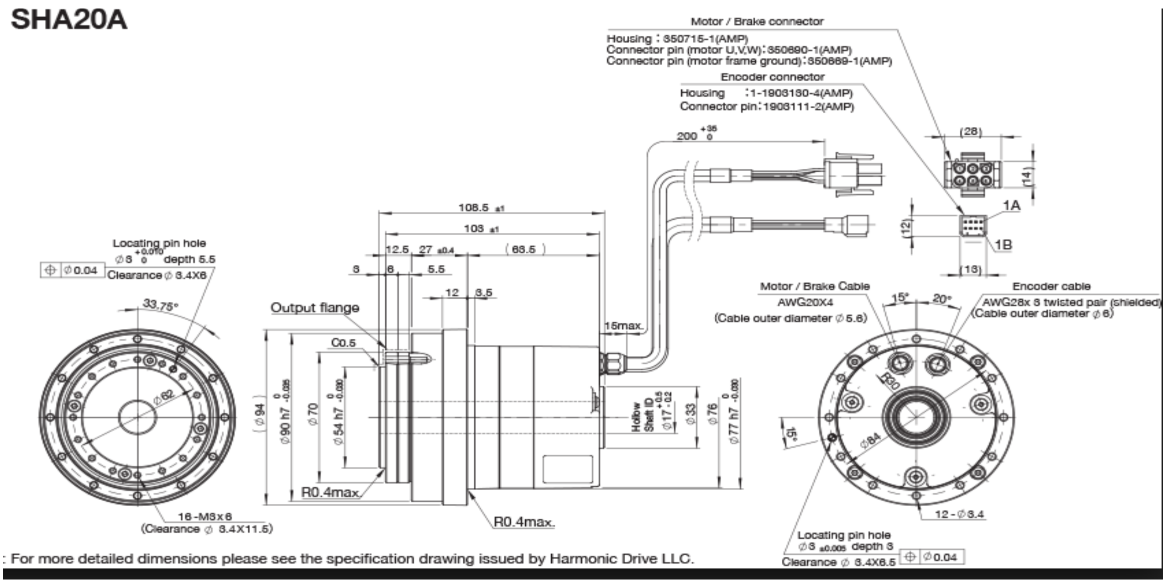

Figure 40: "SHA-SG" rotary servo actuator dinemsions[30]

3.4.2.2 Absolute encoder

Absolute rotary encoders can provide position values from the moment they are switched on. This is accomplished by scanning the position of the encoder's coded element. All positions in these systems correspond to a unique code. Even movements that occur while the system is powered off are translated into accurate position values once the encoder is powered up, that allows knowing the measure of the angle, to control the output torque of the servo actuator. The absolute encoder calculates the angle θ, which is the angle between the vertical axis Z and the trunk, as shown in (fig.41).

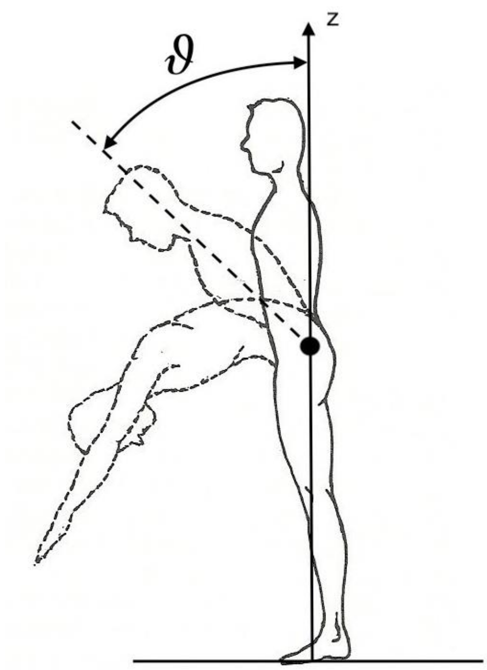

Figure 41: Angle Θ (angle between the vertical axis Z and the trunk)

After we had looked at the possible absolute encoder typologies available on the market, it was found out that Dynapar© company provides a very compact absolute encoder.
The chosen model is a single turn absolute encoder "HENGSTLER (SERIES: AD35, Spring Tether "U")" (fig.42), whose specifications are shown below (fig.4) [31].

SPECIFICATIONS

STANDARD OPERATING CHARACTERISTICS:

Code: Absolute
Resolution Single-turn: 12-22 Bit
Absolute Accuracy: ±35"
Repeatability: ±10"

ELECTRICAL:

Interface: BiSS & SSI
Input Power: DC 5 V -5 %/+10 % or DC 7 - 30 V
Current w/o load typ.: 100 mA
Permissible load: Max. 30 mA
Output Code: Gray
Drives: Clock and Data / RS422
Incremental Signals: Sine-Cosine 1 Vpp
Number of Pulses: 2048
3dB Limiting Frequency: 500 kHz
Alarm Output: Alarm bit (SSI Option), Warning bit and alarm bit (BiSS)
Frequency Response (Baud Rate):
SSI: 100kHz ... 1,5MHz
BiSS-B/ BiSS-C: 100kHz ... 10 MHz

ELECTRICAL (Cont.):

Noise Immunity: Tested to EN61326-1
Electrical Immunity: Reverse Polarity and Short Circuit Protected for the 7-30 VDC Only
Termination: Cable, PCB connector, 12 pole

MECHANICAL:

Housing Diameter: 38.1 mm
Shaft Diameter: 8mm (Hub Shaft)
Shaft Material: Stainless Steel
Shaft Load (solid-shaft): Axial ≤5 N; Radial ≤10 N
Shaft Load (hubshaft): Spring Tether Tolerance: Axial ±0.5mm; Radial ±0.05mm
Maximum Speed: max. 10,000 rpm (continuous), max. 12,000 rpm (short term)
Starting torque typ.: ≤ 1 Nm
Moment of inertia: Approx. 2.5 gcm^2
Mounting: Spring Tether (Hub Shaft)
Housing Material: Plastic
Disc Material: Glass
Weight: 80g (2.8 oz), (ST)

ENVIRONMENTAL:

Standard Operating Temperature: -15 °C ...+120 °C
Storage Temperature: -15 °C ...+85 °C
Shock (DIN EN 60068-2-27): 1,000 m/s^2 for 6 msec duration (IEC 68-2-27)
Vibration (DIN EN 60068-2-6): 100 m/s^2 (10 to 2000 Hz) (IEC 68-2-6)
Humidity: 75%, non-condensing
Enclosure Rating: (EN 60529/A1:2000-02): IP40 Housing & Shaft

CONNECTIONS

PIN	1b	2b	3b	4b	5b	6b
Function	DC 5V / 7-30V (U_p)	Clock	B -	0 V (U_n)	A -	Data
Color	White	Yellow	Gray/Pink	Brown	Brown/Green	Pink
PIN	1a	2a	3a	4a	5a	6a
Function	$\overline{\text{Data}}$	A +	0 V -Sen	B +	$\overline{\text{Clock}}$	5V Sensor
Color	Gray	White/Green	Black	Red/Blue	Green	Violet

U_p = power Supply
Sensor is connected to Power Supply and 0 V (U_n)
Shield connected to case

Analog signals (1Vpp) only available with interface SC (SSI Gray +1Vpp), BC (BiSS-B +1Vpp) and BV (BiSS-C +1Vpp)

Figure 43: Dynapar© absolute encoder specifications[31]

Figure 32: Dynapar© absolute encoder[31]

The selected encoder has the following key features:

1- Short mounting depth allows installation in tight motor end bells.
2- Up to 10,000 RPM speed capability.
3- 8mm hub shaft mount for easy installation.

Moreover, a 3D model is shown below (fig.44), and dimensional drawings in (fig.45)

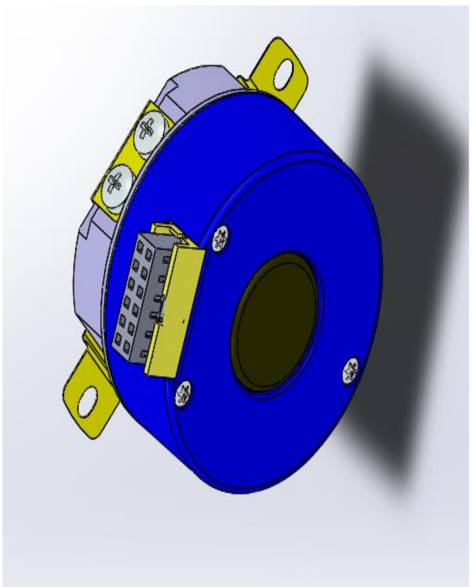

Figure 44: CAD model of the absolute encoder [32]

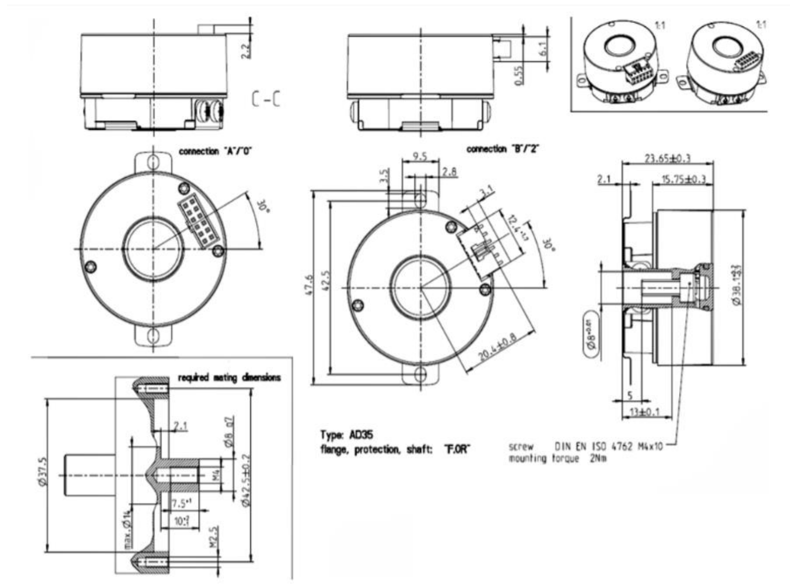

Figure 45: Absolute encoder dimensions[31]

3.4.2.3 Radial spherical plain bearing

The bearing selection for an exoskeleton-based device could be a little bit tricky due to the high flexibility of the system. Indeed, it has many DOFs, different kinds of loads in terms of distribution and amount.

For those reasons, the “maintenance-free radial spherical plain bearing” is one of the most suitable and cost-effective solutions.

Spherical plain bearings are ready-to-mount, standardized, mechanical components that enable multidirectional and self-aligning movements.

The inner ring has a sphere convex external surface, while the outer ring has correspondingly concave internal surface (fig.46). Just consider that the forces acting on the bearing may be statics or dynamics at quite low speeds [33].

Moreover, the 3D model is shown below (fig.47).

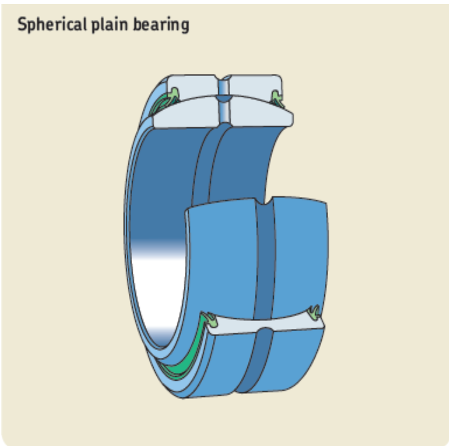

Figure 46: Spherical plain bearing[33]

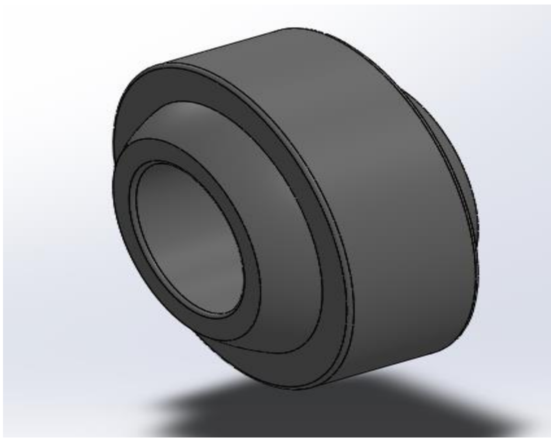

Figure 47: Spherical plain bearing CAD 3D model

Here are listed some advantages inherent to the spherical plain bearing performance:

1- Accommodate misalignment. (fig.48)
2- Virtually eliminate edge stresses and excessive stressing of adjacent components. (fig.49)
3- Accommodate deformation of surrounding components in operation. (fig.50)
4- Accommodate wide manufacturing tolerances and the use of cost-effective, welded assemblies. (fig.51)

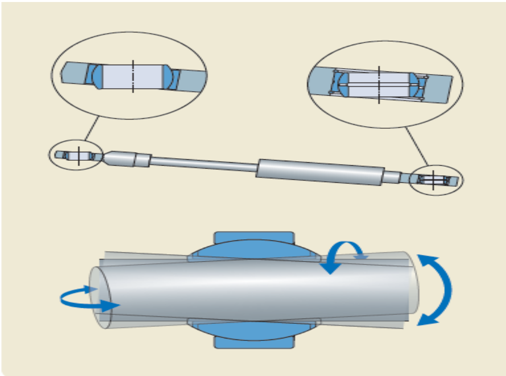

Figure 48: Spherical plain bearing misalignment accommodation [33]

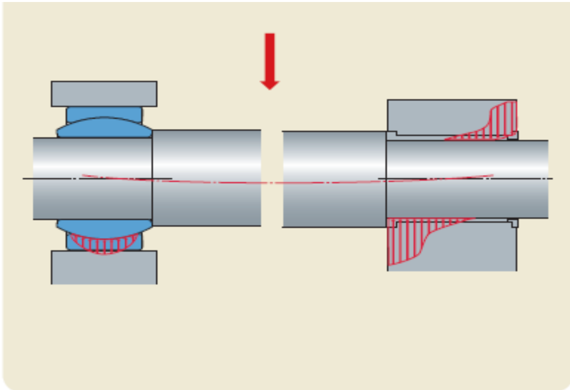

Figure 49: Spherical plain bearing tolerances accommodation [33]

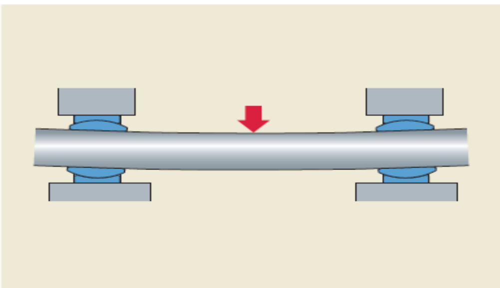

Figure 50: Spherical plain bearing shaft deflection accommodation [33]

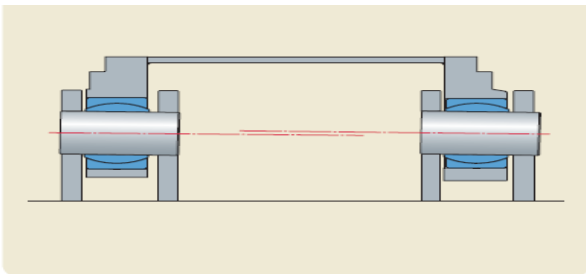

Figure 51: Spherical plain bearing edge stresses and overloading elimination [33]

3.4.2.4 Power transmission shaft

The “power transmission shaft” is referred to a component of circular cross-section that rotates and transmits power from a driving device, such as motor or engine, to a load.
In our case, it is aimed to transmit the motion to the end-user torso and it has at one side a threaded whole (fig.52) that should be fixed to the absolute encoder grub screw.
The shaft was designed to be able to pass through all the hollow body of the servo actuator (fig.53) and it has a variable section since it must fit all the different components diameter (DC motor, harmonic drive, bearing). The disadvantage of this solution could be that we should expect consistent losses with the long single shaft.

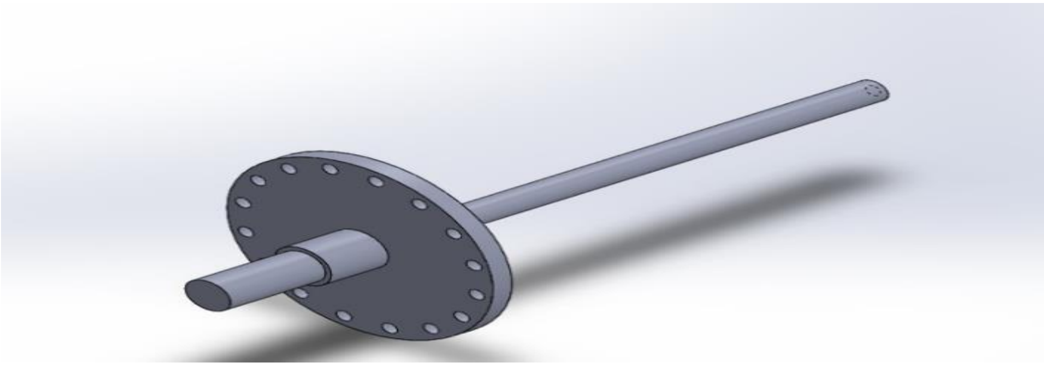

Figure 52: Power transmission shaft CAD 3D model

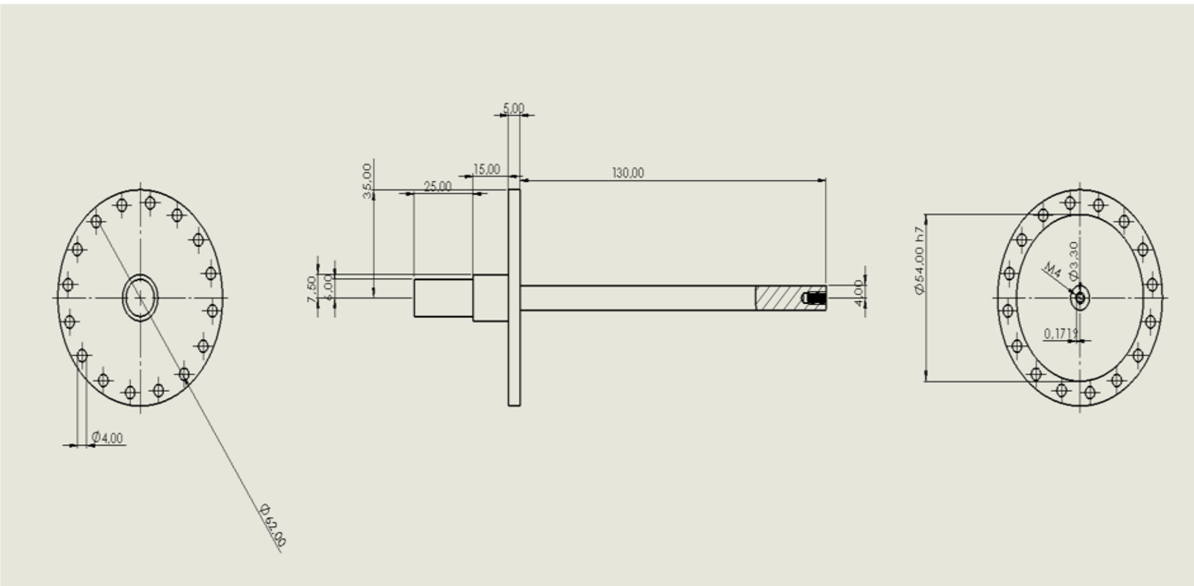

Figure 53: Power transmission shaft dimensional drawings

Chapter 4

Detailed mechanical design

4.1 Permanent magnets stepper motor

The previous DC motor was replaced by a stepper motor as result of the balancing of several design factors. Nowadays they are widely used in robotic projects, since it's not required a continuous rotation for long period at high speed but to result more suitable for precise back-and-forth motions, where accuracy and repeatability of motor operations are fundamental parameters [34].

One of the many stepper motor benefit is what we call the "holding torque", which means the motor can hold the load in place when the rotor is not rotating, that will be useful for us, in the stooping mode.

In addition, despite the stepper motors have lower efficiency than the DC ones, they result more stable and safer against failure, considering that if a mechanical overload happens or anything brakes, the motor stops. This type of motor can drive a wide range of frictional and inertial loads and they can reach maximum torque at start up and low speeds.

This characteristic makes the stepper motor the most suitable for our application, since torque in a low speed range can be up to five times higher than a generic servomotor or a brushless one.

Stepper motors cannot accelerate loads very rapidly and the motor can get very hot in high performance configurations. To minimize the heat radiated from the motor, we chose the one that has the smallest rated current (1A) and a relatively small resistance (6.7 Ohm). In this way, we can reduce copper and iron losses.

It follows that our Joule losses for each phase are:

$$P_j = R * I^2 = 6.7 * 1 = 6.7\ W \tag{9}$$

Where:

P_j are the Joule losses

R is the stepper motor internal resistance

I is the stepper motor rated current

To best fit our study case, we pick out the PM (Permanent Magnets) type as it is several times less expensive than the variable-reluctance and the hybrid ones [35].

The working principle is quite simple since the stator is made of four magnetic poles that are surrounded by a winding in which the current flows [36]. Since our choice consists of a unipolar stepper motor, the excitation is made by sending current through a winding at a time, so that the shaft will rotate of one step each excitation (*fig.54*).

Moreover, we selected the unipolar one as it is simple to control.

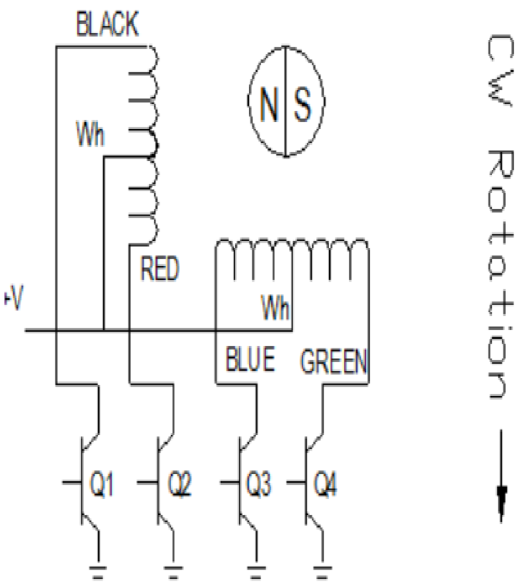

Unipolar Step	Q1	Q2	Q3	Q4
1	ON	OFF	ON	OFF
2	OFF	ON	ON	OFF
3	OFF	ON	OFF	ON
4	ON	OFF	OFF	ON
1	ON	OFF	ON	OFF

Figure 54: Wiring diagram and step sequence of a unipolar stepper motor [37]

The chosen electric motor is the SANMOTION© 2H425U10 (2-phase, unipolar, 42mm), since the Torque/Speed characteristic (*fig.55)* demonstrates that the motor can supply the desired input T_{in} and ω_{in} , as it is shown in the harmonic drive model selection (subparagraph 4.3.3).

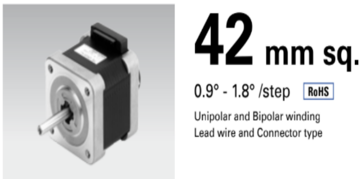

Based motor	Holding torque at 2-phase energization [N.m min.]	Step angle °	Winding type	Rated current A/phase	Wiring resistance Ω /phase	Winding inductance mH/phase	Rotor Inertia [x 10⁻⁴ kg.m²]	Weight kg	Optional motor cable
2P4233B10	0.23	0.9	Bipolar	1	3.3	8.0	0.044	0.24	-
2H4233B05	0.26	1.8	Bipolar	0.48	14	27	0.036	0.23	4835728-1
2H4238B17	0.39	1.8	Bipolar	1.7	1.3	3.4	0.056	0.29	4835728-1
2H4241B05	0.42	1.8	Bipolar	0.5	18	42	0.062	0.31	4835728-1
2H4241U12	0.32	1.8	Unipolar	1.2	3	3.9	0.062	0.31	4835710-1
2H4248U12	0.37	1.8	Unipolar	1.2	3.3	3.4	0.074	0.37	4835710-1

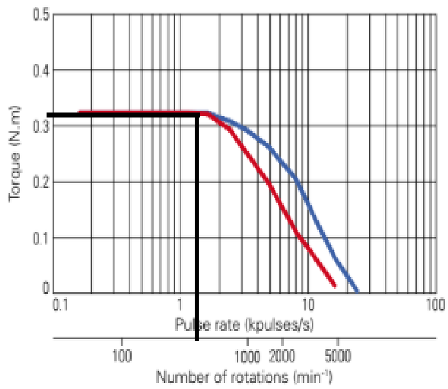

Figure 55: Motor electromechanical datasheet; Torque/speed characteristic [38]

Another parameter to determine is the number of steps our motor requires to perform one full revolution:

$$\frac{\frac{360\ Degree}{1\ Revolution}}{1.8\frac{Degree}{Step}} = 200\frac{Steps\ (Counts)}{Revolution} \tag{10}$$

This value is necessary to select the proper optical incremental encoder (*fig. 56*), that the SANMOTION© Company provides as additional feature for a precise position control, useful to measure the rotation angle (position) of the motor's shaft.

Encoder type	Counts Per Revolution [CPR] 200	400	1000	1024	Pulse index option	Single ended	Differential line driver	Key points
R type	■					■		Compact size Simple interface Cost effective
S type		■			■	■		Medium resolution Pulse index option Simple interface
M type			■	■	■	■		High resolution Pulse index option Simple interface
L type		■					■	Noise immunity Transmitting encoder signal over a long distance

Figure 56: R-type Encoder for 200 step/revolution (Counts per Revolution)[38]

An optical incremental encoder is an electrical device consisting of a rotating disk, mounted around the stepper motor shaft, that has a pattern of alternated opaque and transparent sectors, called code tracks.

The working principle is quite simple. Indeed, as the disk rotates, a light source will send a signal to a light sensor, so that it generates a pulse signal. To monitor the number of pulses and the direction of rotation, our encoder uses two code tracks (A and B) that are associated to two output channels shifted of 90° in phase (*fig. 9*). The relative phase among them gives us the direction of shaft rotation, thus if A is in advance with respect B, rotation happens in clockwise direction and, the other way round.

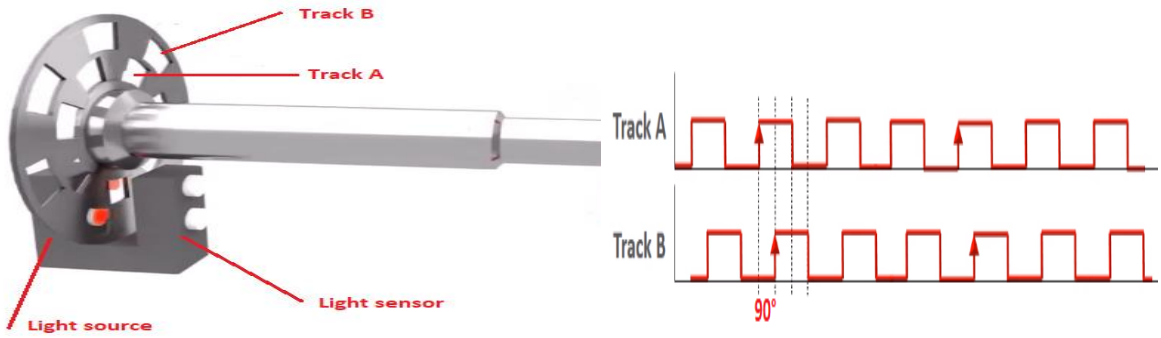

Figure 57: Encoder working principle [39]

In total, our encoder has five pins, and each is connected to a small wire *(Fig.58)*.

Encoder pin-outs

Pins	R220 35, 42mm sq.	R220 56, 86mm sq.
Pin 1	Channel B	GND
Pin 2	5 VDC	NC
Pin 3	Channel A	Channel A
Pin 4	NC	5 VDC
Pin 5	GND	Channel B

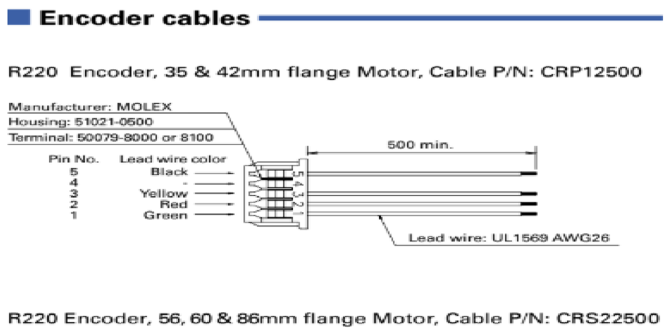

Figure 58: R-type encoder pin-outs and wire connections [38]

Pin 1 is the ground (GND), pin 2 with no connection (NC), pin 3 for track A reading (Channel A), pin 4 is the supply voltage (5V) and pin 5 for track B reading (Channel B). Those 5 pins will be connected to the microcontroller that will be mounted on the back support. This will lead to the use of cable extensions, since jumper cables are not very suitable to span large distances and are also not very robust connections. This step will require some soldering phases.

Note: The main component of the exoskeleton electronics is the microcontroller. Microcontrollers are essentially miniature computers that have all components in the single board. They contain additional interfaces to directly connect to other devices (e.g. analog-to-digital converters and many communication buses).

The microcontroller used for our application is the one in Arduino Uno, whose features are reported in the following table (Table 7):

Microcontroller	ATmega328
Operating Voltage	5 V
Input Voltage (Recommended)	7-12 V
Input Voltage (Limits)	6-20 V
Digital I/0 Pins	14 (6 for PWM output)
DC Current for I/O Pin	40 mA
DC Current for 3.3V	50 mA
Flash Memory	32 KB of which 0.5 KB for BootLoader
SRAM	2 KB
EEPROM	1 KB
Clock Speed	16 MHz

Table7: Features of the Arduino UNO [40]

In the next paragraph, we show how to program the Arduino to read as digital input the pulse signals from the incremental encoder and, in turn, it sends them, through the digital output ports, to the stepper motor driver, that is responsible for converting them into motor motion (*fig. 11*).

Our motor driver is the model SANMOTION© US1D200P [38], that is specific for the selected motor.
The Arduino board can operate on an external supply in the recommended range from 7V to 12V, since it must supply 5V as output. For this purpose, we can find different compatible solutions available on the market.
In addition, as the incremental encoder supply requires a battery of 5V, we use the power outlet of the Arduino board to energize it, while for the motor we require an external power supply, given by a battery of 24V.

To make things clearer, we draw a simple connection scheme, depicted below (fig.59):

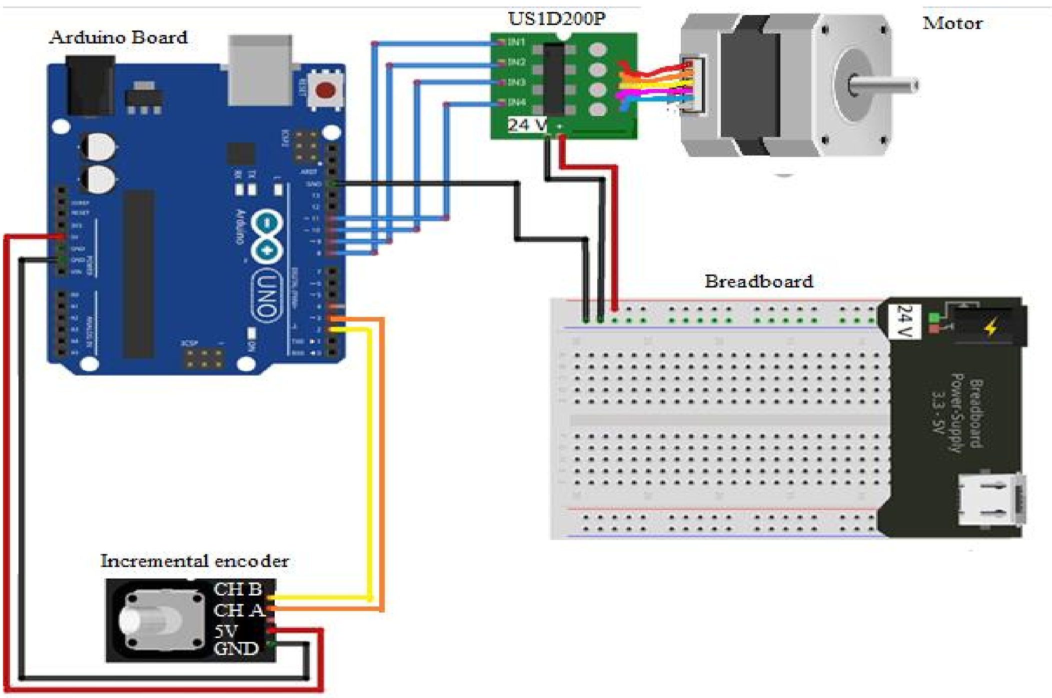

Figure 59: The schematics of how to connect the encoder to the microcontroller. This will enable us to read the motor angle (yellow and orange wires) through two of the Arduino's digital inputs and process them to control the motor angle through 4 of the Arduino's digital outputs.

Note: On the market is also available the "micro stepper motor" technology, that provides miniature components, that are optimal for positioning application. They can reach a very small longitudinal length, but they lose in the encoder resolution, since they provide a minimum step angle of 18 degrees, that is not efficient enough for our application.

4.1.1 Reading the motor angle

Now, we write our first Arduino program, usually called a ‘sketch’, where we implement the first functionality of our exoskeleton that will be compiled and loaded onto the microcontroller.
The program has been written considering the Arduino rotary encoder library[41] available online.
It reads the position of the motor from the encoder digital channels A and B.
It consists in reading the digital signals received by the two code tracks, and when the serial communication is started, they are compared so that each pulse updates the variable associated to the motor steps.
At the same time, depending on the order of low-to-high switch of the two tracks, we can keep track of the direction of rotation of the motor.
This code will be of special interest, for a possible future work of control algorithm implementation.
The full sketch is attached in the annexes of the thesis (Annex 1).

4.2 Electromagnetic single disc clutch

A dry electromagnetically actuated clutch is needed to disengage the input (stepper motor) and the output (harmonic drive), when the end-user is wearing the exoskeleton, but the assistive torque is not required, as it occurs in the "free mode".

The single disc friction surface is responsible for the torque transmission that happens when there is current running through the field coil. Indeed, the electric actuation convert the coil into an electromagnet that generates magnetic lines of flux.

The flux is therefore transferred to the rotor that becomes magnetized and it attracts the armature. This leads to a fully engaged clutch and a 100% rotary motion transfer because there is no relative slippage between the field coil and the magnetized rotor (fast response time).

When the coil is no more energized, it is up to the compression spring to create a small gap between the field coil and the rotor so that the clutch disengages.

The electromagnetic clutches provide high torque capacity in the smallest package size, without chattering noise.

To make things clearer a CAD model of a multi plates clutch is reported below (fig.60).

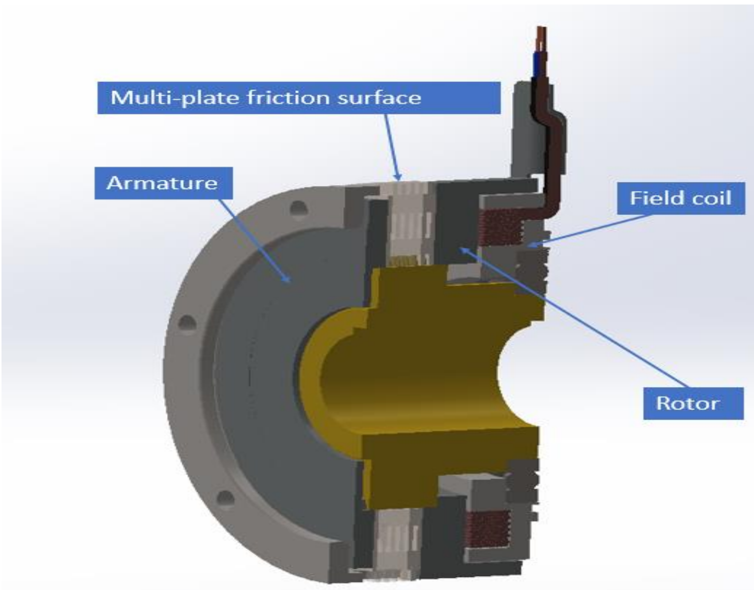

Figure 60: Multi plate electromagnetic clutch CAD model [42]

The chosen clutch is the Warner Electric© "SMF VAR 00-10" model [43], that can provide a maximum torque equal to 7Nm, that is several times higher than the one actually transferred by the motor (fig.61).

A Solidworks® model that respect the main dimensions has been implemented (fig.62), based on the company datasheet.

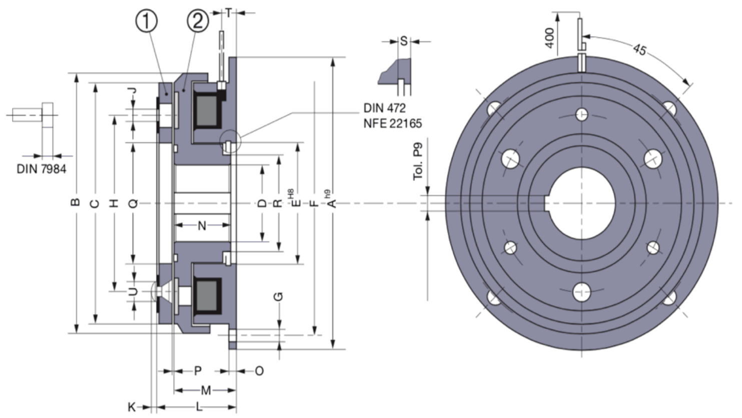

Sizes			**10**
Nom. Torque		[Nm]	7
Max. Speed		$[min^{-1}]$	8000
Power	P20[U=12/24/103,5V]	[W]	12,5
	A		80
	B		68
	C		63
	D min		10H8
	D Std		10/15/17
	D max		17H8
	E		35
	F		72
	G For screw		4xM4
	H		46
	J (1) For screw		3xM3

	K		1,5
	L		28
	M		24
	N		22
	O		2
	P		0,2
	Q		35
	R		23
	S		3,5
	T		5,6
	U		6
Inertia	❶	$[kgm^2]$	0,00004
Inertia	❷	$[kgm^2]$	0,00011
Weight		[kg]	0,5
Connection			**Leads**

Figure 61: Chosen clutch specifications and dimensions [43]

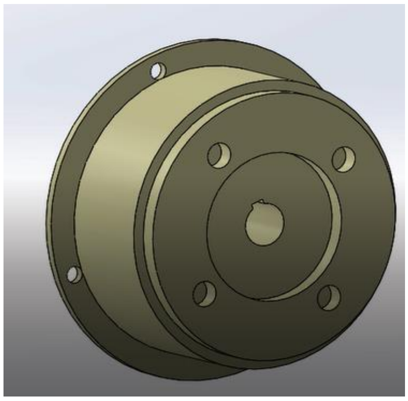

Figure 62: Clutch 3D model

4.3 Harmonic drive

C.W.Musser introduced the basic concept of the strain wave gearing since 1957, and it was first used successfully in 1960 [44], and from that moment the harmonic drives found widespread use and acceptance among mechanical designers due to the very high reduction ratios in a tiny package with a wide range of advantages like:

1- Excellent positional accuracy and repeatability.
2- Single-stage very high reduction ratio.
3- High torque capacity.
4- Zero backlashes.
5- In-line configuration.
6- Very high efficiency.
7- Back driving.
8- Lightweight.

For all these reasons the Harmonic drive is an excellent choice to be used in powered exoskeletons for providing more compact design according to size and weight limitations, giving very high reduction ratios which allow using a smaller motor, reducing both size and weight of the exoskeleton, providing higher efficiency and repeatability.

4.3.1 Operating principle

Each harmonic drive is composed of three main components illustrated in fig(63), the wave generator, the flex spline, and the circular spline. The wave generator consisting of a ball bearing assembly with a rigid elliptical inner-race and a flexible outer thin-walled race. The flex spline looks like a shallow cup with small external gear teeth around its edge. When the wave generator is assembled with the flex spline it causes the flexible gears-tooth circumference of the flex spline to adopt the elliptical profile of the wave generator.

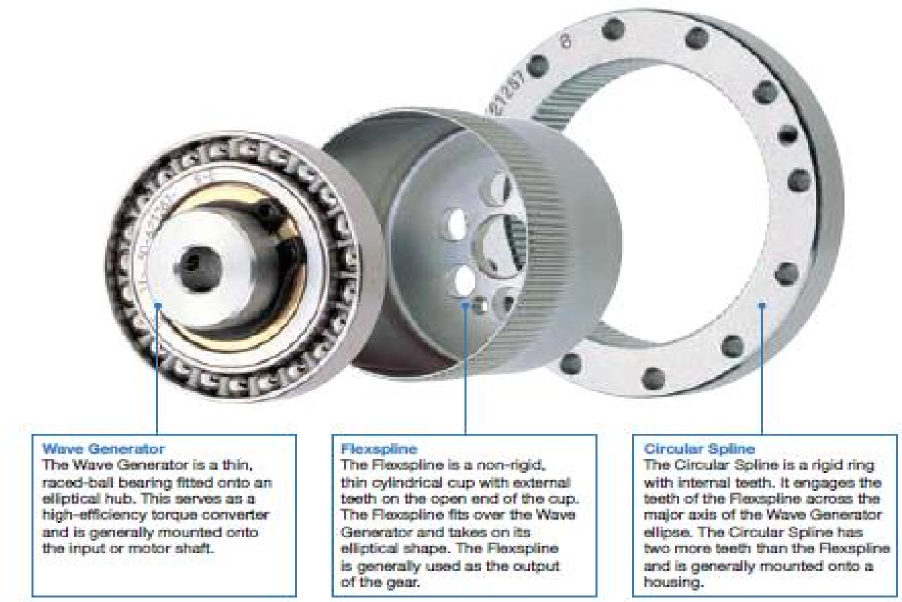

Figure 63: Harmonic drive components [45]

The circular spline is a rigid annular ring with internal teeth machined along a slightly larger pitch diameter than those of the flex spline on the inside. The flex spline and wave generator are placed inside the circular spline of the harmonic drive, meshing the teeth of the flex spline and the circular spline. The flex spline is deformed into an elliptical shape, and its teeth mesh with the teeth of the circular spline in two contact points on opposite sides of the flex spline.

When the three components assembled, they can rotate in different velocities on the same axis, starting by the rotation of the wave-generator which is the rotation input which carries the zone of the gear tooth engagement with its primary shaft. When this zone propagated 180 degrees around the circumference of the circular spline the flex spline, which usually contains two fewer teeth than the circular spline, which will lag by one tooth relative to the circular spline as a result of this gradual and continuous engagement of slightly offset gear teeth, each rotation of the wave generator moves the flex spline two teeth back on the circular spline as shown in (fig.64), and through this mechanism gear ratios up to 320:1 could be achieved and the gearing reduction ratio could be calculated according to the following formula [45] :

$$Reduction\ Ratio = \frac{n^{\circ}\ of\ flex\ spline\ teeth - n^{\circ}\ of\ circular\ spline\ teeth}{n^{\circ}\ of\ flex\ spline\ teeth} \tag{11}$$

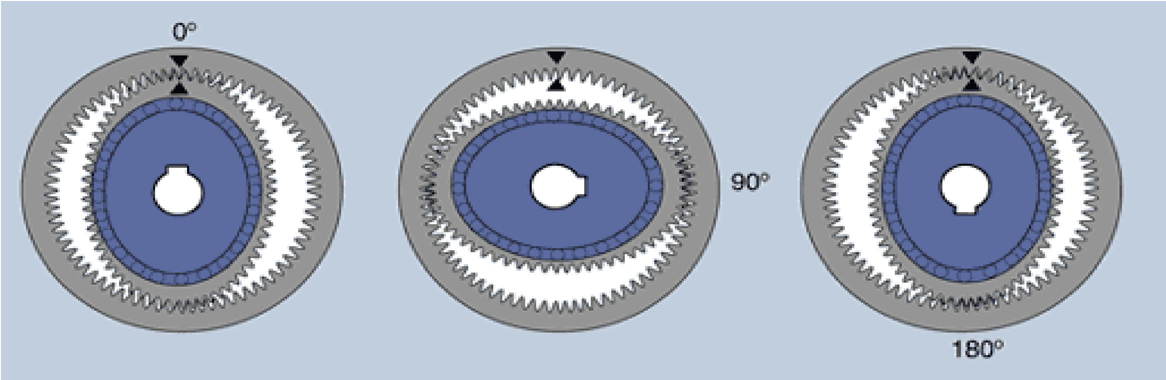

Figure 64: Flexs pline – Circular spline teeth mesh [46]

4.3.2 FB series component type

FB Series is also referred to “pancake style." It consists of four parts and it operates using the same principle as the traditional harmonic drives. The flex spline is shaped like the flex spline of the cup type harmonic drives with a cut cup bottom and it is structured to have an additional circular spline with the same number of teeth as the flex spline [47].
Moreover, it has these features:

1- The flat and thin shape.
2- Compact and simple design.
3- Low axial width.

The structure of the FB series component type has been modeled in Solidworks®, as shown in the figure below (fig.65).

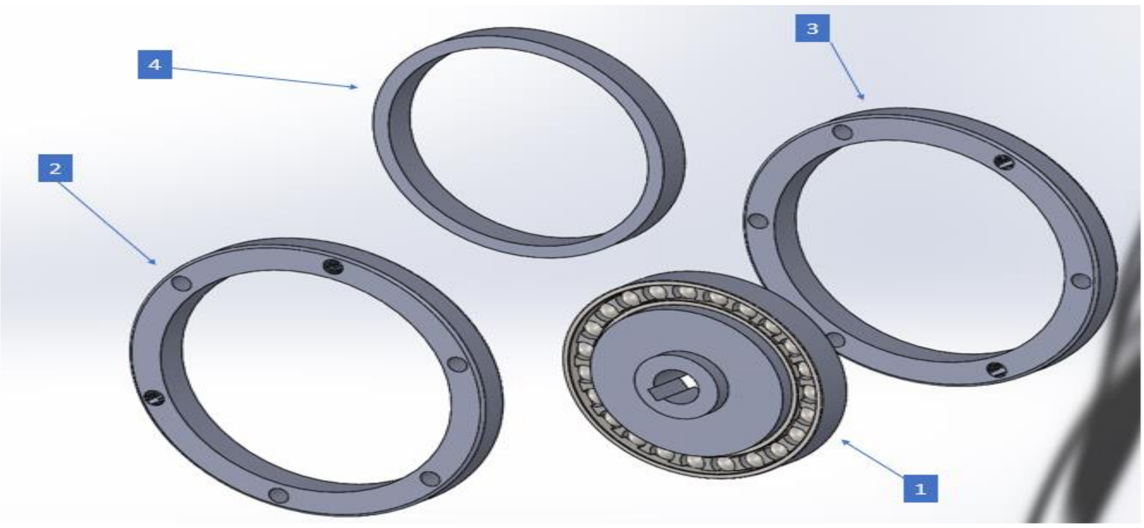

Figure 65: Solidworks® model of the FB series component type

Item Number	*Item Name*
1	Wave generetor (WG)
2	Circular spline S (CSS)
3	Circular spline D (CSD)
4	Flexspline (FS)

Table 8: List of model items

It turned out that using the Harmonic Drive® FB series component is an appropriate choice for our design, due to its features that fit for a perfectly compact design.

4.3.3 Model selection

To select the proper harmonic drive model, we must guarantee that both the input and output torque/speed are associated to the right gear ratio.

From the stepper motor torque/speed characteristic, shown in the fourth chapter, we can derive the input parameters:

$$T_{in} \cong 0.32\ Nm\ ;\ \omega_{in} \cong 600\ RPM \tag{12}$$

Instead, from the hip torque calculation made in the second chapter, we can extract the output parameters:

$$T_{out} = 42\ Nm\ ;\ \omega_{out} = 5\ RPM \tag{13}$$

Now it is possible to find the right torque/speed reduction ratio as follow:

$$R = \frac{T_{out}}{T_{in}} = \frac{42}{0.32} = 131.15 \tag{14}$$

$$R = \frac{\omega_{in}}{\omega_{out}} = \frac{600}{5} = 120 \tag{15}$$

By following the above parameters and after having consulted the Harmonic Drive® FB series catalogue [48], we found out that the "FB-32-131-2-GR" is the most appropriate model.

Indeed, it provides a reduction ratio equal to 131 and a rated torque of 82 Nm, corresponding to the allowable continuous torque load at 2000rpm rated speed (fig.66).

Moreover, even if unexpected impact torque may occur, the maximum average load torque is high enough to consider the system safe.

Size	Ratio	Rated torque at 2000rpm		Repeated Peak Torque		Max. Average Load Torque		Max. Momentary Torque		Rated input rotational speed	Max. Input Speed (rpm)		Limit for Average Input Speed (rpm)		Moment of Inertia	
		Nm	kgfm	Nm	kgfm	Nm	kgfm	Nm	kgfm	rpm	Oil lubricant	Grease lubricant	Oil lubricant	Grease lubricant	I $\times 10^{-4}$ kgm²	J $\times 10^{-4}$ kgfms²
14	50	2.6	0.27	3.2	0.33	3.2	0.33	6.9	0.7	2000	6000	3600	4000	2500	0.033	0.034
	88	4.9	0.5	7.8	0.8	7.8	0.8	15.7	1.6*							
	100	5.9	0.6	9.8	1.0	9.8	1.0	15.7	1.6*							
	110	5.9	0.6	9.8	1.0	9.8	1.0	15.7	1.6*							
20	50	14	1.4	18	1.8	18	1.8	34	3.5	2000	6000	3600	3600	2500	0.135	0.138
	80	17	1.7	21	2.1	21	2.1	35	3.6							
	100	22	2.2	26	2.7	25	2.5	47	4.8							
	128	24	2.4	33	3.4	25	2.5	58	5.9							
	160	24	2.4	38	3.9	25	2.5	59	6.0*							
25	50	23	2.3	30	3.1	30	3.1	54	5.5	2000	5000	3600	3000	2500	0.36	0.37
	80	31	3.2	39	4.0	39	4.0	70	7.1							
	100	39	4.0	52	5.3	52	5.3	91	9.3							
	120	39	4.0	61	6.2	61	6.2	94	9.6*							
	160	39	4.0	76	7.8	61	6.2	86	8.8*							
32	50	44	4.5	60	6.1	60	6.1	108	11	2000	4500	3600	2500	2300	1.29	1.32
	78	63	6.4	75	7.7	75	7.7	127	13							
	100	82	8.4	98	10	98	10	176	18							
	131	82	8.4	137	14	118	12	235	24*							
	157	82	8.4	157	16	118	12	235	24*							
40	50	88	9	118	12	118	12	216	22	2000	4000	3300	2000	2000	3.38	3.45
	80	118	12	147	15	147	15	265	27							
	100	157	16	186	19	186	19	343	35							
	128	167	17	235	24	235	24	372	38*							
	160	167	17	284	29	274	28	353	38*							
50	80	216	22	265	27	265	27	480	49	1700	3500	3000	1700	1700	9.9	10
	100	284	29	253	36	353	36	627	64							
	120	304	31	421	43	421	43	706	72*							
	160	304	31	510	52	490	50	666	68*							

* Torque value limited by ratcheting.

(Note)

1. Moment of inertia: $I=\frac{1}{4}GD^2$
2. See "Engineering data" on Page 012 for details of the terms.

Figure 66: Harmonic drive rating table [48]

Once selected the size 32, we draw a 3D model (fig.68) based on the outline dimensions (fig.67).

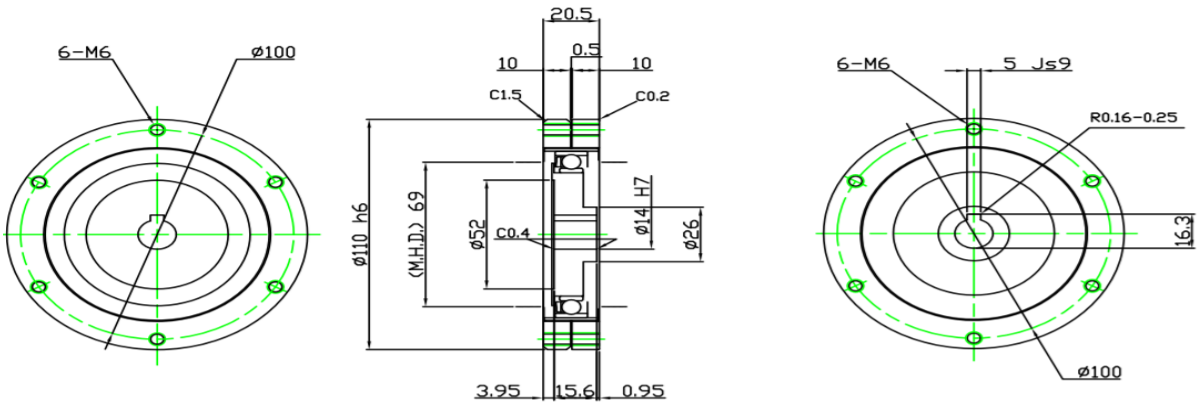

Figure 67: HD outline dimensions [48]

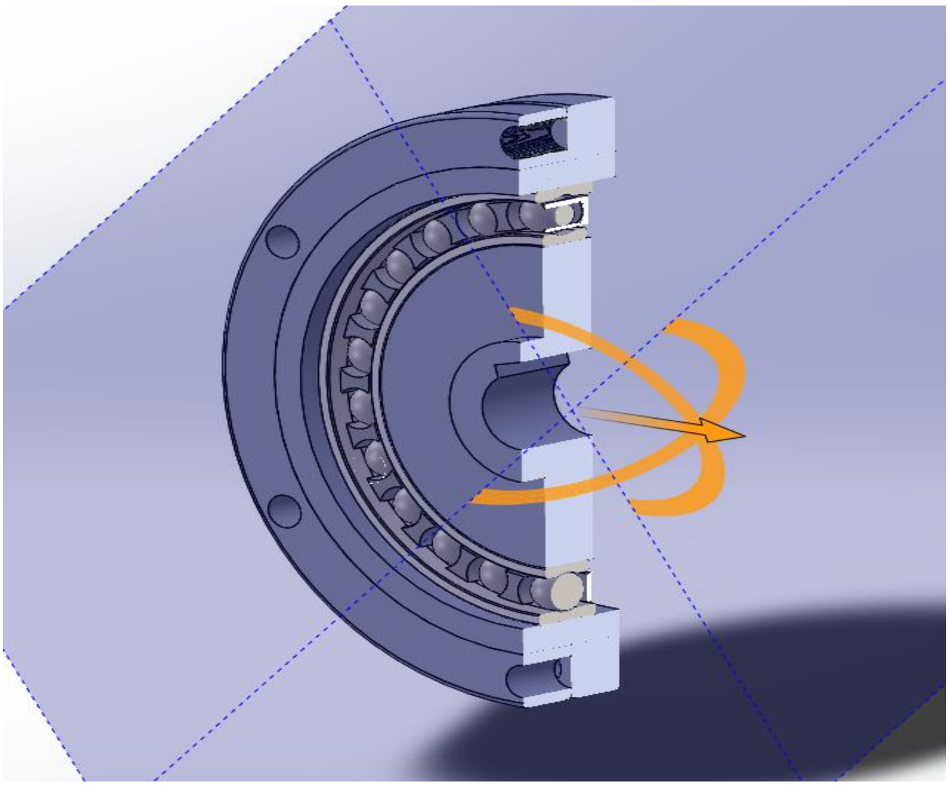

Figure 68: Solidworks® model of the selected harmonic drive (Section view)

4.3.4 Components connections

In our system we use the wave generator as the HD input component, which is taking its motion from the stepper motor through an interconnected clutch.

At the same time, both circular splines S and D are working as output elements.

The circular spline S is transferring the motion, through a flanged shaft (fig.70), to one of the two four-bar linkage crank that can rotate around its axis. Meanwhile, the latter will ideally transmit all the torque to the second crank, through the two horizontal rods, which is in turn linked to the back-side shaft. This shaft is then fixed to the back frame so that the torque is delivered to the user trunk, through the backpack straps.

The circular spline D, instead, it is connected to the leg frame (fig. 69), through threaded fasteners.

It's quite important to underline that both the leg frame and the flanged shaft should be manufactured to match the threaded holes of the two circular splines, so that we can have a restricted number of items, thereby facilitating the mounting and handling processes.

They have been modeled on SolidWorks respecting those functional requirements, as reported below.

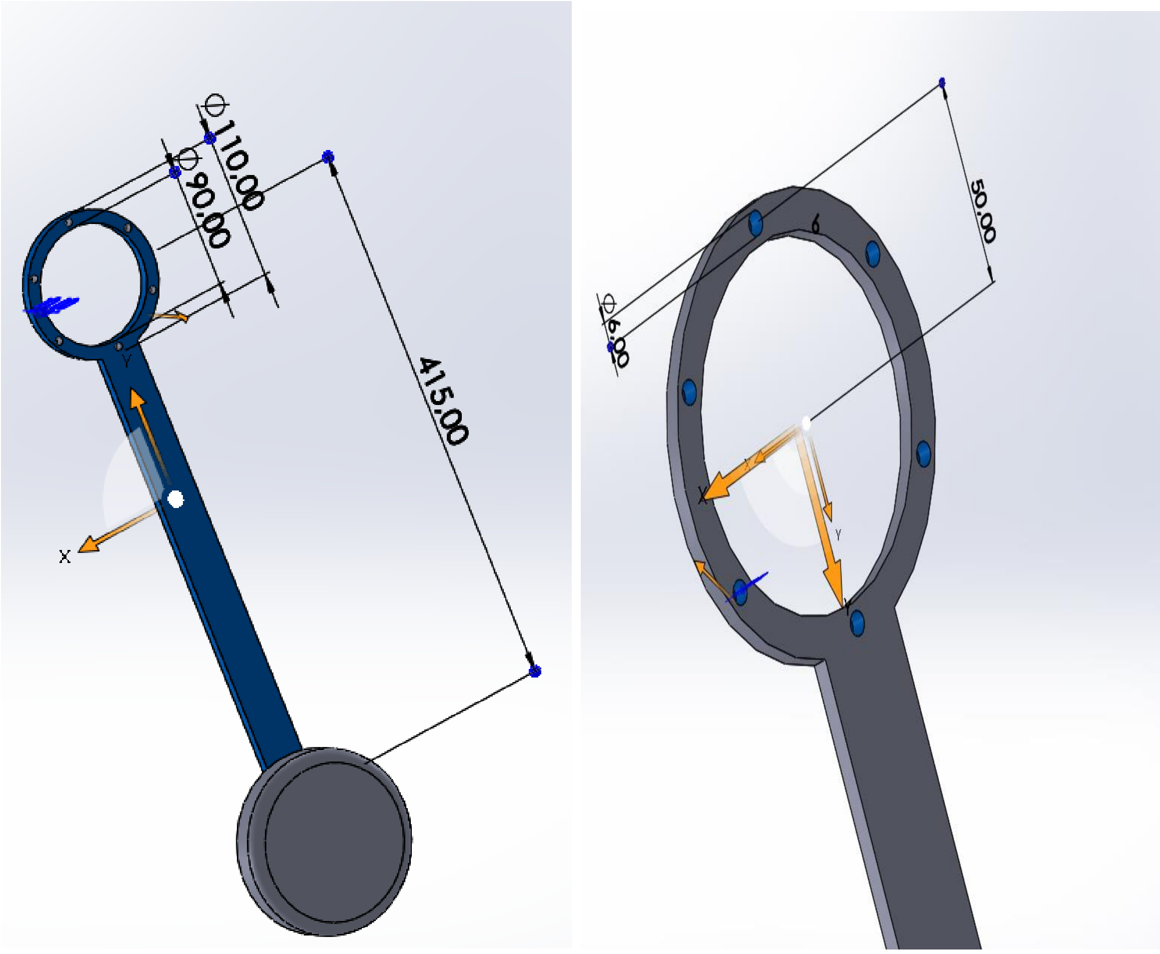

Figure 69: Leg support CAD model details matching the circular spline D connection

Note that the vertical length of the leg support has been chosen respecting the anthropometric data, whose values are presented in the chapter 2.

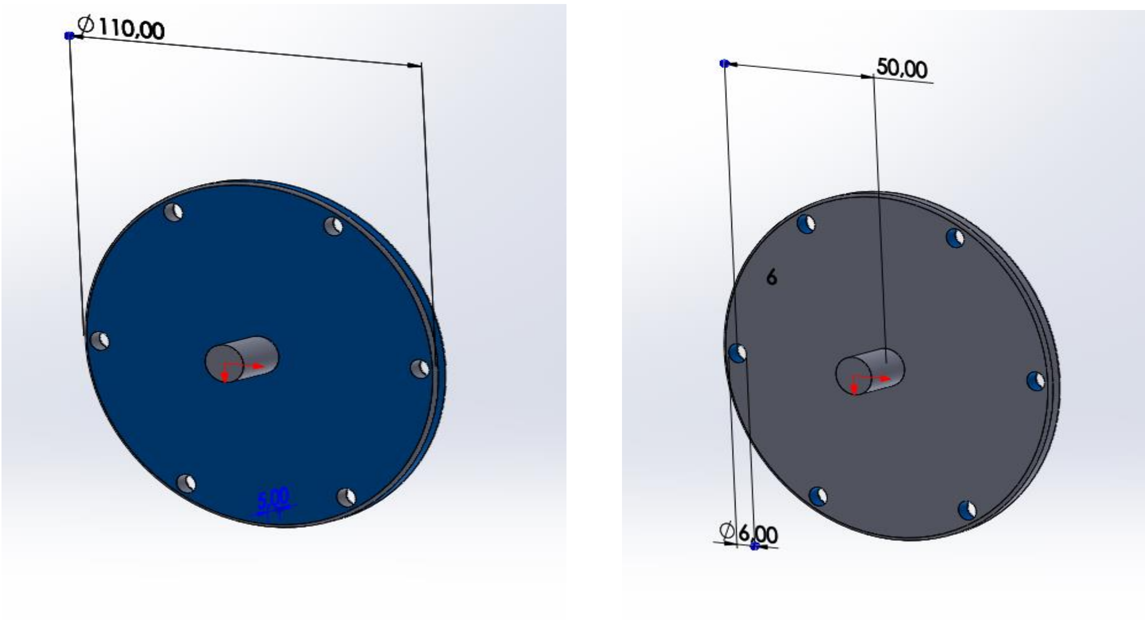

Figure 70: Flanged shaft CAD model details for matching the circular spline S – four-bar linkage connections

The next figure shows all the possible rotational directions, input and output elements and the reduction ratios characterizing the FB Series harmonic drive(fig.71).

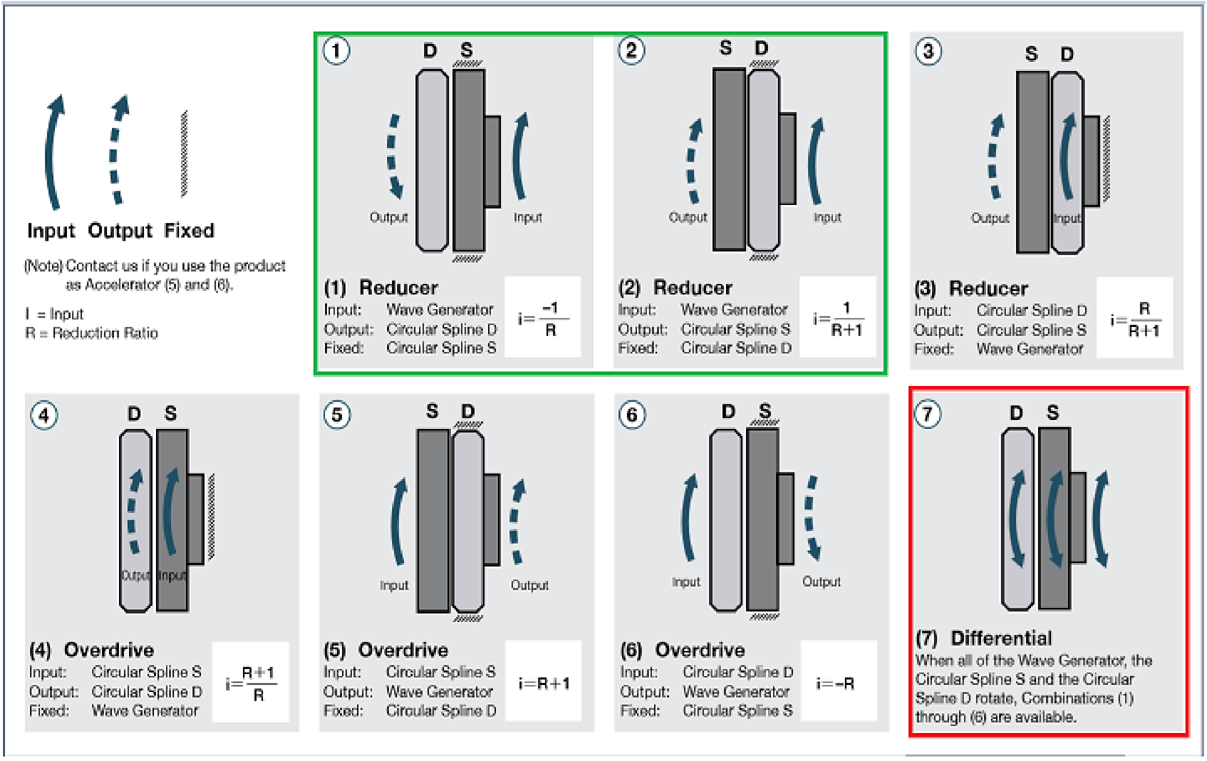

Figure 71: FB Harmonic Drive catalogue rotational direction and reduction ratio [48]

The selected configuration is the (7) Differential one (red square), as< our hip joint is alternatively working between the combination (1) and (2) (green square).

More precisely, the combination (1) provides that the circular spline S is fixed, and the circular spline D works as output. As the transmission ratio is negative, we have an output rotational direction that is the opposite of the input one (wave generator).

The combination (2), instead, it provides the reverse of the previous one, as the circular spline S is the output, and the circular spline D is fixed. In this case the transmission ratio is positive, and we have an output rotational direction that is equal to the input one.

That means that the two circular splines are rotating in the opposite directions, as our leg and back do with respect to the hip.

Moreover, to decide which of the two circular spline has to provide torque to the back, we chose the one with the transmission ratio much higher than is the D one [48].

Resuming the two possible combinations:

- Combination (1):
  If the leg moves → CSS Output → $i = \frac{-1}{R}$ → $R = -131$ (16)
  (back is fixed) CSD fixed

- Combination (2):
  If the back moves → CSD Output → $i = \frac{1}{R+1}$ → $R = 132$ (17)
  (leg is fixed) CSS fixed

For a better understanding, we chose to make a draw of one of the two possible operational cases. As it is shown in the (fig.72), we consider the combination (2), in which the leg is assumed to be fixed and the motor is transferring the torque to the back.

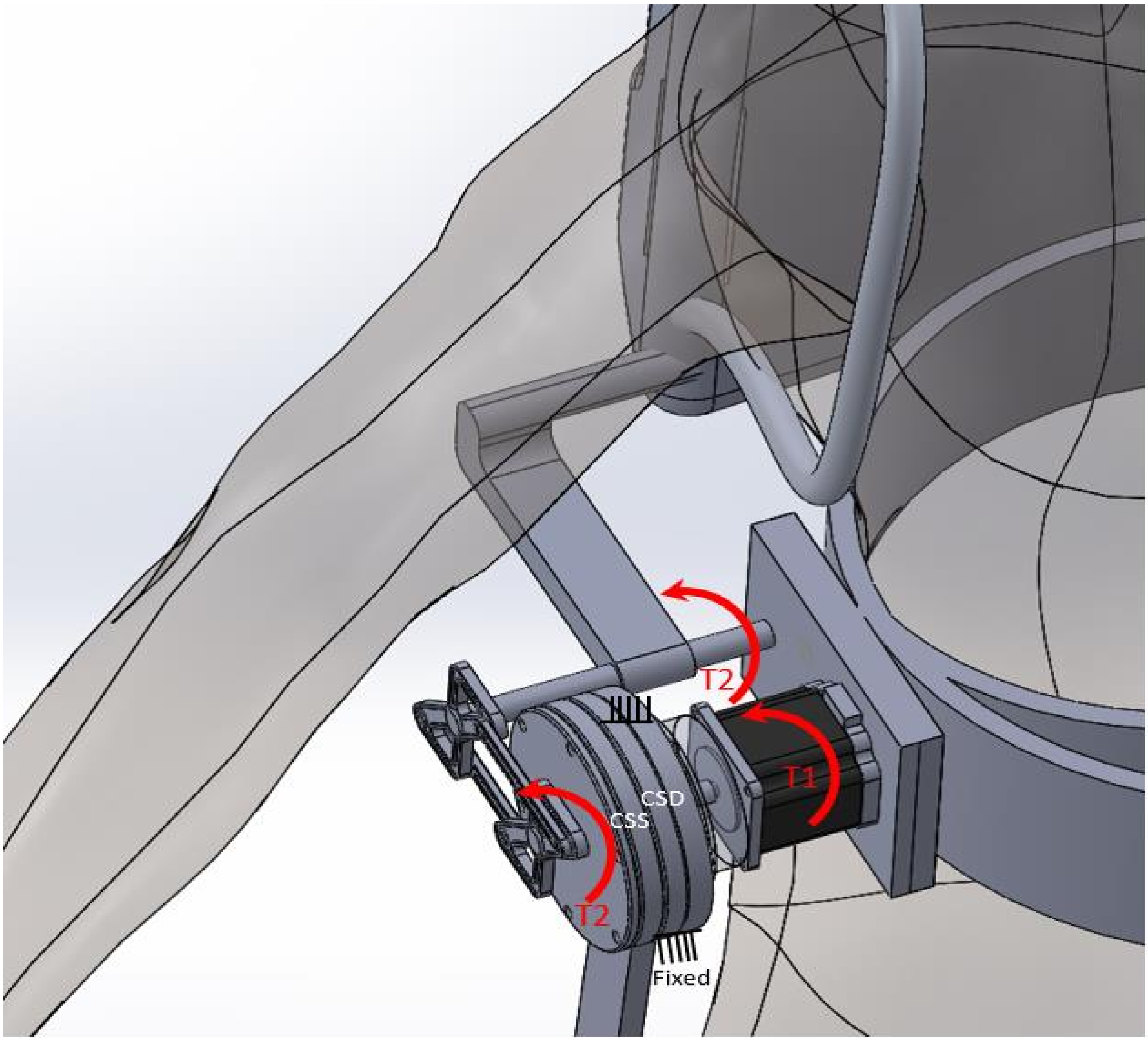

Figure 72: "Bending mode", fixed leg, user torso rising case

4.3.5 Efficiency

The efficiency of the harmonic drive depends on the following conditions:

1- Input rotational speed.
2- Load torque.
3- Reduction Ratio.
4- Temperature.
5- Lubrication type (oil or grease).

The relation between the harmonic drive efficiency, input rotational speed, and reduction ratio is shown in fig (73) [48].

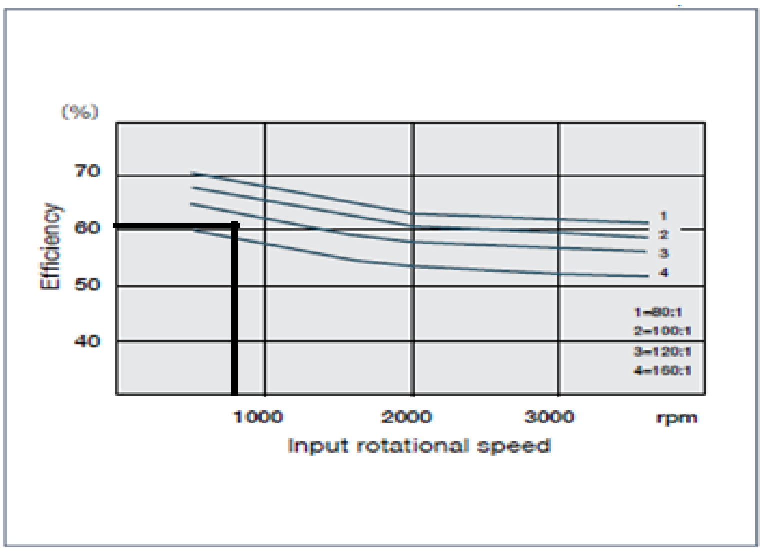

Figure 73:speed/efficincy graph[48]

However, as the maximum input rotational speed is around 700 RPM, it means that we are working in the most efficient section.

The only disadvantage is that we chose a high reduction ratio that decreases the efficiency a little bit (approximately 10%). To compensate for this loss, a more powerful motor should be used, but it would increase the side thickness of the harmonic drive. In conclusion, we are keeping everything as it is, for the sake of having the exoskeleton as compact as possible.

4.3.6 No-load running torque, starting torque and back driving torque

1. The “no-load running torque” is the torque which is required to rotate the wave generator, that works as input (high-speed/low-torque side), when there is no load on the output (low-speed/high-torque side).

2. The “starting torque” is the static torque required to start the wave generator in a no-load condition.

3. The “back driving torque” is the static torque required to start the output shaft if the input side is in a no-load condition.

Those three parameters depend on the model and size of the harmonic drive (fig.74).
In our condition we are using the 32 size [48].

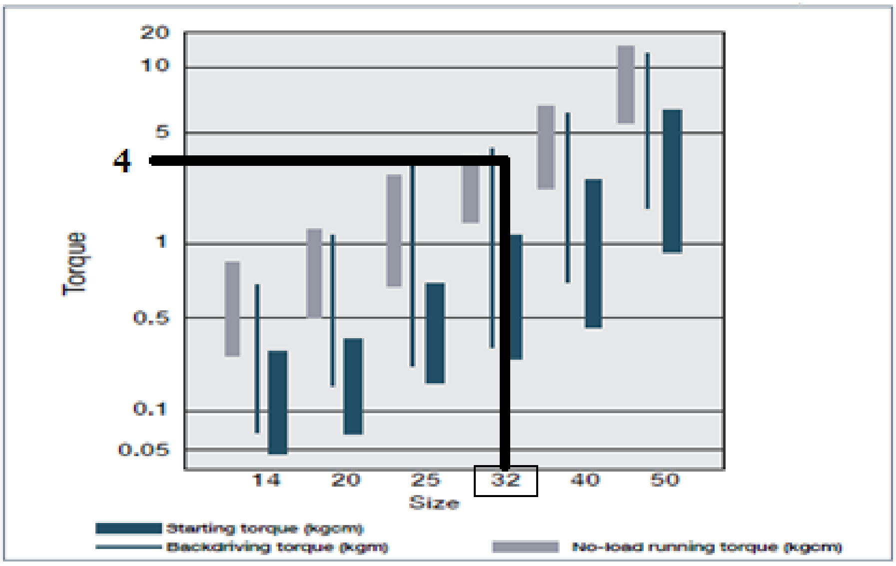

Figure 74: No-load running torque, starting torque and back driving torque graph [48]

Anyhow, the input torque of the motor is bigger than the needed torque to rotate the harmonic drive in the three different conditions. This means we are working in the safe side.

4.4 Bearing calculation

Bearings are necessary for our application to support and to guide the rotating shafts, so that the friction is reduced at minimum levels and, at the same time, they can take care of the noise, energy consumptions and heating problems. To make the right choice we must assure a high level of performance and the opportune grade of robustness, following the right design procedure that is proposed by the SKF © bearing company.

This is just a preliminary bearings evaluation because a more precise load calculation should be made to determine which are the actual operational shaft loads[49].

Indeed, the bearing evaluation is done for the drive shaft, but the same procedure should be separately done for the driven shaft, that is the one that supports the back frame.

Moreover, we suppose two bearings to be enough for the drive shaft(fig.75).

One bearing, called for simplicity reasons “bearing A”, it should be mounted on the shaft adapter coupled with the motor shaft, and it is rotating at the maximum rotational speed (n_{max}).

The second bearing, called for simplicity reasons “bearing B”, it should be mounted on the flanged shaft that is connected to the HD circular spline D, and it is rotating at the minimum rotational speed (n_{min}) as shown below.

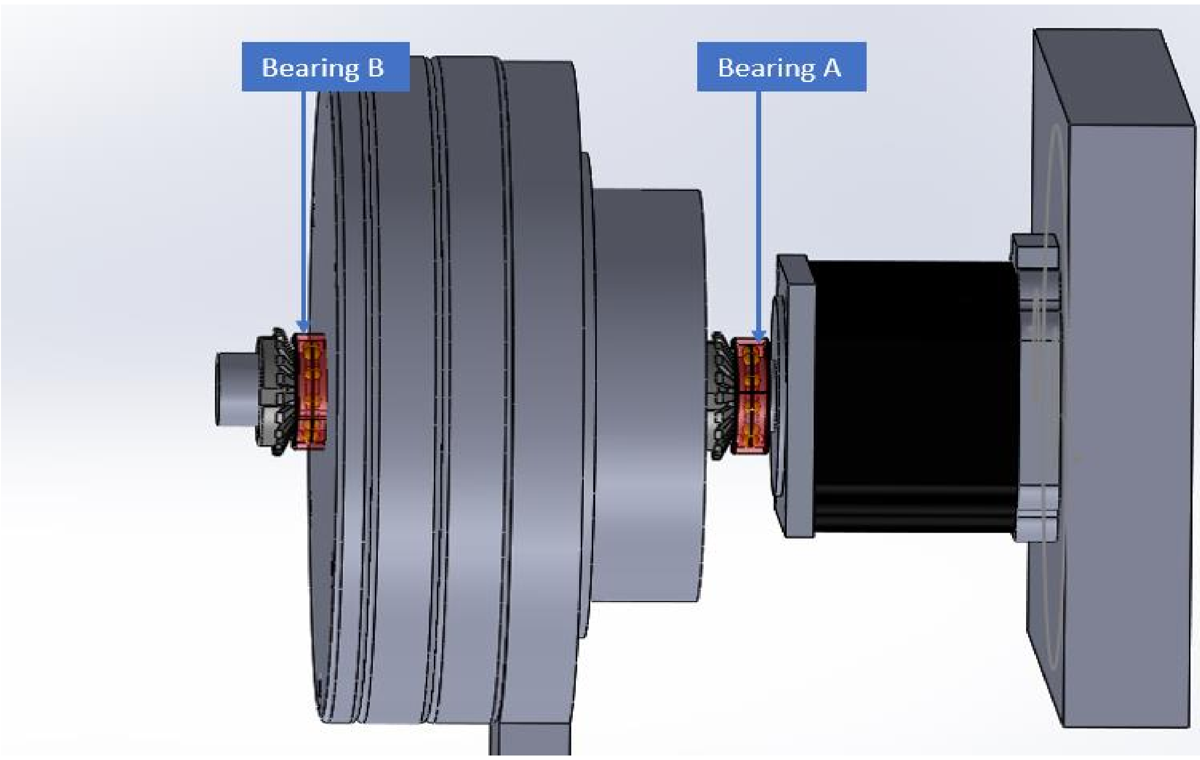

Figure 75: Solidworks® model of bearings (A and B)

Note that, according to the SKF © design procedure, the two bearings are designed separately, even if we assume the equivalent radial/axial loads and the selected bearing series to be the same.

4.4.1 Drive shaft model

The input parameters of the bearings selection are:

Shaft diameter (d)	10mm
Maximum rotational speed (n_{max})	655rpm
Minimum rotational speed (n_{min})	5rpm
Lubrication	Maintenance-free

Table 9: Bearings input parameters

The shaft diameter (d) is the same for both the two bearings A and B since they are mounted on two shafts having the same diameter.

Further, as lubrication parameter we consider the maintenance-free one, as our goal is to avoid replacing the bearings.

The drive shaft bearings shall support both a radial load Fr due to the gravitational force of all the components, as well as the reaction forces of the leg frame, and an axial load Fa, that is generated during the working phase.

Either forces are supposed to be constant in magnitude and direction, while the elastic deformations and torques are neglected for simplicity, as suggested by the SKF © design guidelines[50].

Hence, we can model our isostatic mechanical structure(fig.76) as a simply supported beam with a point load at centre and an axial load, as follow:

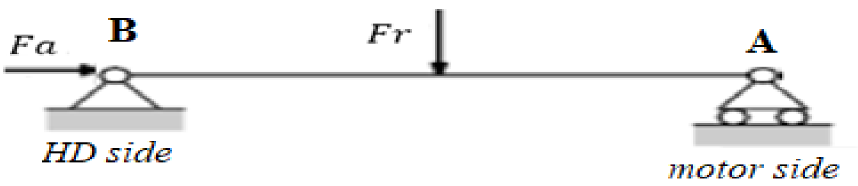

Figure 76: Isostatic mechanical structure of the drive side shaft

Note that the hinge has been placed in correspondence of the axial force application point because this force can be balanced by the hinge horizontal reaction force[51].

Now we compute separately the equivalent radial and axial loads, that are valid for both the bearings.

4.4.2 Equivalent radial load

The point load is the sum of all the component weights and the reaction force of the leg frame:

$$Fr = m_{tot} * g = \left(m_c + m_{HD} + m_{lf}\right) * g = (0.5 + 1 + 0.280) * 9.81 \cong 20\ N \qquad (18)$$

Where:

$m_c,\ m_{HD}, m_{lf}$ are respectively the clutch, the HD and the leg frame masses

g is the gravitational acceleration

All the masses are taken from their relative catalogue specifications [52-53], except for the leg frame one (Fig.77), that has been measured from the *SolidWorks Mass Properties* function.

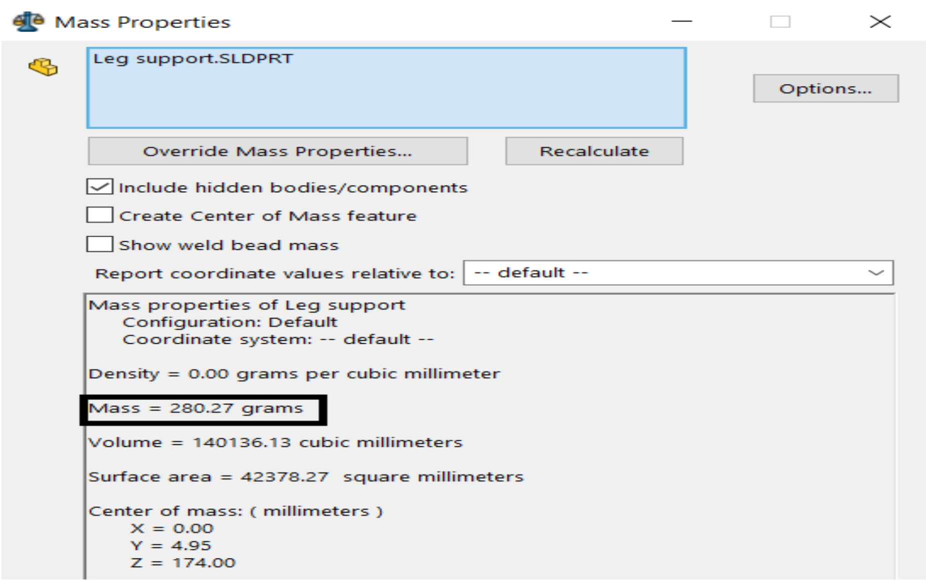

Figure 77: Leg frame mass

We supposed it to be of carbon fiber. This assumption is explained in the material selection paragraph.

4.4.3 Equivalent axial load

The total axial load is the sum of the clutch and the HD normal forces, since the leg frame is assumed to give only a radial contribution.

For the computation of the single disc electromagnetic clutch axial force, since there is no relative information in the catalogue, we use the mathematical expression of the *"torque capacity"*[54], from which we derive the inverse formula:

$$Tc = \frac{2}{3}\,\mu\,\frac{r_2^3 - r_1^3}{r_2^2 - r_1^2}\,Fa_C \quad \rightarrow \quad Fa_C = Tc\,\frac{3}{2\mu}\,\frac{r_2^2 - r_1^2}{r_2^3 - r_1^3} = 0.35\,\frac{3}{2*0.7}\,\frac{0.063^2 - 0.035^2}{0.063^3 - 0.035^3} = 9N \quad (19)$$

Where:

Fa_C is the clutch axial force

Tc is the torque capacity

μ is the friction coefficient in case of steel-steel contact

r_1, r_2 are the internal and external clutch radius

Furthermore, about the HD contribution, the company datasheet provides a table, in which the calculation formula is function of the reduction ratio[55].

That is because, when operating, an axial force is generated on the wave generator and the bearings must be selected to accommodate this axial load.

$$Fa_{HD} = 2 * \frac{T}{D} * 0.07 * \tan 20° = 2 * \frac{42}{32} * 0.07 * \tan 20° = 0.0668\ \mathrm{N} \qquad (20)$$

Where:

T is the output torque

D is the HD size

Fa_{HD} is the harmonic drive axial force

The resulting load is:

$$Fa = Fa_C + Fa_{HD} \cong 9\,N \tag{21}$$

4.4.4 Bearing selection

To avoid the bearings replacement, we initially had a look at the SKF© catalogue and we found the *"maintenance-free spherical plain bearings"* typology, consisting of steel and polymeric (PTFE) materials [56].
Even if they respect our desired characteristic, the lateral encumbrance and the basic load ratings were too high for our application.

For this reason, we decided to choose the *"SKF© - Single row deep groove ball bearing"* typology, that also assure an infinite life of the bearings, as shown in the basic rating life calculation below.
The selected bearing series is the "61800-2RS1", as shown below:

1.1 Single row deep groove ball bearings
d **9 – 10** mm

Principal dimensions			Basic load ratings		Fatigue load limit	Speed ratings		Mass	Designations	
			dynamic	static		Reference speed	Limiting speed[1)]		Bearing open or capped on both sides	capped on one side[1)]
d	D	B	C	C_0	P_u					
mm			kN		kN	r/min		kg	–	
9 cont.	24	7	3,9	1,66	0,071	–	19 000	0,015	► 609-2RSH	609-RSH
	24	7	3,9	1,66	0,071	70 000	34 000	0,014	► 609-2RSL	609-RSL
	24	7	3,9	1,66	0,071	70 000	34 000	0,015	► 609-2Z	609-Z
	26	8	4,75	1,96	0,083	60 000	38 000	0,02	► 629	–
	26	8	4,75	1,96	0,083	–	19 000	0,02	► 629-2RSH	629-RSH
	26	8	4,75	1,96	0,083	60 000	30 000	0,02	► 629-2RSL	629-RSL
	26	8	4,75	1,96	0,083	60 000	30 000	0,021	► 629-2Z	629-Z
10	19	5	1,72	0,83	0,036	–	22 000	0,0055	**61800-2RS1**	–
	19	5	1,72	0,83	0,036	80 000	38 000	0,0055	**61800-2Z**	–
	19	5	1,72	0,83	0,036	80 000	48 000	0,0053	**61800**	–
	22	6	2,7	1,27	0,054	–	20 000	0,01	**61900-2RS1**	–
	22	6	2,7	1,27	0,054	70 000	36 000	0,01	**61900-2Z**	–
	22	6	2,7	1,27	0,054	70 000	45 000	0,01	**61900**	–

Figure 78: SKF© Datasheet of single-row deep groove ball bearings [56]

Both the speed ratings and the basic load ratings are more suitable for our input parameters and we can save half space and mass, with respect to the previous topology.

4.4.5 Bearing A - Equivalent dynamic bearing load

To calculate the bearing A rating life, we must evaluate the "*equivalent dynamic bearing load " (P)*, that is defined as: the equivalent hypothetical load acting on the bearings, as combination of both radial and axial forces[50].
This load is determined according to the following formula:

$$P = 0.5 * [(X * Fr) + (Y * Fa)] = 0.5 * [(1.9 * 20) + (0.55 * 9)] \cong 21.5\ N \qquad (22)$$

Where:
Fr, Fa are the equivalent radial and the axial loads

X, Y are the radial and the axial load factors (provided by the SKF© catalogue)

0.5 is the scaling factor (assuming the load to be equally split between the two bearings)

4.4.5.1 Bearing A - life estimation

To ensure the infinite life of the bearings, we evaluate the "*basic rating life"*[57] as:

$$L_{10h}(n_{max}) = \left(\frac{10^6}{60\ n_{max}}\right)\left(\frac{C}{P}\right)^p = \left(\frac{10^6}{60*655}\right)\left(\frac{1740}{21.5}\right)^3 = 13 * 10^6\ h \quad (8) \rightarrow \text{maintenance-free}$$

Where:
L_{10h} is the bearing life expressed in operating hours
C is the dynamic basic load
p is the bearing factor (equal to 3 for the spherical bearings)

A second check-test can be carried out by determining the *"SKF© rating life"*[9], according to the *"ISO 281"* method, that is more accurate, since it takes care of a variety of influencing factors, according to the formula:

$$L_{10m} = a_1 * a_{SKF} * \left(\frac{C}{P}\right)^p \qquad (23)$$

The a_1 is the *"reliability factor"*, that is unitary, since we consider a reliability of 90%, as it is the suggested value.

The a_{SKF} is the "*life modification factor"*, that is function of the contamination level η_C, of the lubricant viscosity ratio κ and of the fatigue load limit P_u.

It can be calculated with the following procedure:
- We first evaluate the contamination factor η_C , from the following table (*fig. 79*).

Guideline values for factor η_c for different level of contamination

Conditions	Factor η_c 1) for bearings with diameter $d_m < 100$	$d_m \geq 100$ mm
Extreme cleanliness • Particle size of the order of the lubricant film thickness • Laboratory conditions	1	1
High cleanliness • Oil filtered through an extremely fine filter • Typical conditions: sealed bearings that are greased for life	0,8 ... 0,6	0,9 ... 0,8
Normal cleanliness • Oil filtered through a fine filter • Typical conditions: shielded bearings that are greased for life	$\boxed{0,6 ... 0,5}$	0,8 ... 0,6
Slight contamination • Typical conditions: bearings without integral seals, coarse filtering, wear particles and slight ingress of contaminants	0,5 ... 0,3	0,6 ... 0,4
Typical contamination • Typical conditions: bearings without integral seals, coarse filtering, wear particles, and ingress from surroundings	0,3 ... 0,1	0,4 ... 0,2
Severe contamination • Typical conditions: high levels of contamination due to excessive wear and/or ineffective seals • Bearing arrangement with ineffective or damaged seals	0,1 ... 0	0,1 ... 0
Very severe contamination • Typical conditions: contamination levels so severe that values of ηc are outside the scale, which significantly reduces the bearing life	0	0

1) The scale for η_c refers only to typical solid contaminants. Contamination by water or other fluids detrimental to bearing life is not included. Because of strong abrasive wear in highly contaminated environments ($\eta_c = 0$), the useful life of the bearing can be significantly shorter than the rating life.

Figure 79: SKF© Contamination factors [56]

We choose $\eta_C = 0.5$, as the worst reasonable case condition for shielded bearings, having a mean diameter of:

$$d_m = 0.5\,(d + D) = 0.5\,(10 + 19) = 14.5\,mm < 100mm \qquad (24)$$

- As a second step, we must evaluate the viscosity ratio κ, that is given by the ratio between the actual operating viscosity of our selected grease v, and the rated viscosity v_1.

The value v, it is a combination of the operating temperature and the ISO standard designation of our lubricant.
To choose the right grease, we must firstly extrapolate the diameter series number from the *"SKF© bearing designation system"*(fig.80), entering the table with the selected bearing series previously found (61800).

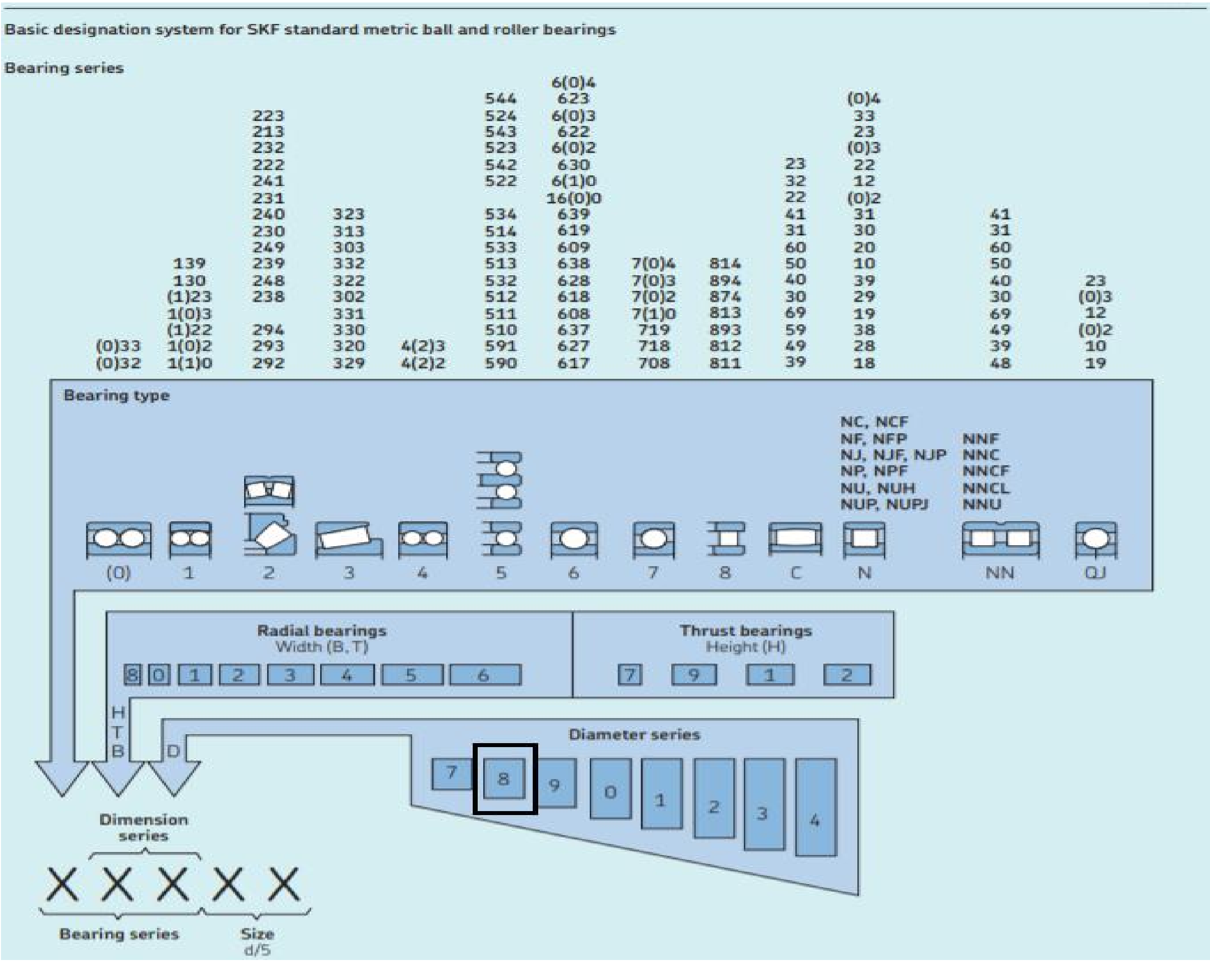

Figure 80: SKF bearing designation system [56]

Then, according to the bearing diameter series (= 8), we can select the grease from the table below(fig.81), that is the low temperature "LT10". This grease has a unitary *"Grease performance factor" (GPF)* and it consists of a diester oil containing a lithium soap thickener (fig.82).

SKF standard greases for capped single row deep groove ball bearings made of carbon chromium steel

Bearings in diameter series	SKF standard greases in bearings with outside diameter			
	D ≤ 30 mm d < 10 mm	d ≥ 10 mm	30 < D ≤ 62 mm	D > 62 mm
8, 9	LHT23	LT10	MT47	MT33
0, 1, 2, 3	MT47	MT47	MT47	MT33

Figure 81: SKF© standard greases selection [56]

Technical specifications of SKF standard and special greases for capped deep groove ball bearings

Grease	Temperature range[1)] –50 0 50 100 150 200 250 °C –60 30 120 210 300 390 480 °F	Thickener	Base oil type	NLGI grade	Base oil viscosity [mm²/s] at 40 °C (105 °F)	Base oil viscosity [mm²/s] at 100 °C (210 °F)	Grease performance factor (GPF)
MT33		Lithium soap	Mineral	3	100	10	1
MT47		Lithium soap	Mineral	2	70	7,3	1
LT10		Lithium soap	Diester	2	12	3,3	2
LHT23		Lithium soap	Ester	2–3	27	5,1	2
LT		Lithium soap	Diester	2	15	3,7	1
WT		Polyurea	Ester	2–3	70	9,4	4
GJN		Polyurea	Mineral	2	115	12,2	2
HT		Polyurea	Mineral	2–3	96	10,5	2
VT378		Aluminium complex soap	PAO	2	150	15,5	–[2)]
GFJ		Aluminium complex soap	Synthetic hydro-carbon	2	100	14	1
GE2		Lithium soap	Synthetic	2	25	4,9	2

1) Refer to the SKF traffic light concept (page 117).
2) For bearings filled with VT378 grease, use the scale corresponding to GPF = 1 and multiply the value obtained from diagram 1, page 246, by 0,2.

Figure 82: SKF© greases technical specifications [56]

From the selected grease viscosity grade “ISO VG 10”[58], by assuming an operating temperature of 60°, we get $v \cong 6\, mm^2/s$ (fig.83).

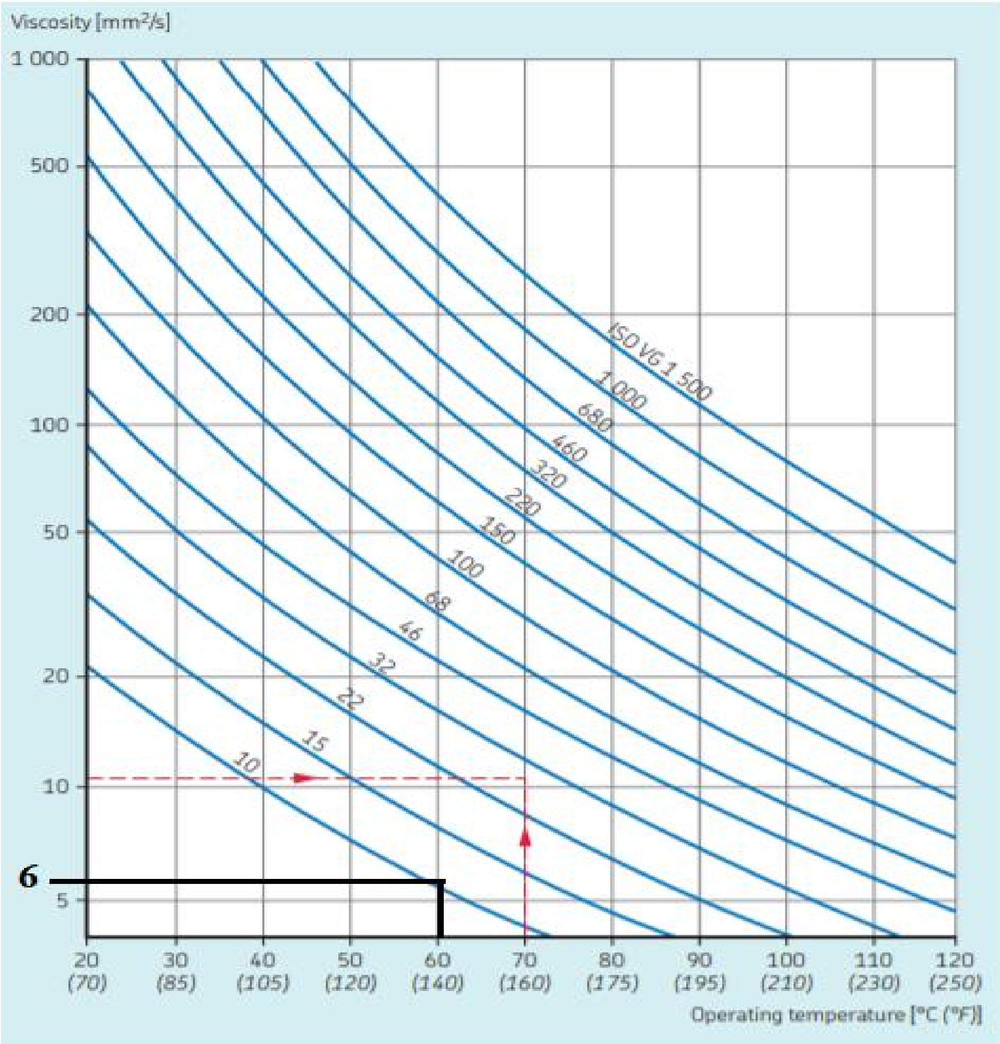

Figure 83: SKF© greases technical specifications [56]

Conversely, the v_1 factor is function of the mean diameter d_m and of the rotational speed n (fig.84).

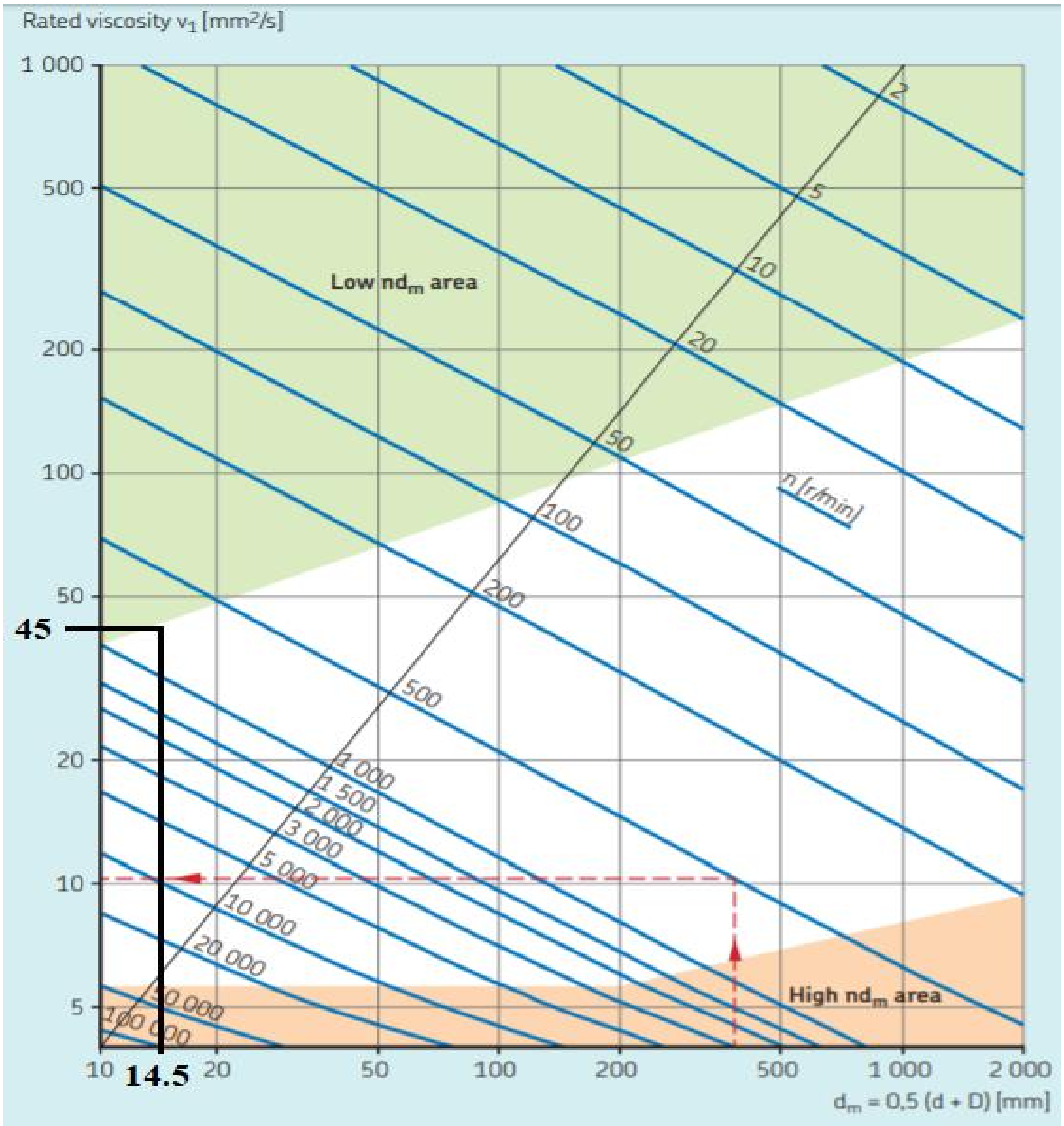

Figure 84: Rated viscosity [56]

We get the value $v_1(n_{max}) = 45\ mm^2/s$. Therefore, the viscosity ratio is:

$$\kappa\,(n_{max}) = \frac{v}{v_1(n_{max})} = \frac{6}{45} \cong 0.133 \qquad (25)$$

At this point, we can determine the a_{SKF} factor (*fig.85*), choosing as input parameters:

$$\kappa\,(n_{max}) = 0.133 \qquad\qquad \eta_C * \frac{P_u}{P} = 0.2 * \frac{36}{21.5} = 0.34 \qquad (26)$$

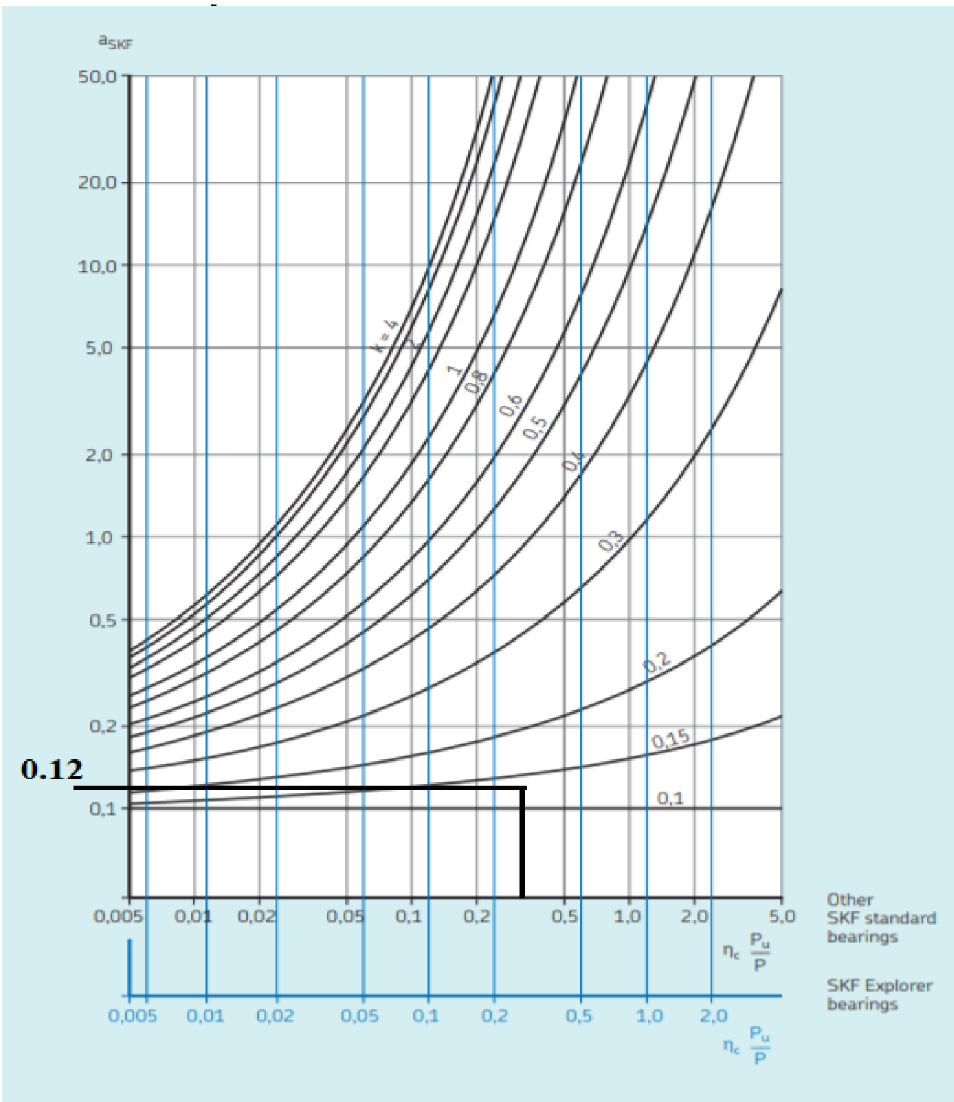

Figure 85: Bearing life modification factor [56]

We get a value of $a_{SKF}(n_{max}) = 0.12$.

By substitution, we obtain a SKF© rating life of:

$$L_{10m}(n_{max}) = a_1 * a_{SKF}(n_{max}) * \left(\frac{C}{P}\right)^p = 1 * 0.12 * \left(\frac{1740}{21.5}\right)^3 = 63608.2 * 10^6 \ rev. \ (27)$$

The same life expressed in hours is:

$$L_{10mh(n_{max})} = \left(\frac{10^6}{60\ n}\right) * L_{10m} = \left(\frac{10^6}{60*655}\right) * 63608.2 = 1618529h\ maint.\ free \qquad (28)$$

This means that the infinite life of the bearing A is definitely granted.

4.4.6 Bearing B - Equivalent and required static bearing loads

Since the bearing B has a rotational speed n_{min} < 10rpm, the SKF© suggest a different procedure to verify the selected bearing model. Indeed, according to the *"ISO 76:2006"* [56], the bearing must be verified based on the *"required basic static load rating"* C_0, that for the selected bearing is equal to 0.83 kN (fig.78).
The first step consists of an evaluation of the "equivalent static bearing load" P_0.
By considering the *"radial/axial load factor"* X_0 and Y_0, with a scaling factor of 0.5, as the load is assumed to be equally split between the two bearings, we get:

$$P_0 = 0.5 * [(X_0 * Fr) + (Y_0 * Fa)] = 0.5 * [(0.6 * 20) + (0.5 * 9)] \cong 8.25\ N \qquad (6)$$

Then, we must select the bearing "static safety factor" s_0 (fig.86). By assuming a rotating ball bearing with normal condition of operation and performance requirements, we get s_0= 1.

table 1 - Guideline values for the static safety factor s_0

Type of operation	Rotating bearing Performance requirements (e.g. quiet running or vibration-free operation)						Non-rotating bearing	
	unimportant		normal		high			
	Ball bearings	Roller bearings	Ball bearings	Roller bearings	Ball bearings	Roller bearings	Ball bearings	Roller bearings
Smooth, vibration-free	0,5	1	1	1,5	2	3	0,4	0,8
Normal	0,5	1	1	1,5	2	3,5	0,5	1
Pronounced shock loads[1)]	≥ 1,5	≥ 2,5	≥ 1,5	≥ 3	≥ 2	≥ 4	≥ 1	≥ 2

Figure 86: SKF© static safety factor [59]

Now, it is possible to verify the static load according to the following formula:

$$\frac{C_0}{P_0} \geq s_0 \rightarrow \frac{830}{8.25} = 100 \geq 1 \quad (7)$$

As it is evident, the bearing working at low speed is not at risk of permanent deformations.

In summary, both bearings can achieve the required levels of robustness and support.

4.5 Material selection

Choose the right material to build an exoskeleton is a complicated mission. Indeed, a wearable robot that should be flexible, elastic and soft, at the same time, it should give strength to the end-user. Moreover, the exoskeleton should be as light as possible, and it should allow most of the human body DOMs. A wide range of materials is used in manufacturing different parts of an exoskeleton, where each part has a different function and interacts with the human body differently. In the following chapter, we introduce different materials that could be used in producing different parts of an exoskeleton. The aim is to show the advantages and the mechanical properties of each material, trying to explain why those materials were chosen for manufacturing the various parts.

Exoskeleton parts are separated, mentioning the used materials for manufacturing each one of them, the parts are divided as follows:

1- Power transmission shafts.
2- Exoskeleton leg frame.
3- Waist belt.
4- Flange and four bar linkage.
5- Back frame.
6- Hip joint housing.
7- Straps and adjustable release buckle.

4.5.1 Power transmission shafts

In our design, shafts are connected between the different power transmission elements and they have been used to transfer both different torques and speeds between those elements. Among them, the first shaft is connecting the electric stepper motor output with the electromagnetic clutch input. The second one, that is coming out of the other side of the clutch is coupled with the wave generator of the harmonic drive. Then, the third shaft is connecting one of the two harmonic drive output (circular spline S) with the four-bar linkage. The last one receives the power from the four-bar linkage and it makes this power available to the back frame.

Shafts are designed as short as possible, as our target is to reach a compact design. Meanwhile, the diameters of the shafts vary due to different dimensions of the exoskeleton components.

For example, to connect the motor`s output shaft with the electromagnetic clutch input bore, a hollow shaft with inner and outer keys has been fitted inside the electrical motor`s output shaft, where a groove screw is penetrating from top the outer diameter of the connecting shaft passing through the key and the motor`s output shaft to fasten them all together. This kind of shaft coupling is called “shaft adapter” (fig.87) and it is used to couple two different shafts when the available distance is limited and to make shafts larger.

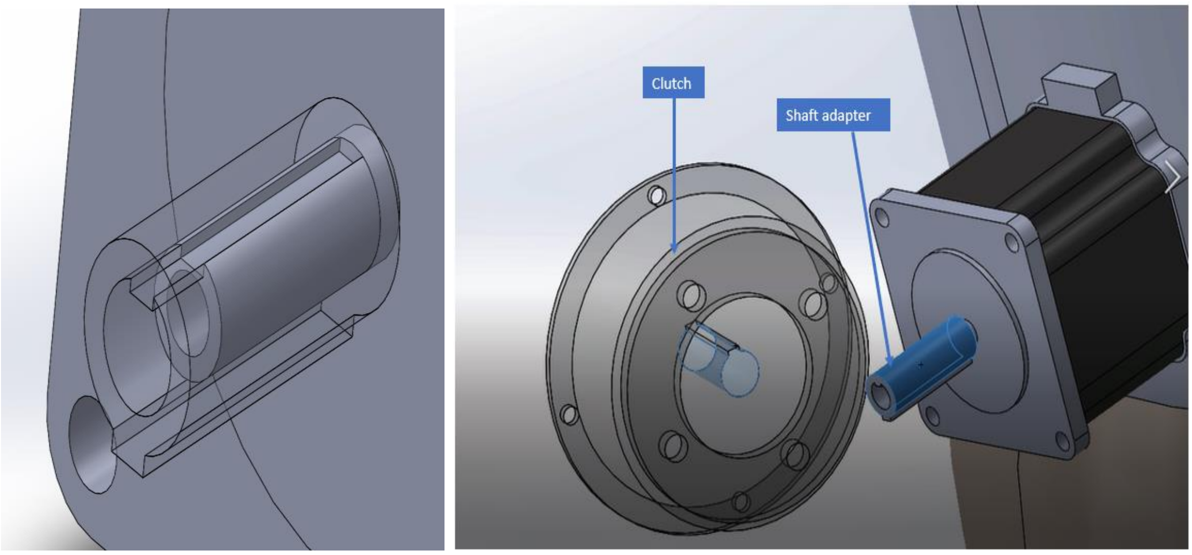

Figure 87: Two views of the shaft adapter 3D model

4.5.2 Mechanical key

The mechanical keys are mechanical elements used to connect shafts with rotating machine parts; the key prevents the relative rotation between two connected rotating parts, enabling torque transmission. A shaft key requires a matching keyway and seat. Those components are mostly made of the same material of the shaft rods, for the sake of avoiding overload failures. The key length should be at least equal to the shaft diameter, and this is because the torque is partially transmitted through the shaft, the key, the keyseat and keyway (fig.88) [60].

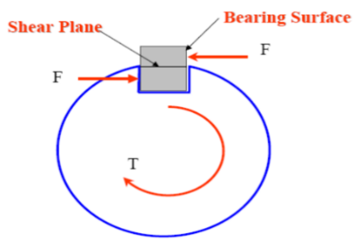

Figure 88: Key transmitted torque [61]

4.5.3 Shafts

In our study case, the shafts are not transmitting very high torque, and due to that, mild or low carbon steel alloys could be used as materials for our shafts as well as for our keys. Some advantages of these materials are: the low prize, the high strength and the malleability. In addition, as these steels are quite softs, they could be easily machined compared to harder steels. In particular, this type of steel alloy is quite easy to weld, it has an excellent surface finish(fig.89) and it is widely available in the market with a wide range of diameters. The mechanical properties are shown in (fig.90). [62-63]

Figure 89: Mild steel[62]

Mechanical Properties	Metric	Imperial
Hardness, Brinell	126	126
Hardness, Knoop (Converted from Brinell hardness)	145	145
Hardness, Rockwell B (Converted from Brinell hardness)	71	71
Hardness, Vickers (Converted from Brinell hardness)	131	131
Tensile Strength, Ultimate	440 MPa	63800 psi
Tensile Strength, Yield	370 MPa	53700 psi
Elongation at Break (In 50 mm)	15.0 %	15.0 %
Reduction of Area	40.0 %	40.0 %
Modulus of Elasticity (Typical for steel)	205 GPa	29700 ksi
Bulk Modulus (Typical for steel)	140 GPa	20300 ksi
Poissons Ratio (Typical For Steel)	0.290	0.290
Machinability (Based on AISI 1212 steel. as 100% machinability)	70 %	70 %
Shear Modulus (Typical for steel)	80.0 GPa	11600 ksi

Figure 90: Mild steel mechanical properties [63]

4.5.4 Leg frame

The leg frame (fig.91) is one of the exoskeleton's main parts, as it delivers the output torque of the harmonic drive (circular spline D) to the user's leg. This frame is attached to the user's leg through a tight pad with an adjustable strap, and to the harmonic drive (circular spline D) by fastening bolts. The material for the two leg links should withstand high strength, meanwhile it should be lightweight to not add loads neither on the legs nor on the hip-joint structure. Moreover, the adjustable strap is placed at the end of the leg frame and it should secure tightly around the user leg, to not slip. Additionally, it should have extra soft and malleable materials to do not harm the worker.

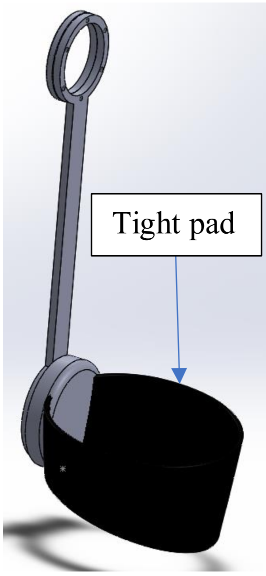

Figure 91: Leg frame + tight pad Solidworks® model

Carbon fibers could be a reasonable choice of material to build the structure of the leg frame of an industrial exoskeleton. Carbon fibers is a material widely used nowadays in manufacturing of robotic links and exoskeleton frames (fig.92). This material is best suited to meet the design requirements of various industrial applications[64]. Here is reported the full range of mechanical proprieties[65], that are:

1- Fatigue resistance.
2- High strength to weight ratio.
3- Corrosion resistance.
4- Good tensile strength.
5- Fire resistance.
6- Rigidity.
7- Low coefficient of thermal expansion.
8- Shock resistance.

Figure 92: Carbon fibre robotic arm [64]

The standard carbon fiber properties[66] are shown in the next table (fig.93).

Standard Fiber Properties

	US Units	SI Units
Tensile Strength	600 Ksi	4137 MPa
Tensile Modulus	35 Msi	242 GPa
Elongation	1.5%	
Density	0.065 lb/in^3	1.81 g/cc
Fiber Diameter	0.283 mils	7.2 microns
Carbon Content	95%	
Yield	400 ft/lb	270 m/kg

Figure 93: Standard carbon fibre mechanical properties [66]

Anyhow, the tight pad and adjustable strap should be made of softer and more ductile material. Carbon fibers are not a proper choice for those parts, because they do not have good malleability. Therefore, polycarbonate polymers could be an excellent choice for the tight pad, as they are enough ductile and they provide a reasonable strength, needed for that kind of application. In addition, they also have other advantages like:

1- Lightweight.
2- High impact strength. (Compared to acrylic and High-Density Polyethylene)

3- Cheap.

4- Easily machined.

5- Heat formed.

6- Chemical resistance.

7- Excellent dimensional stability.

The mechanical properties of polycarbonate polymers compared to different plastic polymers [67] are shown in the next graphs(fig.94). From these graphs, we can say that polycarbonate is one of the most efficient materials to be used for that kind of devices, especially for an industrial exoskeleton which is working in a harsh environment.

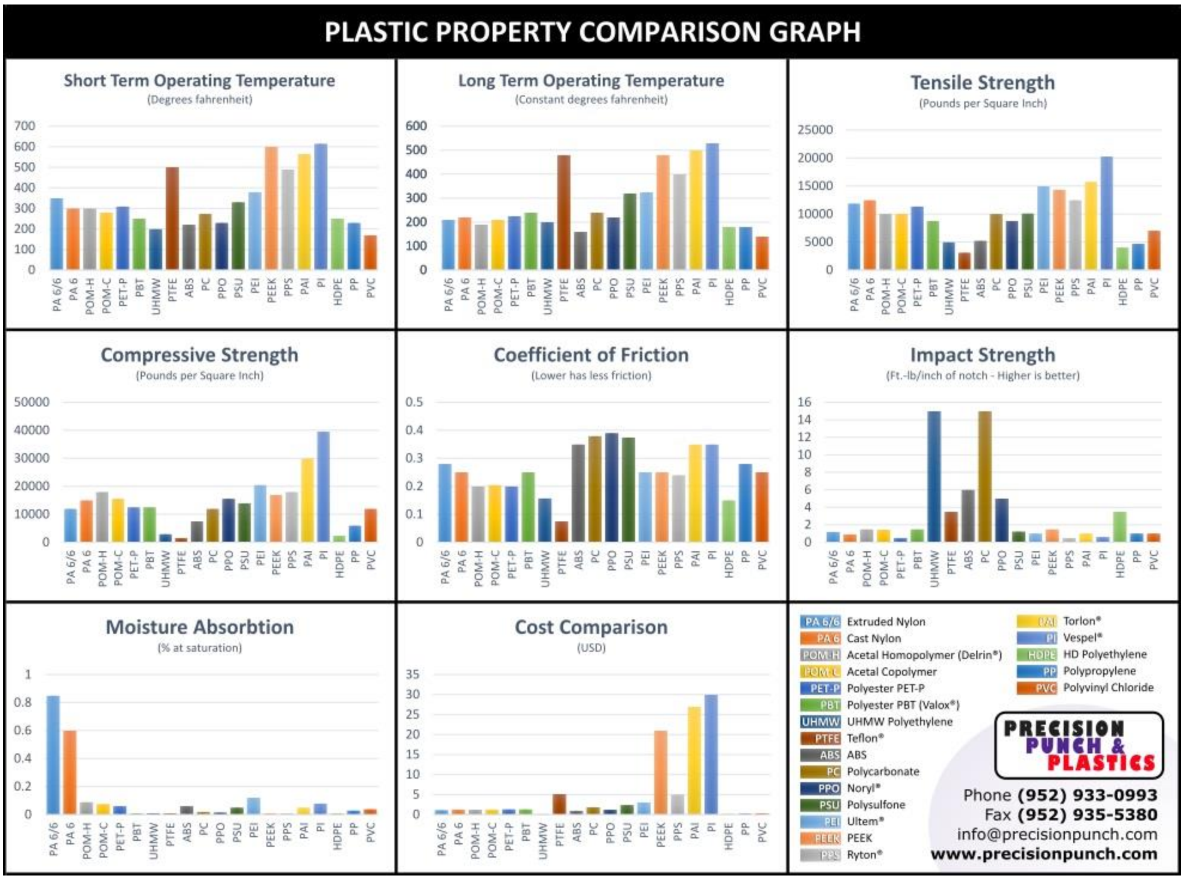

Figure 94: Plastic property comparison graph [67]

The tight pad could take half circle shape made from polycarbonate, to give strength to the whole component, and to follow the shape of the human leg. This pad could be covered by two layers, to provide a soft leg contact. The first layer could be made of "EVA foam", that is like a soft touch sponge. The second layer could be a "two-part epoxy", as it could fasten the first layer on the pad body. Then, a textile cover, made from Dyneema® material, could cover all the layers from the inner side of the pad. Furthermore, two pieces of long straps could be connected to both ends of the pad and by a plastic lock, allowing straps adjustment.

4.5.5 Waist belt

The waist belt is the heart of our exoskeleton structure. A flange is attached to the middle of this belt, carrying all the rotational elements. The waist belt should be made of flexible and elastic materials; at the same time, it should have high strength.

This belt is placed around the waist of the user to provide stabilization of the torso, as it has been proven that: by increasing the intra-abdominal pressure, that is to say, by increasing the pressure around the pelvis, we can aim to reduce the lumbar intradiscal pressure.[68]

The waist belt dimensions should be adjustable to fit the average dimensions of the human hip width which varies between 30-43cm (fig.95) [69].

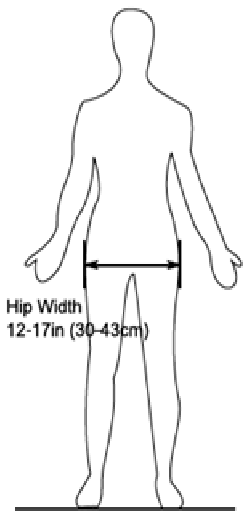

Figure 95: Human hip width average [69]

High-density polyethylene is a suggested material for building the waist belt for a prototype, rather than carbon fibers, due to the complex production procedure. High-density polyethylene is one of the world's most famous plastic polymers. It is an enormously versatile polymer which is suited to a wide range of applications, that vary from the heavy-duty damp proof membrane for new buildings, to light, flexible bags and films. It is flexible, waterproof, easy to process by most methods and low cost. Moreover, it has a good low temperature toughness and an excellent chemical resistance[70]. The waist belt (fig.96) could contain two more layers on its inner side. The first one could be made of EVA foam, while the second one of a covering textile made from Dyneema® material.

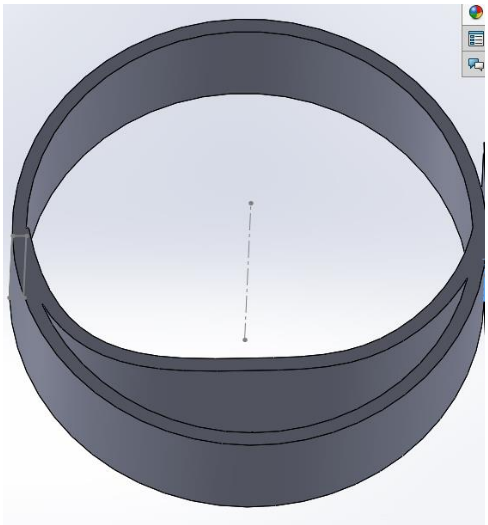

Figure 96: Waist belt Solidworks® drawing

4.5.6 Flange and four bar linkage

The flange is the element that carries the main elements of our exoskeleton, like the motor, the electromagnetic clutch, the harmonic drive, the power transmission shafts, the bearings, and the four-bar linkage. This flange is attached to the waist belt (fig.97). The components that are fastened on the flange should be fastened in a very secure way; for this reason, we would opt for the "aluminum alloy 6061", which is one of the most used aluminum alloys in industrial applications [71]. It has excellent mechanical properties, it exhibits good weldability and it is very commonly extruded. This alloy could be also used to manufacture the four-bar linkage(fig.98), due to its characteristics, providing secure fastening, high strength, easy machining and lightweight.

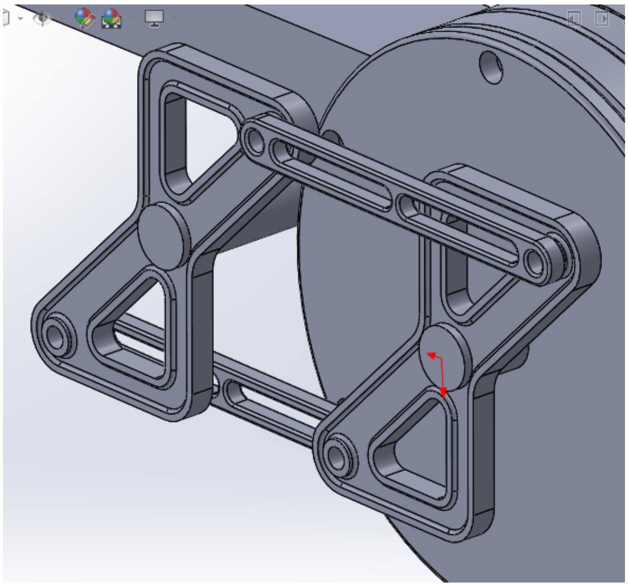

Figure 98: Four-bar linkage Solidworks® drawing

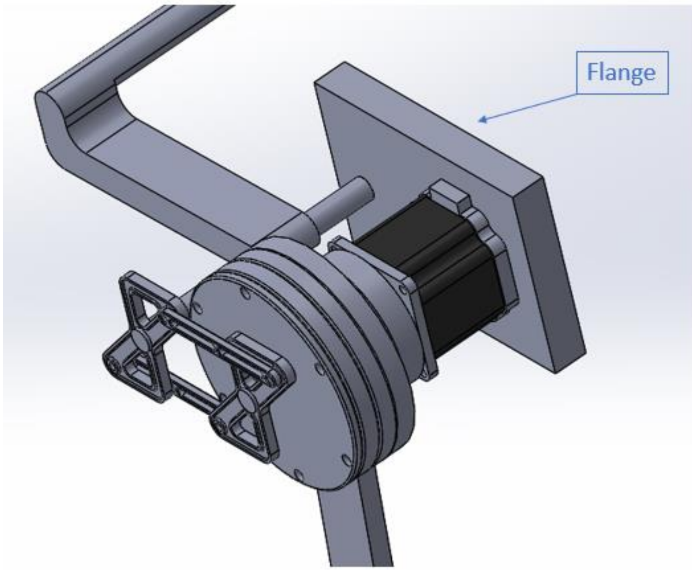

Figure 97: Main flange Solidworks® drawing

The mechanical properties of "aluminum alloy 6061"[72] are shown below (fig.99).

Material	Temperature (°C)	Thermal conductivity ($W.m^{-1}.K^{-1}$)	Heat capacity ($J.kg^{-1}.K^{-1}$)	Density ($kg.m^{-3}$)	Thermal expansion ($\times10^{-6}$ K^{-1})	Young's modulus (GPa)	Yield stress (MPa)	Poisson's Ratio	Melting point (°C)
Aluminum alloy 6061-T6	0	162	917	2703	22.4	69.7	277.7	0.33	582-652
	98	177	978	2685	24.61	66.2	264.6		
	201	192	1028	2657	26.6	59.2	218.6		
	316	207	1078	2630	27.6	47.78	66.2		
	428	223	1133	2602	29.6	31.72	17.9		
	571	253	1230	2574	34.2	0	0		

Figure 99:Aluminum alloy 6061 mechanical properties [72]

4.5.7 Back frame

To transmit the power delivered by the four-bar linkage to the human trunk, a carbon fiber pad could be connected to the power transmission back shaft. Carbon fiber sheets are available with different thicknesses in the commercial market. This carbon fiber pad are sometimes built in the back pad of the traditional backpack. Backpacks are available in the commercial market (fig.100) [69] with shoulder straps, lumbar area padding, and hip belt. A layer of “ROHO inflatable pad”[10] could be built in, to distribute pressure across the area. By using an inflatable pad as part of the support structure, the pressure across the bony spinous processes and sacral tuberosities of the lumbar regions can be minimized (fig.101). Moreover, a CAD model of the backpack is shown below(fig.102).

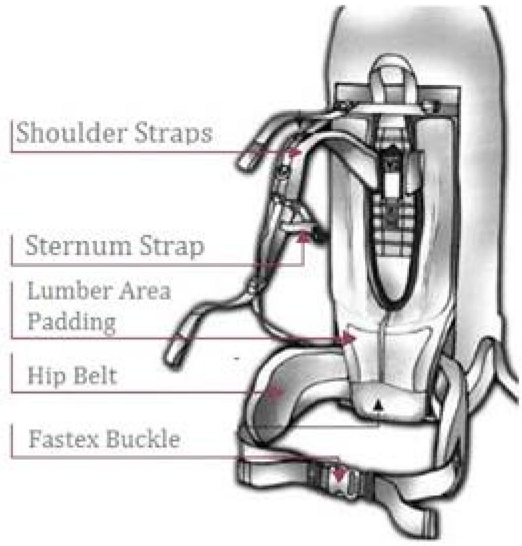

Figure 100: Backpack main elements [69]

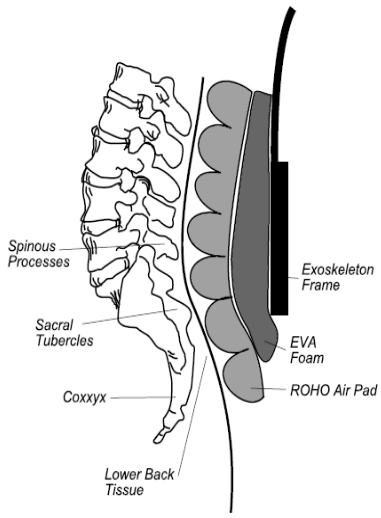

Figure 101: Back frame structure [69]

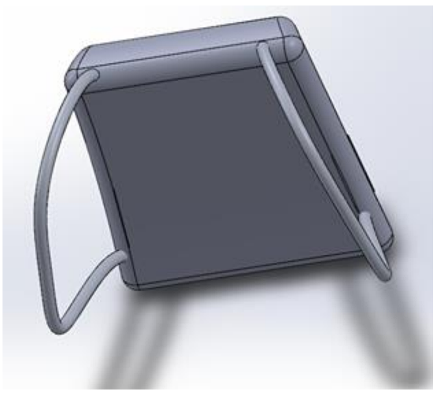

Figure 102: Backpack Solidworks® model

4.5.8 Hip joint case

The hip joint case, that has not been modeled, it should cover all the components placed on the aluminum flange. It should have a good surface finish, giving a high-quality profile and a high impact strength, due to the high exposure to sudden shocks. Using the carbon fiber as a material for the case could be a smart choice due to its mechanical properties, that cover all that has been mentioned above.

4.5.9 Straps and adjustable release buckle

For the straps(fig.103) we could use the regular backpack straps, meanwhile, we could adopt some adjustable release buckle(fig.104) to fix the exoskeleton to the user. Straps are usually made from ballistic nylon [73], which refers to a specific type of nylon, designed for maximum durability and abrasion resistance.

Figure 103: Ballistic nylon straps [73]

Figure 104: Adjustable release buckle [73]

4.6 Fastening solutions for composites

To fasten components to a composite material, such as carbon fibers, it has always been a challenge. Lightweight composite panels need to be thin, but machining processes like drilling or grinding, they may cause the composite thin sheets to deteriorate. For that reason, more than one method is used to fasten components to the carbon fiber panels[74].

4.6.1 Fasteners embedded in composites

Embedding fasteners in composites are among the most common methods used in locking different parts with composites. When integrated during the composite manufacturing process, the fasteners become a part of the carbon fiber panel, giving as a result a robust final assembly (fig.105).

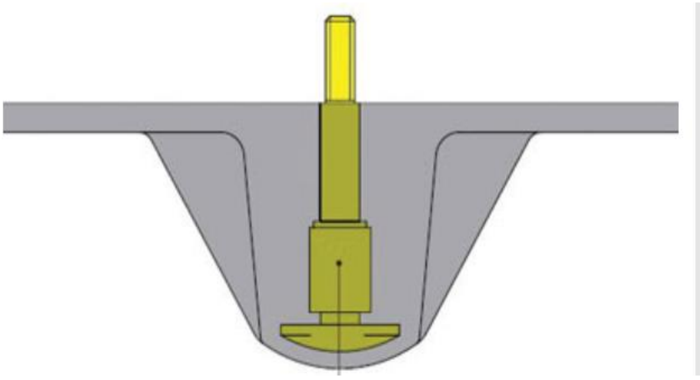

Figure 105: Fasteners embedded in composites [74]

However, embedding fasteners in the composite material is weakening it, increasing its weight and thickness. Thus, we should not use it in our design, to keep the exoskeleton as compact as possible.

4.6.2 Surface bonding in composites

Surface bonding in composites (fig.106) is an alternative method to the embedding fasteners in carbon fiber panels, without the need for the material to be thickened. The thin flat head, which is perforated to allow the flow of the composite material covering the fastener plate (fig.107), it helps to transfer the load efficiently into the composite structure.

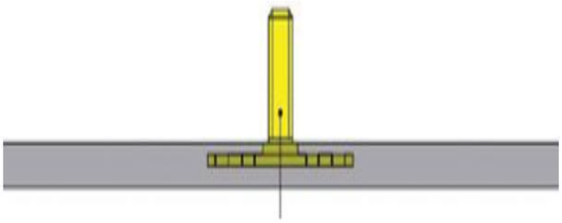

Figure 106: Surface bonding in composites [74]

Figure 107: fastener plate [74]

This method could be the best one for our application for many reasons, such as:

1- Saving space and weight.
2- Reduce composite curing time.
3- Higher tensile and torsional loads.
4- More compact design.

A practical example is shown in the following figure (fig.108).

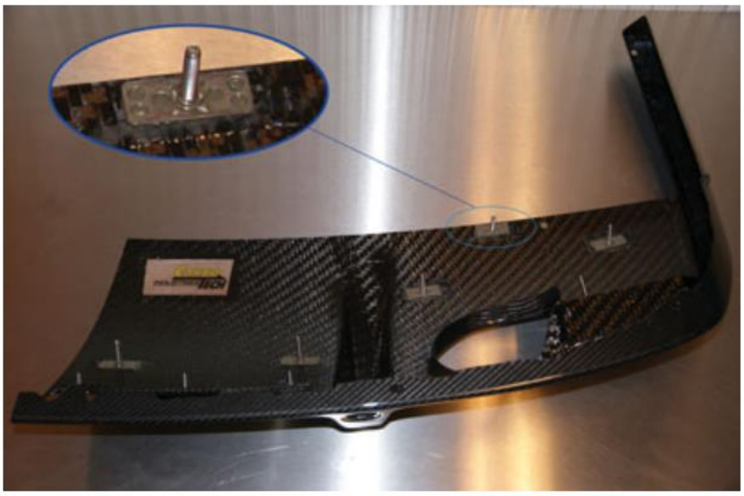

Figure 108: Practical example [74]

Chapter 5

Conclusion and future work

5.1 Conclusions

A study was done, reviewing the first conceptual design of the hip joint industrial exoskeleton. Since industrial exoskeletons is a new field of research, we were affected by the lack of scientific papers that could afford helpful information and more consistent background. Anyhow, we were able to implement a detailed design of the actuation unit considering the relative contact surfaces and the proper components coupling.

Some additional interfaces were chosen after studying the available commercial solutions that could fit with our specifications, to provide a more compact design. It was decided to decrease the assistive holding torque from 70% of the user`s resulting total working torque to be only 30%. This modification has been done after understanding that offering a 70% of assistive torque is an exaggerated value, and it is not a reasonable amount of a helping power afforded to a healthy worker. Moreover, it could increase much the weight of the exoskeleton and increase its lateral dimensions, since heavier and bigger component should be selected to afford that high amount of torque. In other words, it could affect also the comfortably of the worker, that should hold a massive structure for a long-time interval in the working environment By decreasing the holding torque value, a new required torque calculation has been done and more compact and lightweight power transmission components has been chosen, providing a more robust connection of the mechanical components. In addition to that, an elementary bearing calculation has been done, to figure out which is the amount of load that is affecting our system shafts, and we have defined the bearing model, the size, their relative positions and the rating life.

Furthermore, the material selection of different exoskeleton parts has been made, to understand which is the right combination that could be used to build the different exoskeleton parts, according to the functionality required by each part and the mechanical proprieties needed.

A detailed SolidWorks® model has been provided, to visualize how could look the whole system, once the exoskeleton is worn by the user. A harmonic drive analysis has been made to comprehend the working principles and to understand the possible combinations of operational configurations. The operating modes of the exoskeleton has been reviewed, to keep in mind always which are the functionality that should be provided by the studied assistive exoskeleton device. From the obtained results it is quite evident that the primary challenge is to find the best trade-off between compact size and efficiency.

5.2 Future work

In a future work some considerations should be made to make the entire structure adjustable for different user sizes and weights. In addition, a system optimization could be done, deciding if the electromagnetic clutch is a functional component for the system or not. Slimmer commercial electromagnetic clutches could replace the proposed one. Moreover, a material stress analysis and a more detailed bearing calculation could be performed to verify the whole structure robustness. We did not have the opportunity to get more in deep with electronic components, software design and coding.

Finally, the implementation of a specific test bench equipped with power transmission elements, sensors and transducers is a fundamental procedure, in order to have empirical results to compare with the concluded ones.

Annexes

1. Arduino program for motor angle reading

MOTOR_ANGLE_READ | Arduino 1.8.8

File Modifica Sketch Strumenti Aiuto

Verifica

MOTOR_ANGLE_READ §

```

// Variables initialization

int encoderChA = 2;
int encoderChB = 3;
int encoderPos = 0;
int encoderChAInit = LOW;
int turn = LOW;

//Communication setup

void setup() {
  pinMode (encoderChA, INPUT);
  pinMode (encoderChB, INPUT);
  Serial.begin (9600);
}

// Main program loop

void loop() {
  turn = digitalRead(encoderChA);
  if ((encoderChAInit == LOW) && (turn == HIGH)) {
    if (digitalRead(encoderChB) == LOW) {
      encoderPos++;
    } else {
      encoderPos--;
    }
    Serial.print (encoderPos);
   delay(10);
  }
  encoderChAInit = turn;
}

```

Figure x: Arduino program to read the motor angle

The first section is used to define our variables. The first two integers *encoderChA* and *encoderChB* are used to store the pulse signals of the encoder, that are assigned to the input pins 2 and 3 (as shown in the connection scheme of *fig. 10*) thanks to the function *pinMode*. The following variable *encoderPos* is used to initialize the encoder position to 0 at the beginning of the serial communication. Next, the *encoderChAInit* and *turn* are respectively the channel A initial value and the actual one, whose value is read trough to the function *digitalRead*.

Once the communication setup has been called , we can refer to the heart of the code, that is the *loop()* function. Here, the if conditions allow us to compare the read Channel A and B value so that we can update the *encoderPos* value, following the encoder logic explained in the previous paragraph. In other words, when Channel A is high and B is low the position is incremented and vice versa.

The line 28 is used to print the encoder position (*Serial.print*), so it can be displayed on the serial monitor while the program is running.

As any code requires some time to execute, we intentionally implement a delay of 10ms, and lastly, we update the *encoderChAInit* value.

References

[1] https://exoskeletonreport.com/2016/04/exoskeletons-for-industry-and-work/
[2] Davies Robert E., Mewsom-Davis et al., “Muscle”, Encyclopaedia Britannica, Oct. 2018
[3] https://biologydictionary.net/synovial-joint/
[4] https://teachmeanatomy.info/the-basics/anatomical-terminology/planes/
[5] https://opentextbc.ca/anatomyandphysiology/chapter/9-5-types-of-body-movements/
[6] https://en.wikipedia.org/wiki/Exoskeleton
[7] https://en.wikipedia.org/wiki/Powered_exoskeleton
[8] https://exoskeletonpowersuits.weebly.com/history.html#
[9] https://exoskeletonreport.com/2016/08/exoskeleton-industry-2016/
[10] https://exoskeletonreport.com/2015/02/businesses-that-have-or-are-exploring-exoskeleton-products-in-alphabetical-order/
[11] https://exoskeletonreport.com/2015/08/types-and-classifications-of-exoskeletons/
[12] https://exoskeletonreport.com/2015/03/from-hulc-to-mantis-to-fortis-exoskeleton-development-history/
[13] http://hart.berkeley.edu/exoskeletons.html
[14] https://forums.spacebattles.com/threads/how-heavy-should-a-realistic-power-armor-powered-exoskeleton-be.380733/
[15] https://www.therobotreport.com/industrial-exoskeletons-arrive/
[16] http://www.bestdevlist.com/5-ways-powered-exoskeletons-improving-way-live/
[17] Bosch T. , Van Eck J. , Knitel K. , De Looze M., “The effects of a passive exoskeleton on muscle activity, discomfort and endurance time in forward bending work”, The Netherlands, *Appl. Ergon.*, 2016
[18] https://www.zhaw.ch/en/engineering/institutes-centres/institute-of-mechatronic-systems-ims/
[19] https://www.suitx.com/backx
[20] Dan Kara, “Industrial exoskeletons: new systems, improved technologies, increasing adoption”, December 6, 2018 [ONLINE]
[21] https://exoskeletonreport.com/2015/08/soft-exoskeletons-and-exosuits/
[22] https://www.engr.ncsu.edu/theengineeringplace/educators/
[23] ISO/TR 7250-2:2010 – Basic human body measurements for technological design – Part 2: Statistical summaries of body measurements from individual ISO populations
[24] Herman, Irving P.,“Physics of the Human Body”, Berlin, Springer, 2016
[25] https://www.britannica.com/science/centre-of-gravity
[26] Francesco Giovacchini, Federica Vannetti, Matteo Fantozzi, Marco Cempini, Mario Cortese, Andrea Parri, Tingfang Yan, and al., “A light-weight active orthosis for hip movement assistance”, Robotics and Autonomous Systems 73, 2015
[27] Harmonic Drive© AG, “CPL-2A Components Sets Engineering Data”, December 2014 product catalogue
[28] http://www.harmonicdrive.net/products/rotary-actuators/hollow-shaft-actuators/sha-sg
[29] https://learn.adafruit.com/analog-feedback-servos/about-servos-and-feedback
[30] Harmonic Drive®LLC, “AC Servo Actuator – SHA SG and CG series manual”, 2019 product catalogue
[31] Dynapar ™, “Encoders & Resolvers”, 2010 product catalogue
[32] https://www.dynapar.com/
[33] SKF®, “SKF spherical plain bearings and rod ends”, September 2011 product catalogue
[34] https://www.orientalmotor.com/stepper-motors/technology/everything-about-stepper-motors.html

[35] https://www.academia.edu/4777256/Stepper_Motor_Advantages_and_Disadvantages
[36] https://www.sciencedirect.com/topics/engineering/stepper-motor
[37] http://www.motioncontrolproducts.com/pages/applications-stepper-motor.php
[38] SANYO DENKI EUROPE SA©, "SANMOTION – 2-PHASE STEPPING SYSTEMS F2", 2012 product catalogue
[39] https://www.brainy-bits.com/stepper-motor-rotary-encoder-p1/
[40] http://www.hobbytronics.co.uk/arduino-uno-r3
[41] https://playground.arduino.cc/Main/RotaryEncoders
[42] https://www.machinedesign.com/archive/basics-electromagnetic-clutches-and-brakes
[43] Altra Industrial Motion©, "Clutches and Brakes", 2018 product catalogue
[44] http://www.designfax.net/cms/dfx/opens/article-view-dfx.php?nid=4&bid=183&et=featurearticle&pn=06
[45] http://hades.mech.northwestern.edu/index.php/Gears
[46] http://www.harmonicdrive.net/
[47] Harmonic Drive®LLC, " Speed reducers for precision motion control – Reducer catalog", 2019 product catalogue (Page 3)
[48] http://www.harmonicdrive.net/_hd/content/documents/FB_Component.pdf
[49] NTN Corporation, "Ball and Roller Bearings",2018 product catalogue
[50] https://www.skf.com/group/products/bearings-units-housings/principles/bearing-selection-process/bearing-size/size-selection-based-on-rating-life/equivalent-dynamic-bearing-load/index.html
[51] Somà A., "Fondamenti di meccanica strutturale", Torino, Levrotto & Bella, 2013
[52] https://www.warnerelectric.com/products/clutch-products/shaft-mounted-clutches/sfm-series/sfm-var-00-clutches
[53] Harmonic Drive®LLC, " Speed reducers for precision motion control – Reducer catalog", 2019 product catalogue (Page 106)
[54] https://x-engineer.org/automotive-engineering/drivetrain/coupling-devices/calculate-torque-capacity-clutch/
[55] Harmonic Drive®LLC, " Speed reducers for precision motion control – Reducer catalog", 2019 product catalogue (Page 27)
[56] SKF®, "Rolling bearings", October 2018 product catalogue
[57] https://www.skf.com/group/products/bearings-units-housings/principles/bearing-selection-process/bearing-size/size-selection-based-on-rating-life/bearing-rating-life/index.html
[58] PIRTEK©, "Lubrication, Refueling and Spill control", 2019 product catalogue
[59] https://www.skf.com/us/products/bearings-units-housings/principles/bearing-selection-process/bearing-size/size-selection-based-on-static-load/index.html
[60] Calistrat M. M., "Shaft key rivisited", Michael Calistrat & Associates, Texas, May 2000
[61] Shigley J., Mischke C. R., Budynas R. G., "Mechanical Engineering Design", McGraw-Hill Education, July 2003, 7th edition
[62] https://www. azom.com/article.aspx?ArticleID=6115
[63] https://ndassistive.org/blog/jaco2-robotic-arm-a-new-generation-of-assistive-technology/
[64] https://www.christinedemerchant.com/carboncharacteristics.html
[65] https://infogram.com/carbon-fiber-vs-fiberglass-1gdk8pd471dvpq0
[66] https://precisionpunch.com/plastic-materials-index/
[67] Gonzalez-Vargas, Jose & Ibáñez, Jaime & Contreras-Vidal, José & van der Kooij, Herman & Luis Pons, José. (2017). Wearable Robotics: Challenges and Trends: Proceedings of the 2nd International Symposium on Wearable Robotics, WeRob2016, October 18-21, 2016, Segovia, Spain. 10.1007/978-3-319-46532-6.

[68] M. G. McKinley, “Design of lightweight assistive exoskeletons for individuals with mobility disorders”, University of California, Berkeley, Spring 2014
[69] https://www.bpf.co.uk/plastipedia/polymers/HDPE.aspx
[70] Sanders Robert E., “Technology Innovation in Aluminum Products”, JOM 53 (2), 2001
[71] https://www.researchgate.net/figure/Material-properties-of-aluminum-alloy-6061-T6-alumina-and-steel_tbl1_262512682
[72] http://www.fasteningsystems.com/side_release_buckles_1.html
[73] https://www.fastfixtechnology.com/news/fastener-solutions-for-composites/
[74] Tilloca G., "Study and design of a hip joint for exoskeleton applications", Torino, Politecnico di Torino, Dicembre 2018